Dissertation
submitted to the
Combined Faculty of Natural Sciences and Mathematics
of the Ruperto Carola University Heidelberg, Germany
for the degree of
Doctor of Natural Sciences

Presented by

Christian Kischnick, M.Sc.
Born in: Bremen, Bremen (Germany)
Oral examination: 19.07.2018

Role of Phosphoinositides in Cellular Polarity and Immunity

Referees: Prof. Dr. med. Alexander Dalpke

Dr. Steeve Boulant

ACKNOWLEDGEMENTS

First of all I want to thank Dr. Steeve Boulant for the opportunity to work on this project. I further would like to thank Dr. Megan Stanifer. They gave me fantastic support, guided me through my PhD, and helped me through tough times.

I also want to thank Prof. Dr. Alexander Dalpke for agreeing to be the first supervisor and for his participation in my TAC meetings. Furthermore I want to thank Dr. Volker Lohmann for his participation in my TAC meetings and Prof. Dr. Gislene Pereira as well as Dr. Pierre-Yves Lozach for being part of my defense committee.

Furthermore I want thank our collaboration partner Prof. Dr. Volker Haucke and his group, especially Dr. Haibin Wang and Guan-Ting Liu. Without their help and expertise this project would not have been possible.

I am grateful for getting the chance to work with the whole Boulant group; they have made stressful years more fun and my PhD a memorable time.

Ganz besonders möchte ich mich bei meiner Familie bedanken, insbesondere bei meinen Eltern und meiner Schwester. Ohne euer Verständnis und eure Hilfe hätte ich es nie an eine Universität und bis zur Promotion geschafft!

TABLE OF CONTENT

List of Figures

List of Tables

SUMMARY

Cell polarity describes the asymmetric distribution of proteins, RNA, organelles and lipids. One of the best studied models of polarity are epithelial cells. They form the barriers that separate and protect the organism from the outside environment. Establishment and maintenance of polarity is ensured through a highly complex network of proteins and lipids that mediate asymmetry through trafficking processes and reorganization of the cytoskeleton. One of the key players in polarity are phosphoinositides, phosphorylated forms of the lipid phosphatidylinositol. In this thesis I investigated the role of one such phosphoinositide, PI(3)P, on cellular polarity and immunity in human intestinal epithelial cells.

In my work I used established methods to evaluate the role of PI(3)P in human intestinal epithelial cells. These three methods were (1) the use of specific inhibitors targeting VPS34 (2) the development of cell lines depleted of kinases and phosphatases needed for PI(3)P biogenesis and (3) on demand depletion of PI(3)P from endosomes using a chemical dimerizer system. Each of these methods were evaluated both for their ability to modulate PI(3)P levels and for their impact on cellular polarity and immune response. While I could demonstrate that all three methods successfully modulated PI(3)P levels the chemical dimerizer (AP21967) interferes with polarity and immunity itself and we require a new dimerizer before conclusions can be made using this method. Interestingly, I determined that reduced PI(3)P levels, either by chemical inhibition or knock-down of the kinase VPS34, impaired cellular polarity in T84 cells indicating a critical role of PI(3)P in the polarity program. Additionally, knock-down of the PI(3)P metabolizing enzymes VPS34 and MTM1 showed interesting results for IFNλ production upon reovirus infection. IFNλ production in MTM1 and VPS34 knock-down cells is increased and decreased respectively. This could be due to the previously reported PI(3)P dependent TLR3 sorting adaptor WDFY1 and should be further investigated.

In parallel I also created a novel viral vector system in our lab. This viral vector is based on the BacMam system which are baculovirus based vectors with a large cargo capacity. The BacMam was initially modified with an S/MAR sequence to allow for its persistence in cells. The vector was then further modified to allow expression of reporter genes. Both vectors were shown to be fully functional and will provide a valuable tool for future projects.

ZUSAMMENFASSUNG

Zellpolarität bezeichnet die asymmetrische Verteilung von Proteinen, RNS, Organellen und Lipiden. Epithelzellen sind eines der am besten untersuchten Modelle für Polarität. Sie bilden eine Barriere die das Innere des Organismus vor der Außenwelt schützt. Ein hochkomplexes Netzwerk aus Proteinen und Lipiden stellt Polarität durch asymmetrische Transportvorgänge und Veränderungen im Zytoskelett her und erhält sie aufrecht. Phosphoinositole sind Lipide und eine der wichtigsten Komponenten in diesem Netzwerk. In dieser Arbeit wurde die Rolle eines dieser Lipide, PI(3)P, in der Polarität und der Immunantwort in menschlichen Darmepithelzellen untersucht.

Um die Rolle von PI(3)P in menschlichen Darmepithelzellen zu untersuchen wurden drei gängige Methoden verwendet: (1) Spezifische Inhibitoren gegen die Kinase VPS34, (2) Knock-down von VPS34 und MTM1, Enzymen die an der Biogenese von PI(3)P beteiligt sind, und (3) Reduzierung des endosomalen PI(3)P mit einem System zur chemisch-induzierten Dimerisierung von Proteinen. Diese Methoden wurden in auf ihre Fähigkeit PI(3)P Level zu verändern hin untersucht. Während alle drei Methoden die PI(3)P Level veränderten, zeigte sich, dass der Dimerisierungsinduktor AP21967 sowohl Polarität als auch die Immunantwort negativ beeinflusst. Wir benötigen einen neuen Dimerisierungsinduktor bevor wir diese Methode tatsächlich nutzen können. Eine Verringerung der PI(3)P Level, entweder durch Inhibierung oder Knock-down der Kinase VPS34, hatte eine Beeinträchtigung der Polarität und der Immunantwort zur Folge. Das deutet auf eine entscheidende Rolle von PI(3)P in diesen Prozessen hin. Knock-down von VPS34 oder MTM1, resultierte in interessanten Ergebnissen bei der IFNλ Immunantwort auf eine Reovirus Infektion. Diese ist nach MTM1 Knock-down erhöht und nach VPS34 Knock-down verringert. Das könnte durch die bereits publizierte Rolle des TLR3 Adapters WDFY1 zustande kommen und sollte genauer Untersucht werden.

Zudem wurde parallel ein neuer viraler Vektor in unserem Labor etabliert. Dieser basiert auf BacMam, virale Vektoren basierend auf Baculoviren die eine sehr hohe Verpackungspakazität haben. Das BacMam System wurde mit einer S/MAR Sequenz modifiziert die es dem Virus erlaubt dauerhaft in Zellen zu verbleiben. Dieser Virus wurde dann weiter verändert um die Expression von Reporter Genen zu erlauben. Beide Vektoren sind funktional und werden von großer Hilfe für zukünftige Projekte sein.

ABBREVIATIONS

bp	Base pair
BSA	Bovine serum albumin
coGFP	Copepod green fluorescent protein
DAG	Diacylglycerol
DAPI	4',6-diamidino-2-phenylindole
DMEM	Dulbecco's Modified Eagle Medium
DNA	Deoxyribonucleic acid
EDTA	Ethylenediaminetetraacetic acid
EtOH	Ethanol
FBS	Fetal bovine serum
GEF	guanine nucleotide exchange factor
GFP	Green fluorescent protein
GOI	Gene of interest
GPCR	G-protein coupled receptor
HBSS	Hank's Balanced Salt Solution
HMW	High molecular weight
IC_{50}	Half maximal inhibitory concentration
IF	Immunofluorescence
IFA	Immunofluorescence assay
IMDM	Iscove's Modified Dulbecco's Medium
IPTG	Isopropyl β-D-1-thiogalactopyranoside, Isopropyl β-D-thiogalactoside
kb	Kilo base pairs
LB	Lysogeny broth
LB-Amp	Lysogeny broth with ampicillin
LB-Kan	Lysogeny broth with kanamycin
LMW	Low molecular weight
MEM	Minimum essential medium
MOI	Multiplicity of infection
NGS	Normal Goat Serum
mRFP	Monomeric red fluorescent protein
MRV	Mammalian reovirus
NBCS	Newborn calf serum

OD	Optical density
PCR	Polymerase chain reaction
PEI	Polyethylenimine
PFA	Paraformaldehyde
Poly(I:C)	Polyinosinic-polycytidylic acid
qRT-PCR	Quantitative reverse-transcription polymerase chain reaction
rcf	relative centrifugal force
RIPA	Radioimmunoprecipitation assay buffer
RNA	Ribonucleic acid
rpm	Revolutions per minute
S/MAR	Scaffold / matrix attachment region
SDS	Sodium dodecyl sulfate
SDS-PAGE	Sodium dodecyl sulfate polyacrylamide gel electrophoresis
shRNA	Short hairpin RNA
TBE	Tris-Borate-EDTA
TE	Tris-EDTA
TEER	Trans-epithelial electrical resistance
tGFP	Turbo green fluorescent protein
wt	wildtype
X-Gal	5-Bromo-4-chloro-3-indolyl β-D-galactopyranoside

1 INTRODUCTION

1.1 EPITHELIAL POLARITY

Cellular polarity is a term that describes the asymmetric distribution of cellular components such as proteins, lipids, RNA and even whole organelles[1]. It is a phenotype that is found in many cells. Commonly studied examples include neurons (axon - dendrites), migrating cells (directional polarization with leading and trailing edge), asymmetrically dividing stem cells, and epithelial cells (apico-basal axis)[1,2]. Monolayered epithelia have an apical site facing the outside, e.g. lumen of the gut or urinary tract, and a basolateral site with which the cells are in contact with one another and the extracellular matrix on the inside of the body[3,4].

The intestinal epithelium is composed of five different cell types that arise from a common stem cell niche. The vast majority of cells are the absorptive enterocytes[5]. Besides their barrier function, they are involved in nutrient uptake and secretion of antimicrobial peptides (AMPs)[6,7]. These cells are what we will focus on in this thesis and refer to them as intestinal epithelial cells (IECs). In addition to the enterocytes there are the hormone secreting enteroendocrine cells, mucus secreting goblet cells, Paneth cells that secrete AMPs, and microfold cells (M-cells) that sample antigens by transcytosis to underlying immune cells[7–10]. One of the primary functions of the intestinal epithelium is that of a physical barrier. It separates the inside of the body from the lumen of the intestine and its microbiome[11]. To fulfill this task, the cells have to form a tight monolayer of polarized cells. This epithelial polarity is established and maintained by an intricate network of proteins and lipids termed the epithelial polarity program (EPP)[12]. This part of the introduction will provide a general overview of the EPP without the lipids which will be discussed in section 1.3.

To investigate how apico-basal polarity is initially established, epithelial cells can be grown in an artificial extracellular matrix (ECM) either composed of collagen or Matrigel, a commercial ECM secreted by a murine tumor cell line[13,14]. Single cells will start dividing and ultimately form a three dimensional structure named spheroid or cyst (Figure 1)[15]. The most common model for mammalian epithelial cells are Madin-Darby canine kidney (MDCK) cells. When MDCK cells are grown as spheroids, they initially express the apical marker protein Podocalyxin everywhere in the plasma membrane (Figure 1 A). In the two cell stage they display an inverted polarity

phenotype. The apical marker Podocalyxin faces the ECM while the basolateral marker β-catenin is localized to the plasma membrane where both cells are in contact (Figure 1 B). At this contact site the first cell-cell connections form, which is known as the apical membrane initiation site (AMIS). As cells grow and divide, polarity markers will start to relocate to their correct membrane domain and Podocalyxin can be found in the pre-apical patch (PAP) where a small lumen forms (Figure 1 C)[14,16]. Upon further cell divisions this small lumen becomes a single, large lumen in the center of the spheroid (Figure 1 D).

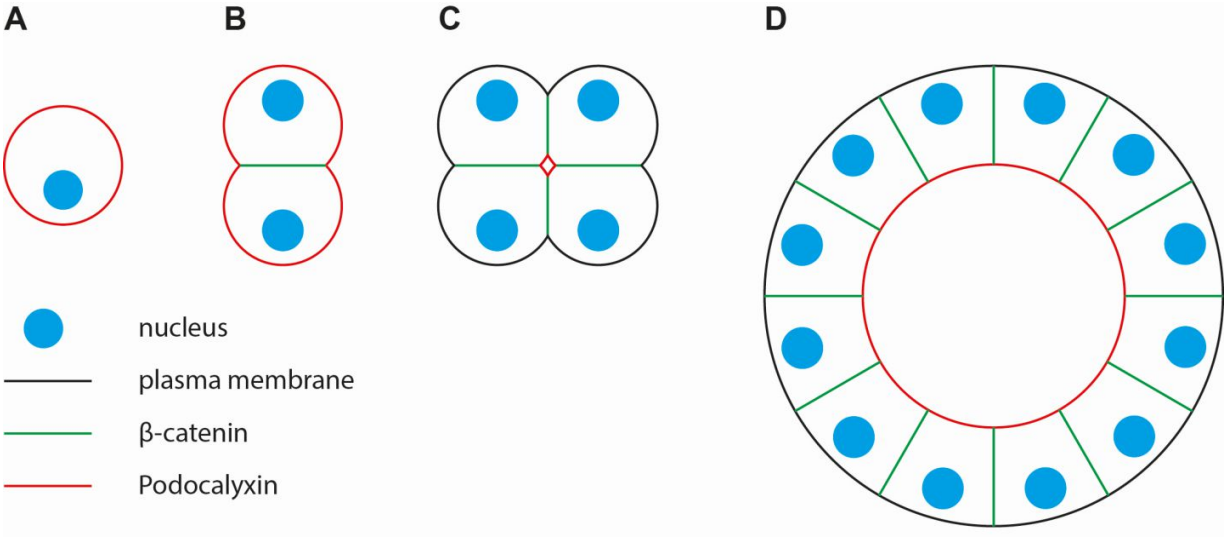

Figure 1: Schematic of MDCK spheroid formation. A) Single cell not showing signs of polarization. Podocalyxin is found everywhere plasma membrane. B) Two cell stage with inverted polarity. The apical marker Podocalyxin faces the extracellular matrix and the basolateral marker β-catenin localizes to the membrane contact site. This is the membrane initiation site (AMIS) forms. C) Small cell aggregate where pre-apical patch (PAP) has formed. Polarity markers show correct localization. D) Fully formed spheroid with a single, large lumen. Data was adapted from[14,16,17].

Even before the pathways establishing apico-basal polarity were elucidated as much as they are today, it was known that MDCK cells secrete laminin at their basal side to form a basement membrane[18]. It has been shown that the GTPase Rac1 is a key player in establishing apico-basal polarity by assembling a laminin basement membrane at the basal pole [13]. While Rac1 is a key player, there are a large number of other proteins involved. Some of the most important proteins can be divided into four different groups which will be mentioned here briefly. First there are the apical proteins of the Crumbs (CRB) group: Crumbs itself, membrane palmitoylated protein 5 (MPP5, also known as PALS1), and PALS1-associated tight-junction homologue (PATJ)[12]. Members of the Scribble (SCRIB) group, SCRIB, Discs-large homologue

(DLG) and Lethal giant larvae (LGL), show a polarized distribution to the lateral site of cells[12]. Next there are the PAR proteins, which contains PAR1, 3, 4, 5, 6, atypical protein kinase C (aPKC), and the GTPase Cdc42[12]. PAR3, PAR6, Cdc42, and aPKC are usually considered to be apical determinants[19]. PAR1 and PAR4 are localized in the basolateral domain but still are not considered to be part of either an apical or basolateral complex and PAR5 is found in the cytoplasm[19]. In Drosophila there is also the Coracle group of proteins which in addition to Coracle itself includes Moesin, Yurt, Neurexin IV, and the Na^+, K^+-ATPase[12]. Giving that the p58 subunit of the Na^+, K^+-ATPase is used as a basolateral marker in MDCK cells, one could assume that the Coracle is used in other organisms besides Drosophila[20,21]. Interestingly, only Crumbs, Neurexin IV, and the Na^+, K^+-ATPase are transmembrane proteins. The other proteins mentioned above are kept in their respective domain by interaction with other polarity proteins or membrane proteins[12]. Regulation of polarity requires a complex interplay between all of these components.

PAR3 is one of the earliest proteins found in the future apical domain. It is involved in targeting the Cdc42-PAR6-aPKC complex and PALS1 to the apical side. It also helps recruit E-cadherin to form adherens junctions[19]. When polarization progresses, PAR3 itself becomes a target for aPKC phosphorylation and exclusion from the apical domain, possibly mediated by PAR5 which has been shown to mediate the exclusion of PAR3 from the basal domain after PAR1 phosphorylation[22,23]. This complex interplay allows PAR3 to be localized at a narrow area just between the apical and basolateral domains at the adherens junctions or tight-junctions[14,24]. This mechanism of mutual exclusion is used by several other proteins as well, e.g. aPKC phosphorylation of PAR1 and LGL to exclude them from the apical domain[25,26].

Besides cytoplasmic proteins that are kept in their respective domains by the exclusion mechanisms described above, it is important that cells have intracellular transport mechanisms targeting vesicular carriers to the correct domain. This requires rearrangement of the trafficking machinery which includes a variety of endosomal compartments such as the apical- and basal sorting endosome (ASE, BSE), the apical recycling endosome (ARE) and the common recycling endosome (CRE) in addition to the common components involved in vesicular trafficking such as late endosomes, lysosomes, and Golgi apparatus[27]. This system is different from non-polarized cells as can be seen for Rab11a. Rab11a is involved in transferrin recycling only in nonpolarized MDCK cells but not after polarization when the transferrin receptor is localized to the basolateral

site[28]. The role of the Rab11a compartment in selective apical delivery of cargo has also been shown in human polarized intestinal epithelial cells (Caco-2)[29]. Therefore it is assumed that Rab11a switches from general recycling to predominantly apical recycling (ARE). This change is not absolute as the trafficking of E-cadherin to the lateral site requires Rab11a endosomes[30]. Rab35 is another protein that has been shown to be involved in establishing polarity by apical trafficking, and is involved in bringing Podocalyxin to the AMIS[31]. These vesicles not only contained Podocalyxin but also Crumbs3, Cdc42, aPKC, and Rab11 all of which are important polarity proteins defining the apical pole[31]. However, each polarized system is unique and will show unique factors required for the establishment of polarity[32].

One of the early determinants trafficked to the apical side is the polarity protein Crumbs, which is trafficked to the apical site through Rab11-positive vesicles[19,33]. In *Drosophila*, surface levels of Crumbs have to be tightly controlled by surface delivery and endocytosis. If endocytosis is disrupted by targeting the clathrin adaptor AP-2, the apical domain expands and normally monolayered epithelia are more likely to become multilayered[34].

Cdc42 was so far introduced as being important for establishing the apical membrane domain. But it was also shown that it is involved in the exit of apical as well as basolateral cargo from the trans-Golgi-network (TGN) in MDCK cells[35]. Another group verified the role of Cdc42 in basolateral trafficking by showing hat loss of Cdc42 in MDCK cells resulted in the loss of basolateral polarity while apical polarity was not impaired[36].

One prerequisite of polarity are tight junctions. Tight-junctions separate the apical from the basolateral domain and prevent diffusion between both domains[37]. They are composed of transmembrane proteins (claudins, occludin and junctional adhesion molecules (JAMs)), as well as many interacting proteins such as zonula occludens (ZO) proteins bridging it with the actin cytoskeleton[37]. The ability of tight junctions to prevent passive diffusion across the monolayer can experimentally be measured by the trans-epithelial electrical resistance (TEER). It was shown that aPKC isotype specific interacting protein (ASIP)/PAR3/aPKC positively regulates tight junction formation in MDCK cells which can be shown by an increased TEER[38]. Later another group showed that loss of PAR3 in MDCK cells disrupts assembly of tight junctions in an Rac-dependent pathway[39]. Overexpression of dominant-negative Rac or knock-down of its guanine nucleotide exchange factor (GEF) Tiam1 in cells missing PAR-3 improved tight-junction

formation[39]. Other parts of the epithelial polarity program are involved in tight-junction formation as well. Expressing an inactive PAR6 mutant in murine cancer cells induced ZO-1 structures and reduced their metastasis to the lung when implanted in BALB/c mice and exogenous expression of Crumbs3 induces tight junction formation in the epithelial cell line MCF10A, which normally do not have tight junctions[40,41].

Research over the last decades has helped us to get a better understanding of how epithelial polarity is established and maintained. It has become obvious that it is the result of highly complex and interdependent protein complexes and a rearranged endosomal system all of which participate in defining distinct apical and basolateral plasma membrane domains, cell-cell junctions, and providing specific, polarized trafficking routes.

1.2 Immunity in Intestinal Epithelial Cells

To protect the host form the intestinal microbiome the epithelium works not just as a mechanical barrier but also as a platform to sense and combat viral or microbial infection. In this part I will give a short introduction into how IECs can sense infection and then briefly talk about the interplay between the microbiome and the intestinal epithelium.

The cell's intrinsic innate immunity is based on germ-line encoded pattern recognition receptors (PRRs) which can provide a first line of defense before the more specialized adaptive immune system can provide protection[42]. These sensors include the toll-like receptors (TLRs) and the retinoic acid inducible gene I (RIG-I)-like receptors (RLRs)[42–44]. All of these receptors recognize pathogen-associated molecular patterns (PAMPs) which are conserved structures found on microorganisms and viruses. Since they are not found on the host itself they allow a self – foreign differentiation[42].

All 10 TLRs encoded by the human genome have the same general structure. They have an extracellular domain composed of multiple leucine-rich repeats in a horseshoe shape that mediates pattern recognition. A transmembrane domain connects it to the intracellular Toll/IL-1 receptor (TIR) domain to relay the signal into the cell[42,45]. TLRs can be subdivided according to their localization into cell surface TLRs (TLR1, 2, 4, 5, 6, 10) and endosomal TLRs (TLR3, 7, 8, 9). While having similar structures, they recognize a wide variety of patterns. TLR2 together with TLR1 or TLR6 recognizes triacylated lipopeptides or diacylated lipopeptides respectively. Upon activation they signal via TIR Domain Containing Adaptor Protein (TIRAP) and Myeloid

Differentiation Primary Response 88 (MyD88) to stimulate nuclear factor kappa-light-chain-enhancer of activated B cells (NF-κB) mediated production of proinflammatory cytokines[46]. TLR5 recognizes bacterial flagellin and signals via MyD88 and NF-κB like TLR2/1/6[46]. Plasma membrane TLR4 together with MD2 is activated by bacterial lipopolysaccharide (LPS) and signals via TIRAP and MyD88 to stimulate NF-κB mediated inflammatory cytokine production. TLR4 is then taken up by the cell and signals from within the endosome via TIR-domain-containing adapter-inducing interferon-β (TRIF) and TRIF-related adaptor molecule (TRAM) which continue to signal via NF-κB but also induce interferon regulatory factor 3 (IRF3) mediated type I interferon production[46,47]. TLR7 and TLR9 recognize single stranded RNA and unmethylated CpG sequences in DNA respectively. They signal from the late endosome/endolysosome compartment via MyD88 to induce proinflammatory cytokines and type I interferon through NF-κB and IRF7 respectively[46]. TLR3 signals the late endosomes/endolysosomes as well and upon recognition of double stranded RNA it induces inflammatory cytokines and type I interferon through NF-κB and IRF3 respectively in a TRIF dependent manner[42,46]. TLR10 differs from the other receptors described in that it was reported to act as a negative regulator of TLR signaling[48,49].

RIG-I like receptors are cytoplasmic proteins belonging to the family of DExD/H box RNA helicases. This group encompasses RIG-I, Melanoma Differentiation-Associated protein 5 (MDA5), and laboratory of genetics and physiology 2 (LGP2)[44]. They all have zinc-binding C-terminal domain (repressor domain) and a central helicase domain that mediates double stranded RNA binding. RIG-I and MDA5 also have N-terminal tandem caspase activation and recruitment domains (CARD) necessary for signaling. As LGP2 doesn't have these CARD it can't signal but rather has regulatory functions[44]. Once RIG-I or MDA5 bind their ligand, they can interact with their common adaptor mitochondrial antiviral signaling protein (MAVS). MAVS signals through multiple proteins including TNF receptor-associated factor 2 (TRAF2), TRAF3, and TRAF6[44]. IRF3/7 and NF-κB then drive expression of type I and type III interferon as well as proinflammatory cytokines[44]. It was shown that despite its name, MAVS is also found on peroxisomes which have been identified as the primary signaling hub for the RLR induced type III interferon response[50].

The intestinal epithelium is in contact with the microbiome and needs to be able to tolerate commensals but mount an immune response to pathogens or when the epithelial barrier is

breached. This is especially important for surface expressed TLRs[5]. One hypothesis is that tolerance is achieved by predominantly expressing TLRs on the basolateral surface. There they only get into contact with their ligand if the epithelial barrier is breached and an immune response has to be mounted[5]. When TLR distribution in healthy intestinal tissue samples was compared with samples from ulcerative colitis (UC) and Crohn's disease (CD) patients, an increase in TLR4 expression in both UC and CD patients was found. Furthermore, the TLR4 signal was predominantly basolateral in healthy individuals and UC patients. In CD patients on the other hand a strong TLR4 signal at the apical pole was observed[51]. This points towards a role of TLR signaling in the inflammatory symptoms of CD patients as well as polarity in preventing inflammation in healthy individuals[51]. Also it was shown that the polarized human colon carcinoma cell line HCA-7 responds stronger to basal TLR5 stimulation than to apical stimulation[52]. Reduced expression of the sensor might help to achieve tolerance as well. While TLR4 was barely detectable in biopsies from healthy individuals, patients with ulcerative colitis or Crohn's disease showed a strong upregulation[51]. As it is technically difficult to analyze the exact location of TLRs on the different intestinal epithelial cell types, these results have to be interpreted carefully. Also it might not be necessary that TLRs are strictly localized to one side. It was shown that the outcome of TLR9 signaling in intestinal epithelial cells depends on the site of stimulation. While basolateral stimulation of polarized HCA-7 cells invokes an NF-κB dependent immune response, apical stimulation resulted in accumulated IκBα which prevented NF-κB activation. It also conferred intracellular tolerance to subsequent TLR stimulations[52]. Furthermore they showed that basal TLR3 stimulation elicited a much stronger IL-8 response than apical stimulation[52]. As TLR9 and TLR3 are both endosomal, this would argue for the ability of cells to tell apart which site the stimulation came from and respond accordingly. This is further substantiated by data from our lab. When polarized T84 cells are infected with reovirus Type 3 Dearing (T3D), which is mostly sensed by RIG-I, a site specific immune response is mounted (Figure 2). Infection from the basolateral site results not only in a stronger interferon λ response but also in a longer lasting response (Figure 2 A). Such a difference cannot be seen for interferon β1 (Figure 2 B). Data speaking against a strict localization of receptors to the basolateral site is further substantiated by observations that TLR signaling is indeed beneficial for the host. Examples include experiments with mouse models of inflammatory bowel disease (IBD). For example, mice lacking signaling by most TLRs ($MyD88^{-/-}$) develop much more severe intestinal

inflammation[53]. Other experiments showed that *Bacteriodes fragilis* protected animals from experimental IBD in an TLR2 dependent manner[53].

While there is still much more work to do to gain a more complete understanding of the tolerance to the microbiome, work in our lab and from others indicates that the polarized phenotype of the intestinal epithelium is involved since both, the preferential localization of receptors to the basolateral site and the ability to distinguish which side the signal originates from, requires polarized cells.

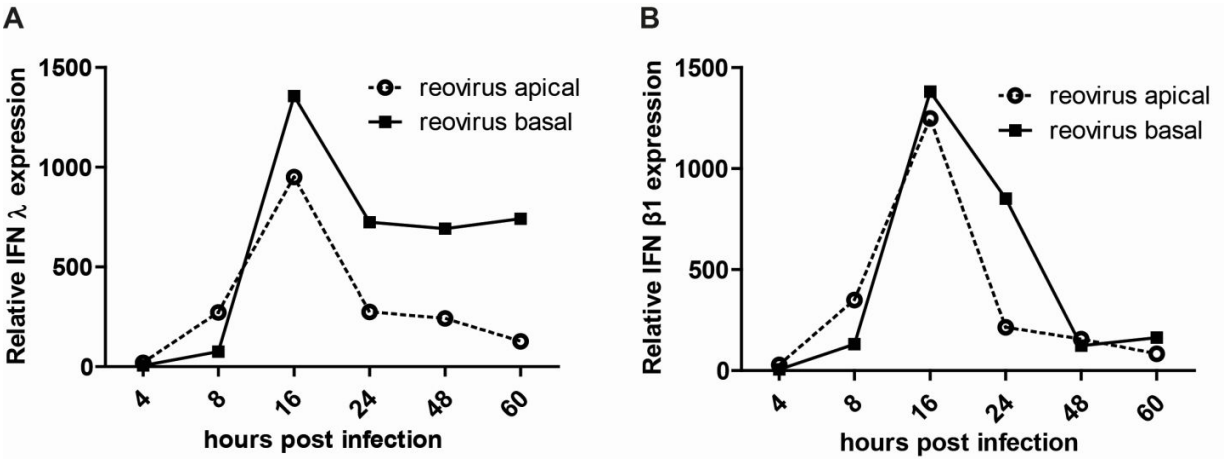

Figure 2: Immune response to reovirus Type 3 Dearing (T3D) infection in polarized intestinal epithelial cells. Polarized T84 cells were infected with reovirus T3D from the apical or basal site. mRNA expression of interferon λ (A) and interferon β1 (B) were analyzed between 4 and 60 hours post infection. Experiment performed by Megan Stanifer.

1.3 LIPIDS

Cellular membranes are an essential pre-requisite of life. They form the borders of cells, protecting the cytosol from the extracellular space. This separation is what makes life possible. What started with a simple membrane surrounding the prokaryotic cytoplasm evolved into highly complex eukaryotic cells with numerous membranous organelles. These membrane separated compartments allow cells to spatially separate processes that require different environments or are incompatible with one another, e.g. the proton gradient over the mitochondrial membrane used for energy generation or the low lysosomal pH required for hydrolytic enzymes to work[54,55].

The major building blocks of all cellular membranes are lipids. While an all encompassing definition of lipids is difficult, the LIPID MAPS Classification System has defined

them as "hydrophobic or amphipathic small molecules that may originate entirely or in part by carbanion- based condensations of thioesters (fatty acids, polyketides, etc.) and/or by carbocation-based condensations of isoprene units (prenols, sterols, etc.)"[56]. Their classification system divides all lipid molecules into eight different categories (fatty acyls, glycerolipids, glycerophospholipids, sphingolipids, sterol lipids, prenol lipids, saccharolipids, and polyketides) that contain further subcategories[57]. Lipids found in membranes are amphiphilic molecules with a hydrophilic head group linked to a hydrophobic tail, most commonly glycerophospholipids[58,59].

1.3.1 PHOSPHOINOSITIDES

Phosphatidylinositol (PI) belongs to the group of glycerophospholipids[57]. It is a minor component of cellular membranes making up between 5% and 10% of a cells lipids, although numbers as low as only 1.2% of all phospholipids were reported for human erythrocytes[58–60]. The structure of a dipalmitoyl phosphatidylinositol (PI(16:0/16:0)) as an example of PIs is shown in Figure 3. PI has an inositol ring (myo-inositol) as a hydrophilic head-group that is connected to the hydrophobic diacylglycerol (DAG) via a phosphodiester bond. The exact structure of DAG can vary in terms of fatty acid chain length or degree of saturation[61]. The relative quantity of such PI species can even change as has been shown in macrophages where activation is accompanied by a 300% increase in PI(20:4/20:4)[62]. Another way in which PI can participate in cellular signaling events is as lysophosphatidylinositol (LPI). This is produced by phospholipase A removing one of the fatty acid chains[63]. LPI has been shown to be the ligand for GPR55, a G-protein coupled receptor which is implicated to be involved in various diseases such as cancer and type 2 diabetes[63,64]. LPI can bind GPR55 directly, making it a good example of how lipids provide more than a barrier function[65].

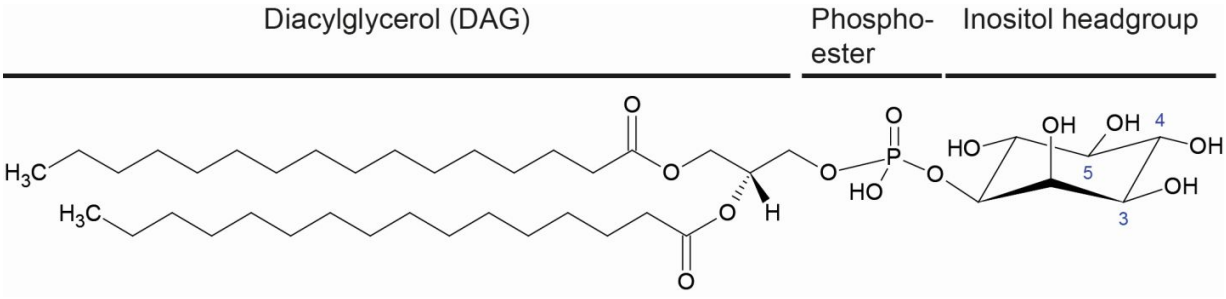

Figure 3: Phosphatidylinositol (PI) schematic. Image depicts dipalmitoyl phosphatidylinositol as an example. Within cells different species of this lipid exist, differing in their side chain lengths and degree of saturation (number of double bonds). PI can be reversibly phosphorylated at the positions 3, 4, and 5 or the inositol ring (blue numbers) giving rise to a total of seven different PI-phosphates (phosphoinositides). Lipid structure was taken from the LIPID MAPS Structure Database (LMGP06010007)[66].

But most of the time when speaking about different PI species it refers to differences in the phosphorylation pattern of the inositol ring. It can be reversibly phosphorylated at positions 3, 4, and 5 which results in a total of seven different phosphatidylinositol phosphate species (PIPs) also known as phosphoinositides: PI(3)P, PI(4)P, PI(5)P, PI(3,4)P_2, PI(3,5)P_2, PI(4,5)P_2, PI(3,4,5)P_3[67]. The seven different phosphoinositides are not all equally abundant. Levels of PI(4,5)P_2 for examples have been reported between 0.3 and 1.5 mol% of total phospholipids in murine BL/VL3 lymphoma cells and human erythrocytes respectively[60,68]. In *Saccharomyces cerevisiae* both PI(4)P and PI(4,5)P_2 have been shown to make up between 1.5 and 2% of total PI each (PI + PIPs)[69]. Levels of PI(3,5)P_2 are ususally lower. In *S. cerevisiae* this lipid was not detectable with a standard chloroform-methanol-HCl extraction. Only when cells were lysed with perchloric acid the recovery improved enough to allow for detection of basal PI(3,5)P_2 levels which are 18 to 28 fold lower than the levels of PI(3)P, PI(4)P, and PI(4,5)P_2[70]. Another publication found that PI(3,5)P_2 made up less than 0.2% of total PI while PI(3)P levels were at approximately 2.5% of total PI[69]. The large span in the reported abundance of phosphoinositides not only stems from the different cell types used, but also from the lipid extraction method, as PI(3,5)P_2 only became detectable once the extraction method was modified[70]. Also it is quite likely that the different detection methods play a role. Often phosphoinositides were labeled with [^{3}H]-inositol, extracted and then separated and phosphoinositide levels analyzed. This could be done by thin layer chromatography (TLC) followed by a phosphate assay or by high-performance liquid chromatography (HPLC) measuring the counts per minute of each peak during elution[68,70]. Alternatively, mass spectrometry is used[71].

Phosphoinositides are not equally distributed within the cell[72]. Due to their differential distribution and because their abundance can change rapidly and transiently upon various stimulations (e.g. osmotic shock, growth factor signaling) they are ideal for defining membrane identity and participating in signaling events[70,73,74]. This is, for the most part, done by interactions of proteins with the headgroup of one or more phosphoinositides. One example of such effectors are the GTPases of the Ras superfamily[72]. As such phosphoinositides play a role in nearly all biological processes and often several phosphoinositide species are involved in these processes. Therefore I will give an overview of different cellular processes and the role phosphoinositides play in them instead of describing each individual phosphoinositide.

1.3.2 PHOSPHOINOSITIDES IN CELLULAR TRAFFICKING PROCESSES

1.3.2.1 Secretory and Recycling Pathway

The secretory pathway allows cells to traffic internal components to the outside, either for secretion, e.g. neurotransmitters and hormones, or to transport trans-membrane proteins to the plasma membrane, e.g. receptors[75]. This pathway starts at the endoplasmic reticulum. From there exocytic cargo is transported to the Golgi apparatus by COP-II vesicles. Secretory cargo is sorted within the Golgi apparatus and secretory vesicles are formed and transported to the plasma membrane[75]. Work, mostly done in yeast, shows that PI(4)P plays important roles in this process[76]. It is formed locally at the ER exit sites (ERES) from which the COP-II vesicles transport cargo to the Golgi. A study showed that PI(4)P is involved in the formation of soluble N-ethylmaleimide-sensitive-factor attachment receptor (SNARE) complexes that mediate the membrane fusion with the Golgi[77]. After the secretory cargo was trafficked through the Golgi, exocytic vesicles form at the trans-Golgi network (TGN) and are transported by myosin V to the plasma membrane. After budding these vesicles are rich in PI(4)P. Together with the GTPase Ypt32 PI(4)P recruits Sec2. Sec2 in turn acts as a guanine nucleotide exchange factor (GEF) for the Rab family GTPase Sec4[76]. During the transport exocyst subunits are recruited to the vesicle. The Sec15 subunit is recruited by interaction with the Sec2/4 complex. This interaction is hindered by PI(4)P and only becomes possible as vesicles gradually lose their PI(4)P content while being transported to the plasma membrane. The removal of PI(4)P requires Osh4. Osh4 is known to exchange PI(4)P with sterols at ER contact sites with the plasma membrane or Golgi apparatus. Therefore it is assumed that Osh4 bridges the exocytic vesicle with the ER membrane, exchanging PI(4)P with sterol using a PI(4)P gradient as an energy source. In mammalian cells the protein OSBP has a similar function as Osh4 in yeast cells. PI(4)P on the ER membrane is then immediately dephosphorylated by Sac1 maintaining the PI(4)P gradient[76]. Finally, more exocyst subunits are recruited and the vesicle is tethered to the plasma membrane. Exocyst subunits Sec3 and Exo70 bind to $PI(4,5)P_2$, which is enriched at the plasma membrane[76].

In line with these observations in the secretory pathway, it was shown that PI(4)P also plays an important role in recycling of endosomal cargo to the plasma membrane[78]. The primary phosphoinositide on early endosomes is PI(3)P. Dephosphorylation of PI(3)P by MTM1 and subsequent phosphorylation by PI4K2α establishes a PI(4)P enriched domain within the endosomal membrane. Interaction of exocyst with PI(4)P as well as PI4K2α allows recycling back to the plasma membrane[78]. The common role for PI(4)P in surface delivery in the

biosynthetic pathway as well as during recycling strengthens the role of phosphoinositides in given membranes a certain identity, in this case defining a portion of the membrane as exocytic.

1.3.2.2 Clathrin Mediated Endocytosis

Clathrin mediated endocytosis (CME) is a process in which cells internalize extracellular cargo and transmembrane proteins. CME starts by adapter proteins, such as the AP-2 complex, being recruited to the plasma membrane. AP-2 localizes to the plasma membrane by binding to $PI(4,5)P_2$ and motifs within the cargo proteins[76]. AP-2 then recruits the phosphatidylinositol 4-phosphate 5-kinase 1γ which further increases the local $PI(4,5)P_2$ levels[79]. Next, clathrin forms what is called a clathrin coated pit and the phosphatase Synaptojanin is recruited, which results in reduced $PI(4,5)P_2$ levels and increased PI(4)P levels[76]. PI(4)P, either generated by the phosphatase or already present at the plasma membrane, is then used as a substrate by class II phosphatidylinositol-3-kinase C2α (PI(3)K C2α) to produce $PI(3,4)P_2$ which is required for the late stages of endocytosis, possibly because as it recruits sorting nexin 9 (SNX9), a BAR protein that helps to promote constriction of the budding vesicle[80]. Finally dynamin is recruited in a $PI(4,5)P_2$ dependent manner mediating scission of the clathrin coated vesicle[81]. Further reduction of $PI(4,5)P_2$ leads to uncoating of the vesicles which continue the transport into the endosomal system. INPP4A/B phosphatases dephosphorylate $PI(3,4)P_2$ enriching the vesicle in PI(3)P, the predominant phosphoinositide on early endosomes[82]. The importance of phosphoinositides for endocytosis was exemplified here by clathrin mediated endocytosis. But other mechanisms of uptake of extracellular matter, such as phagocytosis, macropinocytosis and fast endophilin mediated endocytosis rely on phosphoinositides as well[76].

CME is an excellent example of how different phosphoinositides become important at different stages of a process. It starts with the common phosphoinositide of the plasma membrane, $PI(4,5)P_2$, and through the action of several kinases and phosphatases ends with a vesicle enriched with the phosphoinositide typical for the endosomal system, PI(3)P. It also shows that the changes in phosphoinositide composition are not simple on/off switches but rather finely-tuned gradual changes. While Synaptojanin decreases the $PI(4,5)P_2$ relatively early during CME, the levels remain high enough to help recruiting dynamin to mediate scission at the end of the maturation process. Another noteworthy point is the time scale of these events. The time between initiation to removal of the clathrin coated pit from the plasma membrane is less than one second[83]. The involvement of several phosphoinositides that are converted into one another

in the course of such a process within a relatively short time span nicely shows why phosphoinositides are used as such versatile components in signaling networks.

1.3.2.3 Endosome Maturation

Cells contain several different endosomal compartments, membrane bound organelles that are used in intracellular trafficking, e.g. endocytosis and recycling or biosynthetic delivery of membrane proteins[84]. After endocytosis cargo ends up in the early endosome characterized by the presence of Rab5 and PI(3)P. From there cargo can be recycled or traffic through Rab7 positive late endosomes, enriched in PI(3,5)P_2, to lysosomes for degradation[84,85]. Two models exist how cargo changes from early to late endosomes. Either both are stable organelles and cargo is trafficked by vesicles from early to late endosomes or early endosomes change their identity to late endosomes by replacing Rab5 with Rab7 and increase their PI(3,5)P_2 content. While there is experimental proof for both models, especially the latter is interesting since it involves phosphoinositides[86,87]. In *C. elegans* Rab5 on early endosomes is kept active by the GEF Rabex5. A complex of SAND-1 and CCZ1 can bind and remove Rabex5 thereby deactivating Rab5. Furthermore SAND-1/CCZ1 recruits Rab7 to endosomes and activates it, maybe by supported the VPS/HOPS complex which has been linked to Rab7 activation[86,88,89]. When PI(3)P is removed with the PI3K inhibitor Wortmannin, SAND-1 is not recruited, therefore PI(3)P levels seem to play an important role in the maturation from early to late endosomes. Change from early to late endosomes via Rab conversion has been shown in a mammalian cell line as well, pointing toward a general principle of endosome maturation[90]. A recent publication found that the WDR91 is a Rab7 effector that binds to active Rab7 and Beclin1, a component of the PI(3)P producing VPS34 complex. This inhibits the VPS34 complex, reducing the PI(3)P levels of late endosomes[89]. PI(3)P levels can then be further reduced by MTMR2 dephosphorylation and conversion to PI(3,5)P_2 by PIKfyve[91]. PI(3,5)P_2 has been described to be more prominent on late endosomes and being important for these organelles[85,92,93]. Therefore these experiments showed how early endosome PI(3)P contributes to late endosome maturation which includes a phosphoinositide shift towards PI(3,5)P_2.

1.3.2.4 Autophagy

Macroautophagy is a process in which different stimuli such as starvation or certain cytosolic pathogens induce the formation of double membrane organelles engulfing parts of the cytoplasm. This so-called autophagosome is delivered to the lysosomes for the cargo to be

degraded[94,95]. One of the core components of autophagy is the class III PI3-kinase Vacuolar Protein Sorting 34 (VPS34). This enzyme works in two different complexes[96]. Both share three components: the catalytic subunit VPS34, the regulatory subunit VPS15, and Beclin-1. While complex II is associated with endosomal PI(3)P, complex I contains Atg14 and is involved in autophagy[96]. This class I complex is recruited to ER-mitochondria contact sites by the ULK complex, an inductor of autophagy[97]. PI(3)P is produced at the initiation site of the isolation membrane, which will eventually engulf a part of the cytoplasm, and mediates recruitment of effector proteins. One of the effectors is the protein WIPI which in turn recruits the ATG5-ATG12 complex and ATG16. These proteins promote lipidation and membrane association of LC3 which mediates autophagosome formation[97]. Another PI(3)P effector is the double FYVE-containing protein 1 (DFCP1) that has an ER-binding site as well as PI(3)P binding FYVE domains. This could target it to PI(3)P rich ER domains[76,97].

1.3.3 PHOSPHOINOSITIDES IN EPITHELIAL POLARITY

One important part of epithelial cell polarity not described above was the role of phosphoinositides. In the commonly used model, Madin-Darby canine kidney (MDCK) cells, the most obvious role is the definition of the apical and basolateral plasma membrane domains. $PI(4,5)P_2$ is found more at the apical plasma membrane while $PI(3,4,5)P_3$ defines the basolateral plasma membrane[15,20]. The domains are kept apart by tight-junctions and localized enzymatic activity[76]. If exogenous $PI(3,4,5)P_3$ is added to the apical site of polarized MDCK monolayers it induces the formation of membrane protrusions that have a basolateral characteristic as can be seen by the presence basolateral markers such as p58, syntaxin4, sec8 and the absence of the apical marker Podocalyxin. Also PI3K, the enzyme making $PI(3,4,5)P_3$ re-localized to these protrusions, arguing for a positive feedback loop strengthening the PIP3 signaling. The basolateral proteins found in these protrusions were not delivered via the biosynthetic pathway but relocalized from the basolateral membrane[20]. Class I PI3-kinase p110δ was shown to localize to the basal membrane and inhibition resulted in impaired polarity[98] .This makes it a likely source of basolateral PI(3,4,5)P3, most likely after activation through integrin signaling[99,100]. Similar experiments have been done with the apical membrane which is enriched in $PI(4,5)P_2$ and exogenous $PI(4,5)P_2$ at the basolateral membrane will induce recruitment of apical proteins to the basolateral membrane[15]. This provides another example of how presence of certain phosphoinositides defines membrane identity. In the same way as presence of PI(4)P defines

membrane as exocytic (see above), presence of $PI(3,4,5)P_3$ or $PI(4,5)P_2$ define a membrane as basolateral or apical and intracellular trafficking is directed accordingly.

Furthermore, a role for the $PI(3,4,5)P_3$ specific 3-phosphatase PTEN in polarity and barrier function has been shown in human colorectal cancer cells Caco-2/15, HCT116, and CT26[101]. PTEN is localized at the border between the apical and basolateral domain by interaction with PAR3[102]. This helps to separate both plasma membrane domains as the conversion of $PI(3,4,5)P_3$ to $PI(4,5)P_2$ not only removes the basolateral marker but also accumulates the apical marker. shRNA mediated down regulation of PTEN in Caco-2/15 cells slowed down polarization, reduced the number of apical microvilli, caused disorganized tight junctions and subsequently decreased trans-epithelial electrical resistance (TEER) in Caco-2/15 cells. Loss of PTEN in HCT116 and CT26 cells was shown increase their metastatic potential when they were injected into the tail vein of mice[101].

A recent paper showed the importance of endosomal PI(3)P for epithelial integrity[103]. Loss of the endosomal VPS34 complex, VPS34 complex II, in *Drosophila* resulted in disrupted epithelia as shown by formation of multilayered epithelia, intracellular accumulation of adherence junction proteins and overlap of apical and basolateral marker proteins. This could be reproduced in the human colon carcinoma cell line Caco-2[103]. Inhibition or loss of VPS34 resulted in an increased number of spheroids with multiple lumen. This could be linked to PI(3)P which recruits the protein WDFY2 through interaction with its PI(3)P binding FYVE domain. Other important roles of PI(3)P have been shown in *C. elegans* where early endosome dynamics are involved in keeping PAR proteins polarized or the already mentioned role of endocytosis in regulating Crumbs surface levels[34,104]. Therefore, one can imagine that the initial integrin signaling via PI3K induces the formation of the apico-basal axis in a Rac1-dependent manner and by accumulation of the basolateral marker $PI(3,4,5)P_3$. The induced polarity program will lead PAR3 to the apical pole where it recruits PTEN that, together with kinases, establishes the accumulation of $PI(4,5)P_2$ as a determinant of the apical plasma membrane. Together with the numerous phosphoinositides involved in intracellular trafficking, polarity is established and maintained[72].

1.3.4 PHOSPHOINOSITIDES IN IMMUNITY

Phosphoinositides have also been linked to the immune response. One interesting example is TLR4 signaling that can occur either from the plasma membrane or endosomes resulting primarily in inflammatory cytokine or interferon production respectively[42]. It was shown that the sorting adaptor TIRAP has a $PI(4,5)P_2$ binding domain required for its plasma membrane localization and its subsequent recruitment of the signaling adaptor MyD88[105]. If the $PI(4,5)P_2$ binding domain was removed or replaced with a domain binding PI(3)P, PI(4)P, or $PI(3,4,5)P_3$ LPS signaling was abrogated. Next, TLR4 is taken up by the cell to signal in an TRIF/TRAM dependent manner[106]. It was published that IP_3 production by phospholipase Cγ-2 (PLCγ-2) cleavage of $PI(4,5)P_2$ as well as $PI(3,4,5)P_3$ production by the class I PI3K p110δ are important in TLR4 endocytosis and subsequent TRIF/TRAM signaling[107,108]. It is tempting to speculate that the outcome of TLR4 signaling does not only depend on the receptor's localization but also on membrane phosphoinositide composition. And while the role of phosphoinositides in TRAM/TRIF signaling are not yet clear, it has been shown that another adaptor, WD repeat and FYVE-domain containing protein 1 (WDFY1, FENS-1), mediates TLR3 and TLR4 signaling by recruiting TRIF[109]. WDFY1 function depends on the presence of its PI(3)P binding FYVE domain[109,110]. Therefore WDFY1 links the endosomal phosphoinositide composition to the outcome of TLR4 signaling. The mechanism described above is most likely not complete. When TIRAP's requirement for PI(4,5)P2 was described, it was speculated that loss of PI(4,5)P2 results in dissociation of TIRAP/MyD88 which allows TRIF/TRAM to take over. The same group later found that TIRAP can actually signal from endosomes[111]. This was attributed to its ability to bind phosphoinositides besides $PI(4,5)P_2$. While a $PI(4,5)P_2$ specific TIRAP would allow TLR4 but not TLR9 signaling, a PI(3)P- or phosphatidylserine-specific mutant could be used for TLR9 signaling[111].

Compartment-specific signaling has also been shown for TLR9 where the outcome, proinflammatory cytokines or type I interferon, depends on the endosome[112]. When TLR9 is in $VAMP3^+$ endosomes it induces NF-κB dependent production of proinflammatory cytokines. When TLR9 is trafficked into $LAMP2^+$ lysosome-related organelles (LROs), IRF7 mediated signaling will result in type I interferons. This AP-3 mediated trafficking depends on the PI(3)P 5-kinase PIKfyve which as previously been shown to be involved in maturation of CpG containing endosomes[92]. It also fits well with the requirement for AP-3, as it was reported that

AP-3 can bind PI(3,5)P_2[113]. And while PIKfyve inhibitor treatment could not be counteracted by addition of exogenous PI(5)P or PI(3,5)P_2, this could simply due to the short half-life such lipids have[20].

1.4 Aims of Phosphoinositide Project

Over the last decades, our understanding of the importance of phosphoinositides in many cellular processes has drastically increased. It was shown that phosphoinositides are involved in establishing polarity, either by directly defining the apical and basal pole or by participating in polarized trafficking processes. Also a role for phosphoinositides in the innate immune response in general as well as in polarized cells has been shown. In our lab, we are interested in immunity in the human intestine. Unfortunately most work regarding phosphoinositides and polarity or immunity has not been done in intestinal epithelial cells. In most cases either very different organisms such as *Drosophila* and *C. elegans* or cells from unrelated tissues such as MDCK cells are used. Both polarity and immunity are of paramount importance in this system. Only polarized IECs can form a tight epithelium that serves as a physical barrier. Also the epithelium is in constant contact with a staggering number of microorganisms that have to be tolerated. A phenotype in which not only immune regulation plays a role but also the polarized state of cells. This tight interplay between polarity and immunity make the intestinal epithelium a highly interesting model to investigate both. Therefore the goal of this project is to investigate the role of endosomal PI(3)P on intestinal epithelial cell polarity and immunity and establish the tools necessary to do so.

1.5 INTRODUCTION TO THE BACMAM PROJECT

1.5.1 BACULOVIRUSES

Baculoviruses are insect-specific viruses with large (80-180 kb), circular, double stranded DNA genomes[114]. These viruses have long since been used for various applications such as pest control or for expression of recombinant proteins in biotechnology[115]. Among the different Baculovirus species, the *Autographa californica* multiple nucleopolyhedrovirus (AcMNPV) is the one most commonly used in biotechnology and normally only infect hosts of the *Lepidoptera* order[114]. AcMNPV can be engineered to encode mammalian proteins which can then be produced by insect cells[114,115]. Insect cells such as Sf9 can grow in suspension culture, therefore it is possible to produce very large quantities of proteins and scale up production. While large scale production of recombinant proteins can technically be done in bacteria cells as well, insect cells offer the advantage of a eukaryotic system for posttranslational modifications[114]. While it is not exactly the same as the mammalian system, it is still close enough to produce proteins for application in humans, e.g. the human papillomavirus vaccine Cervarix (Glaxo-SmithKline)[116]. Additionally they are an advantageous system because of the absence of human pathogens in Lepidoptera cell lines and they can grow without serum[114].

With all the advantages of baculoviruses, e.g. large capacity, no replication or integration in mammalian cells, low cytotoxicity, easy production of large quantities with high titers, these viruses unfortunately were not usable as vectors to transduce mammalian cells as there promoters are only active in insect cells[117,118]. In 1996, this changed when the genome of AcMNPV was modified to include a mammalian expression casstte[119]. Now these viral vectors could be used to deliver large cargo into mammalian cells and have been used for a variety of applications. Examples include the expression of shRNAs, tagging HMGA1 by inserting GFP its locus in 293T cells by simultaneously encoding the GFP homology construct, Cas9 and two guide RNAs, and reprogramming MEFs into a neuronal phenotype by using one Baculovirus expressing three factors instead of three lentiviral vectors[120,121].

While this system offers many advantages and has been used for numerous different applications, some uses are hindered because the viral genome remains episomal and expression is lost within two to three weeks (Figure 24 B)[122]. To achieve long lasting expression several different methods were tested. Expression of the Epstein-Barr virus protein EBNA1 and inclusion

of the oriP sequence extended the expression for 35 days[123]. A second method used adeno-associated virus (AAV) inverted terminal repeats (ITRs) and the AAV rep gene in human embryonic stem cells which allowed for the mechanical selection of GFP positive cells during passaging[123,124]. A third method is through integration using the sleeping beauty (SB) transposon. This method was successfully used to achieve prolonged shRNA expression in HEK 293T cells and synoviocytes, GFP expression in HepG2 cells and murine eyes *in vivo*, and GFP expression in HEK293T cells[120,122,123].

1.5.2 Scaffold / Matrix Attachment Region

While the above mentioned methods to prolong maintenance of expression do work, they do raise questions about the biosafety. Normal baculovirus vectors can be handled under S1 biosafety conditions. The vectors described above either rely on integration into the host cell genome (SB transposon or AAV ITRs) or require the expression of a viral gene, EBNA1, that has been associated with the development of B cell neoplasia in mice and induction of epithelial-to mesenchymal transition (EMT) in nasopharyngeal cancer cells, a process linked to metastasis[125,126]. Therefore we decided to try another method of creating a persistent BacMam vector utilizing a scaffold / matrix attachment region (S/MAR). S/MAR regions were first described in 1984 as being involved in organization of chromatin loops[127]. Numerous functions have been assigned to these sequences. It is believed that by interacting with the nuclear matrix, they form loop structures in which active transcription can take place and where they insulate the gene from negative regulators of transcription on the surrounding chromatin[128]. The S/MAR regions have been described as regulating gene expression and enhancing expression. In 1999 it was published that vectors in which the gene encoding the SV40 large T-antigen was replaced with the S/MAR region from the human interferon β gene are stably maintained in CHO cells at low copy numbers without integration, something that since has been shown for other cell lines as well[129–132]. Such vectors can also be used for *in-vivo* applications. When naked plasmid DNA containing S/MAR sequences were injected into mice or rats it resulted in transgene expression for several months[133,134]. As it was shown that S/MAR regions that do not belong to a gene are not anchored to the matrix, active transcription is required for the S/MAR region to work[128]. This was further verified by comparing integration and episomal maintenance of vectors expressing GFP followed by the S/MAR sequence with plasmids lacking the promoter or having the polyadenylation site between GFP and S/MAR. Only vectors in which active transcription that

included the S/MAR region took place were episomally maintained[135]. The S/MAR region can then interact with the nuclear matrix protein SAF-A which explains how the plasmid is anchored[136]. It was shown that typical proteins of the pre-replication complexes are found on episomal S/MAR plasmids which are replicated once per cell cycle early in the S-Phase[137]. Establishment of anchored plasmids that are stably maintained is not an efficient process though, only 1-5% of transfected CHO cells were able to stably maintain an S/MAR plasmid. But once it is established the plasmid is maintained without selection pressure[138]. Also the S/MAR region seems to prevent integration of the plasmid as a vector with S/MAR is maintained episomally in CHO or HeLa cells while the same vector without S/MAR integrates[129,137]. S/MAR also positively influences the transgene's expression. It was shown that S/MAR containing episomes are found in nuclear compartments associated with active transcription and that the CMV promoter on S/MAR episomes is not epigenetically silenced by cytosine methylation while the same plasmid linearized, so that the S/MAR region is removed, integrates into the genome and the CMV promoter is methylated[138,139].

1.6 Aims of BacMam Project

We want to improve the BacMam system already established in our lab by adding an S/MAR sequence, combining the advantages of both systems: the easily produced viral vector with large cargo capacity and a DNA sequence allowing plasmids to be episomally maintained for months. Such a vector can be a tremendous asset for the lab. To modify our model cell line, T84 cells, we have to stably transduce them with lentiviral vectors. BacMam could provide a safer alternative usable in biosafety level 1 environments. Also some constructs used in our lab are close the maximum cargo capacity of lentiviral vectors and if cells have to express several transgenes, we have to go through several rounds of transduction and selection. Making T84 cell lines takes a long time as cells have to be transduced after being seeded very sparse and they grow very slow. Having a vector that can express multiple proteins at the same time would save time due to a single round of transduction. Also such a vector can be modified to deliver large reporters of the immune response which can be interesting for the lab and the immunity part of the phosphoinositide project.

2 MATERIALS AND METHODS

2.1 MATERIALS

2.1.1 BACTERIA AND MAMMALIAN CELLS

Table 1: List of bacteria.

Name	Reference	Description
DH5α	Invitrogen 18265017	Subcloning efficiency bacteria used in routine cloning.
NEB® 5-alpha Competent E. coli (High Efficiency)	New England Biolabs C2987H	Part of NEBuilder Hifi Assembly kit, in some cases also used as an alternative to normal DH5α if higher efficiency was necessary.
DH10Bac	Invitrogen 10361012	MAX Efficiency® DH10Bac™ Competent Cells used to produce recombinant bacmids.
ccdB Survival™ 2	Invitrogen A10460	Cells resistant to the ccdB kill gene used in Gateway cloning. Used to propagate empty Gateway entry- or destination plasmids.

Table 2: List of eukaryotic cells.

Name	Reference	Description
T84	ATCC ATTC-CCL-248	Human colon carcinoma cell line. Maintained in collagen (from rat tail) coated flasks in DMEM/F12 with 10% FBS, 100 U/ml penicillin, and 100µg/ml streptomycin.
HEK-293T	ATCC ATCC CRL-3216	Human embryonic kidney cell line used to produce lentiviral vectors and for standard transfection / transduction tests. Maintained in IMDM with 10% FBS, 100 U/ml penicillin, and 100µg/ml streptomycin.
HeLa Kyoto	Gift from Department of Infectious Diseases, Virology, University Hospital Heidelberg	Human cervical cancer cell line that is easy to transfect and is routinely used as a model system to test outcome of changes in PIP levels introduced by the chemical dimerization system. Maintained in DMEM with 10% FBS, 100 U/ml penicillin, and 100µg/ml streptomycin.

A549	Gift from Department of Infectious Diseases, Molecular Virology, University Hospital Heidelberg	Human lung epithelial cells. Maintained in DMEM with 10% FBS, 100 U/ml penicillin, and 100µg/ml streptomycin.
L929	Terence S. Dermody, Department of Pediatrics at the University of Pittsburgh School of Medicine	Murine fibroblast cell line. After thawing grown as adherent culture in DMEM with 10% FBS, 100 U/ml penicillin, and 100µg/ml streptomycin at 37 °C with 5% CO_2. Then transferred to suspension culture in MEM Eagle (Joklik Modification) with 2 g/L $NaHCO_3$, 2 mM L-Glutamine, 5% (v/v) FBS, 5% (v/v) newborn calf serum. Suspension cultures are grown at 35 °C without CO_2 in spinner flasks at 140 rpm.
Sf9 (SFM adapted)	Gibco 11496-015	Insect cell line (from *Spodoptera frugiperda*) maintained in suspension culture in SF-900 III SFM (1x) medium without serum or antibiotics. Cells were grown at 27 °C without CO_2 at 110 rpm.

2.1.2 Cell culture Media and supplements

Table 3: List of cell culture media and supplements.

Name	Reference
DMEM/F12	Gibco 31330-038
DMEM	Gibco 41965-039
IMDM	Gibco 21980-032
F12 Ham	Gibco 21765-029
MEM Eagle (Joklik Modification)	Sigma, M0518-10X1L
OptiMEM I Reduced Serum Medium	Gibco 31985-062

Sf-900 III SFM (1x)	Gibco 12658-019
Grace's Insect Medium (unsupplemented)	Gibco 11595-030
FBS	Biochrom GmbH S 0615
NBCS	Gibco 26010-074
Pen/Strep (10,000 U/ml penicillin + 10,000 µg/ml Streptomycin)	Gibco 15140-122
0.05% Trypsin-EDTA	Gibco 25300-054
0.25% Trypsin-EDTA	Gibco 25200-056
Puromycin dihydrochloride	Sigma-Aldrich P9620-10ml
Geneticin (G418 Sulfate)	Gibco 10131027
Blasticidin S HCl	Gibco R210-01

2.1.3 ANTIBODIES

Table 4: Primary antibodies.

Antibody	Reference	Raised in	Dilution IF	Dilution Western blot
α-beta-actin	Sigma-Aldrich A5441	Mouse	-	1:5,000
α-VPS34 (D9A5)	Cell Signaling #4263	Rabbit	-	1:1,000
α-MTM1	Volker Haucke, Leibniz Institut für Molekulare Pharmakologie	Rabbit	-	1:250

α-GFP	Abcam ab6556	Rabbit	1:500	-
α-μNS	Steeve Boulant	Guinea Pig	1:5,000	1:5,000
α-PI(3)P	Echelon Biosciences Inc. Z-P003	Mouse	1:200	-

Table 5: Secondary antibodies.

Antibody	Reference	Raised in	Dilution IF	Dilution Western blot
α-rabbit-IgG HRP	GE Healthcare NA934	Donkey	-	1:5,000
α-mouse-IgG HRP	GE Healthcare NA931	Sheep	-	1:5,000
α-mouse IgG-488	Molecular Probes A11001	Goat	1:1,000	-
α-mouse IgG-568	Molecular Probes A11004	Goat	1:1,000	-
α-mouse IgG-647	Molecular Probes A21235	Goat	1:1,000	-
α-rabbit IgG-488	Molecular Probes A11008	Goat	1:1,000	-
α-rabbit IgG-568	Molecular Probes A11011	Goat	1:1,000	-
α-rabbit IgG-647	Molecular Probes A21244	Goat	1:1,000	-
α-mouse-IgG-IRDye 680RD	LI-COR 925-68070	Goat	1:10,000 – 1:20,000	-
α-mouse-IgG-IRDye 800CW	LI-COR 926-32210	Goat	1:10,000 – 1:20,000	-
α-guinea pig-IgG-IRDye 800CW	LI-COR 925-32411	Donkey	1:10,000 – 1:20,000	-

2.1.4 OLIGONUCLEOTIDES

Table 6: shRNA oligonucleotides. Targeting sequence is underlined**.**

Name	Sequence (5' to 3')
shMTM1 #1 fwd	CCGGGCATTGAAGGGTTCGAAATACCTCGAGGTATTTCGAACCCTTCAATGCTTTTTG
shMTM1 #1 rev	AATTCAAAAAGCATTGAAGGGTTCGAAATACCTCGAGGTATTTCGAACCCTTCAATGC
shMTM1 #2 fwd	CCGGGATGCAAGACCCAGCGTAACTCGAGTTACGCTGGGTCTTGCATCTTTTTG
shMTM1 #2 rev	AATTCAAAAAGATGCAAGACCCAGCGTAACTCGAGTTACGCTGGGTCTTGCATC
shScrambled for	CCGGCAACAAGATGAAGAGCACCAACTCGAGTTGGTGCTCTTCATCTTGTTGTTTTTG
shScrambled rev	AATTCAAAAACAACAAGATGAAGAGCACCAACTCGAGTTGGTGCTCTTCATCTTGTTG
shVPS34 #1 for	CCGGGAGGCAAATATCCAGTTATATCTCGAGATATAACTGGATATTTGCCTCTTTTTG
shVPS34 #1 rev	AATTCAAAAAGAGGCAAATATCCAGTTATATCTCGAGATATAACTGGATATTTGCCTC
shVPS34 #2 for	CCGGCCACGAGAGATCAGTTAAATACTCGAGTATTTAACTGATCTCTCGTGGTTTTTG
shVPS34 #2 rev	AATTCAAAAACCACGAGAGATCAGTTAAATACTCGAGTATTTAACTGATCTCTCGTGG
shVPS34 #3 for	CCGGCCCATGAGATGTACTTGAACGTAATCTCGAGATTACGTTCAAGTACATCTCATGGGTTTTTG
shVPS34 #3 rev	AATTCAAAAACCCATGAGATGTACTTGAACGTAATCTCGAGATTACGTTCAAGTACATCTCATGGG

Table 7: Sequencing primers.

Name	Sequence (5' to 3')
Blasticidin-rev	GCTCTTTCAATGAGGGTGGA
ccdB-F	CACCGCGAAAATGAC
M13-FP	TGTAAAACGACGGCCAGT

M13-RP	CAGGAAACAGCTATGACC
Puro-F	GAGGTGCCCGAAGG
Puro-R	GTTCTTGCAGCTCGG
U6	AGATATTAGTACAAAATACG
Gent-F	TACAAAGTTGGGCATACG
Gent-R	CGTAACATCGTTGCTGC
Polyhedrin-F	CTTATTTATTTGCGAGATGG
Polyhedrin-R	ATTCCGGATTATTCATACC
Amp-F	GGCAACTATGGATGAACG
Amp-R	TTTCACCAGCGTTTCTG
pBR322-F	GCAAGCAGCAGATTACG
pBR322-R	TGTGATGCTCGTCAGG

Table 8: qRT-PCR primers.

Name	Efficiency (%)	Sequence (5' to 3')
HPRT1-fwd	102	CCTGGCGTCGTGATTAGTGAT
HPRT1-rev		AGACGTTCAGTCCTGTCCATAA
IFNβ1-fwd	110.7	GCCGCATTGACCATCTAT
IFNβ1-rev		GTCTCATTCCAGCCAGTG
IFNλ-fwd	110.6	GCCACATAGCCCAGTTCAAG
IFNλ-rev		TGGGAGAGGATATGGTGCAG
IL-8-fwd	98.7	GAGAGTGATTGAGAGTGGACCAC
IL-8-rev		CACAACCCTCTGCACCCAGTTT
β-actin-fwd	99.3	CATGTACGTTGCTATCCAGGC
β-actin-rev		CTCCTTAATGTCACGCACGAT

Table 9: Cloning primers.

Name	Sequence (5' to 3')	Description
hMTM1-C375S-F	CAGTGCTTGTGCATTCCAGTGACGGATGGG	Primers for site directed mutagenesis inducing phosphatase-dead mutation in hMTM1.
hMTM1-C375S-R	CCCATCCGTCACTGGAATGCACAAGCACTG	

pCMV-DEST-R	TACCACTTTGTACAAGAAAGC	Primers to amplify the BacMam pCMV-DEST backbone to insert PuroR-S/SMAR with NEBuilder HiFi Assembly.
pCMV-DEST-F	AATCAGCCATACCACATTTG	
P2A-puro-SMAR-F	CTTTCTTGTACAAAGTGGTATCTGGCAGCGG CGCCACC	Primers to amplify the P2A-puro-S/MAR sequence from pMAX-SMAR-GFP-P2A-Puro to create a BacMam backbone with puromycin resistance.
P2A-puro-SMAR-R	CAAATGTGGTATGGCTGATTACCGTCGACTG CAGAATTCTATCAAATATTTAAAGAAAAAAA AATTG	

2.1.5 PLASMIDS

Table 10: Plasmids used or created in this thesis.

Name	Description
BacMam pCMV-Dest	Gateway destination vector for Baculovirus production. Can be transformed into DH10Bac to create recombinant bacmids via transposition. Source: Invitrogen, A24223
pWPI-puro-rfB	Lentiviral Gateway destination plasmid expressing puromycin resistance gene from an IRES. Source: University of Heidelberg Department of Infectious Diseases Molecular Virology
pWPI-neo-rfB	Lentiviral Gateway destination plasmid expressing neomycin resistance gene from an IRES. Source: University of Heidelberg Department of Infectious Diseases Molecular Virology
pWPI-blr-rfB	Lentiviral Gateway destination plasmid expressing blasticidin resistance gene from an IRES. Source: University of Heidelberg Department of Infectious Diseases Molecular Virology
pLKO.1	Lentiviral expression plasmid for shRNAs using a U6 promoter. shRNAs are cloned via AgeI and EcoRI restriction sites. Can be selected with puromycin. Source: The RNAi Consortium[140]

pMD.2G	Second generation lentiviral envelope plasmid expressing VSV-G. Source: pMD2.G was a gift from Didier Trono (Addgene plasmid # 12259)
psPAX2	Second generation lentiviral helper plasmid. Source: psPAX2 was a gift from Didier Trono (Addgene plasmid # 12260)
pDONR221	Gateway donor plasmid with kanamycin resistance. Used to create entry clones. Source: Invitrogen, 12535-019
BacMam pCMV-DEST-puro-SMAR	Gateway destination vector for production of recombinant bacmids. Based on BacMam pCMV-Dest with addition of puromycin resistance gene and S/MAR region allowing episomal maintenance.
BacMam pCMV-DEST-neo-SMAR	Gateway destination vector for production of recombinant bacmids. Based on BacMam pCMV-Dest with addition of geneticin resistance gene and S/MAR region allowing episomal maintenance.
BacMam pCMV-DEST-blr-SMAR	Gateway destination vector for production of recombinant bacmids. Based on BacMam pCMV-Dest with addition of blasticidin resistance gene and S/MAR region allowing episomal maintenance.
pMAX-SMAR-GFP-P2A-Puro	Plasmid expressing coGFP followed by a 'self-cleaving' P2A sequence from porcine teschovirus-1 polyprotein and the puromycin resistance gene. S/MAR sequence allows episomal maintenance. Source: Richard Harbottle, German Cancer Research Centre (DKFZ)
pmCherry-C1	Used to amplify mCherry to construct pCMV-mCherry-puro-reporter. Source: Clontech, 632524
BacMam pCMV-mCherry-puro-reporter	Gateway destination vector for production of recombinant bacmids. Based on BacMam pCMV-DEST-puro-SMAR. The gateway cloning cassette was replaced with constitutively expressed mCherry. A new Gateway cloning cassette was to insert to allow cloning of a promoter with reporter gene.
pWPI-Puro-FRB*-GFP-Rab5	Lentiviral expression plasmid with the GFP-tagged Rab5 anchor for the chemical dimerization system.

pWPI-Puro-FRB*-CFP-Rab5	Identical to pWPI-Puro-FRB*-GFP-Rab5 except CFP is used as a fluorescent marker.
pWPI-Blr-mRFP-FKBP-hMTM1	Lentiviral expression plasmid with the mRFP-tagged recruitable MTM1 wildtype enzyme for the chemical dimerization system.
pWPI-Blr-mRFP-FKBP-hMTM1-C375S	Lentiviral expression plasmid with the mRFP-tagged recruitable MTM1 C375S mutant enzyme for the chemical dimerization system.
pWPI-Blr-GFP-2xFYVE	Lentiviral expression plasmid for GFP-coupled tandem FYVE domains from Hrs. Used as a PI(3)P sensor.

2.1.6 CHEMICALS AND ENZYMES

Table 11: List of chemicals.

1 kb Plus DNA Ladder	Invitrogen, 10787-018
2-butanol	Roth, KK02.2
2-propanol	Roth, T910.1
30% Acrylamide/Bis-acrylamide solution (37.5:1)	Roth, 3029.1
Agarose	Roth, 3810.2
Albumin standard	Thermo Scientific, 23210
Ammonium chloride	Sigma, A9434
Ampicillin (sodium salt)	Roth, K029.2
APS	Roth, 9592.2
Boric acid	Roth, 6943.1
Bromophenol blue	AppliChem, A2331,0005
BSA	New England Biolabs, B9001S
Cesium chloride	Sigma-Aldrich, C3139
CFC-113 (1,1,2-Trichloro-1,2,2-trifluoroethane)	Sigma-Aldrich, 34874
Collagen (from rat tail)	Sigma-Aldrich, C7661
Complete protease inhibitor cocktail EDTA-free	Roche, 04693159001
CutSmart buffer	New England Biolabs, B7204S
D-(+)-Glucose	Sigma-Aldrich, G5767
DAPI	Sigma, D9542
DC Protein Assay Kit II	Bio-Rad, 5000112
Deoxycholate (sodium salt)	Sigma-Aldrich, D6750
ECL Western Blotting Reagents	GE Healthcare, RPN2106

EDTA (disodium salt dihydrate)	Sigma, E5134
ELISA kit: DIY Human IFN Lambda 2/3 (IL-28A/B)	pbl assay science, 61830
ELISA kit: Human IL-6 ELISA MAX Standard Set	BioLegend, 430502
ELISA kit: Human IL-8 ELISA MAX Standard Set	BioLegend, 431502
Ethanol	Sigma-Aldrich, 32205
Ethidium bromide	MPBio, ETBC1001
Gateway® BP Clonase II Enzyme mix	Invitrogen, 11789020
Gateway® LR Clonase® II Enzyme mix	Invitrogen, 11791020
GFP-FYVE (Hrs), purified protein	Gift from Volker Haucke, FMP Berlin
Glycerol	Roth, 7530.1
Glycine	Gerbu , #1023
HBSS (with calcium, with magnesium, without phenol red)	Sigma, 55037C-1000ML
IPTG	Sigma-Aldrich, I6758
iScript cDNA Synthesis Kit	Bio-Rad, 170-8891
LB	Roth, X968.2
LB-Agar	Roth, X969.2
L-Glutamic acid	Sigma, G1251
Lipofectamine 2000	Invitrogen, 11668-019
Methanol	Sigma-Aldrich, 32213
NEBuilder HiFi DNA Assembly Cloning Kit	New England Biolabs, E5520S
Nonfat dried milk powder	AppliChem, A0830
Odyssey® Blocking Buffer (TBS)	Li-Cor, 927-50000
pH-indicator stripes, pH 5.0 – 10.0	Merck, 1.09533.0001
Phosphate buffered saline (PBS)	Sigma, P4417
PhosphoSTOP phosphatase inhibitor cocktail	Roche, 04906837001
Phusion Hot Start II DNA Polymerase	Thermo Scientific, F549S
Poly(I:C) high molecular weight (HMW)	Invivogen, tlrl-pic
Poly(I:C) low molecular weight (LMW)	Invivogen, tlrl-picw
Polybrene (Hexadimethrine bromide)	Sigma-Aldrich, 107689-10G
Polyethylenimine, branched (PEI)	Sigma-Aldrich, 408727
Potassium acetate	Roth, HN10.3
Precision Plus Protein Dual Color	Bio-Rad, 1610374
ProLong Gold Antifade Mountant with DAPI	Molecular Probes, P36935
ProLong Gold Antifade Mountant with DAPI	Molecular Probes, P36934

Rapalog (A/C Heterodimerizer, AP21967)	TaKaRa, 635057
Restriction enzymes	New England Biosciences
RNase A	Qiagen, 19101
SAR405	BioVision, B1286-5,25
Slide-A-Lyzer Dialysis Cassette, 20,000 MWCO	Thermo Scientific, 66003
SOB medium powder	Roth, AE27.1
Sodium bicarbonate ($NaHCO_3$)	Sigma, S5761
Sodium chloride	Roth, HN00.2
Sodium deoxycholate	Sigma-Aldrich, D6750
Sodium dodecyl sulfate (SDS)	Roth, 2326.2
Sodium hydroxide	Roth, 9356.1
Stready-Glo Luciferase Assay System	Promega, E2510
SuperSignal West Femto Chemiluminescent Substrate	Thermo Scientific, 34095
T4 DNA ligase	New England Biolabs, M0202
TEMED	Roth, 2367.1
Tetracycline hydrochloride	Sigma-Aldrich, T7660-5G
Tris base	Roth, 5429.3
Triton X-100	G-Biosciences, 786-513
TurboFect	Thermo Scientific, R0531
Tween 20	MP Biomedicals, TWEEN201
VPS34-IN1	Cayman Chemical, 17392
WesternBright Chemiluminiszenz Substrat Sirius	Biozym, 541021
X-Gal	Sigma-Aldrich, B4252
β- mercaptoethanol / 2-mercaptoethanol	Sigma-Aldrich, M6250

2.1.7 BUFFERS AND SOLUTIONS

0.5x TBE	
Tris base	50 mM
Boric acid	50 mM
EDTA	1 mM

Blocking solution (western blot)	
Nonfat dried milk powder	5% (w/v)
(Tris buffered saline with Tween) TBS-T	1x

Blotting buffer	
Tris base	25 mM
Glycine	190 mM

Laemmli buffer (4x)	
Tris base, pH 6.8	200 mM
SDS	8%
Glycerol	40% (v/v)
β- mercaptoethanol	4% (v/v)
EDTA, pH 8	50 mM
Bromophenol blue	0.08% (w/v)

Resuspension buffer	
Tris base, pH 7.5	50 mM
EDTA	10 mM
RNase A	100 µg/mL

Lysis buffer	
Sodium hydroxide	0.2 M
SDS	1% (w/v)

Neutralization buffer	
Potassium acetate, pH 4.8	1.32 M

TBS-T (pH 7.6)	
Tris base	20 mM
Sodium chloride	137 mM
Tween 20	0.1% (v/v)

RIPA buffer	
Sodium chloride	150 mM
Triton X-100	1% (v/v)
Sodium deoxycholate	0.5% (w/v)
SDS	0.1% (w/v)
Tris base, pH 8.0	50 mM
PhosphoSTOP phosphatase inhibitor cocktail	1 tablet per 10 mL
Complete protease inhibitor cocktail	1 tablet per 10 mL

SDS-PAA running gel buffer (4x)	
Tris base, pH 8.8	1.5 M
SDS	0.4% (w/v)

SDS-PAA stacking gel buffer (4x)	
Tris base, pH 8.8	0.5 M
SDS	0.4% (w/v)

SDS-PAGE running buffer	
Tris-base	25 mM
Glycine	190 mM
SDS	0.1% (w/v)

SDS-PAGE running gel (two 1.5 mm thick gels)	**12%**	**10%**
Acrylamide/Bis-acrylamide solution (30%)	7.2 mL	6 mL
Water	6.3 mL	7.5 mL
Running gel buffer	4.5 mL	4.5 mL
APS (10% w/v)	150 µL	150 µL
TEMED	30 µL	30 µL

SDS-PAGE stacking gel (two 1.5 mm thick gels)	**5%**
Acrylamide/Bis-acrylamide solution (30%)	1 mL
Water	3.5 mL
Stacking gel buffer	1.5 mL
APS (10% w/v)	50 µL
TEMED	10 µL

SOC medium	
SOB-medium powder	2.66% (w/v)
D-(+)-Glucose	20 mM
TBS (pH 7.6)	
Tris base	20 mM
Sodium chloride	137 mM

Virus buffer	
Sodium chloride	150 mM
Tris base, pH 7.4	10 mM
Magnesium chloride	10 mM

Bacmid isolation solution I (filter-sterilize; store at 4 °C)	
Tris-HCl	15 mM
EDTA pH 8	10 mM
RNase A	100 µg/ml

Bacmid isolation solution II (filter-sterilize)	
NaOH	0.2 N
SDS	1% (w/v)

DNA loading dye (6x)	
Glycerol	60% (v/v)
Tris pH 7.5	10 mM
EDTA pH8	60 mM
Bromphenol blue	0.03% (w/v)

LB- ampicillin	
LB powder (Roth, X968.2)	25g
H_2O	1 L
Ampicillin (100 mg/ml)	1 ml

LB-agar-ampicillin	
LB agar powder (Roth, X969.2)	10 g
H_2O	250 ml
Ampicillin (100 mg/ml)	250 µl
Add ampicillin when LB-agar cooled down and pour plates of 25 ml each.	

LB-kanamycin	
LB powder (Roth, X968.2)	25g
H_2O	1 L
Kanamycin (50 mg/ml)	1 ml

LB-agar-kanamycin	
LB agar powder (Roth, X969.2)	10 g
H_2O	250 ml
Kanamycin (50 mg/ml)	250 µl
Add ampicillin when LB-agar cooled down and pour plates of 25 ml each.	

LB for DH10Bac selection	
LB powder (Roth, X968.2)	25g
H_2O	1 L
Kanamycin (50 mg/ml)	1 ml
Gentamycin (50 mg/ml)	140 µl
Tetracycline (10 mg/ml)	1 ml

LB-agar plates for DH10Bac selection	
LB powder (Roth, X969.2)	10g
H_2O	250 ml
Kanamycin (50 mg/ml)	250 µl
Gentamycin (50 mg/ml)	35 µl
Tetracycline (10 mg/ml)	250 µl
X-Gal (100 mg/ml)	200 µl
IPTG (238 mg/ml)	42 µl
Add all chemicals when LB-agar cooled down and pour plates of 25 ml each.	

HO buffer	
Tris base, pH 7.4	10 mM
NaCl	250 mM
2-mercaptoethanol	10 mM
Filter sterilize (0.2 µM membrane) and stored at 4 °C	

Dialysis buffer	
Tris base, pH 7.4	10 mM
NaCl	150 mM
$MgCl_2$	20 mM

Stripping buffer	
HCl	0.1 M
2-mercaptoethanol	0.1 M
Buffer A	
Pipes, pH 6.8	20 mM
NaCl	137 mM
KCl	2.7 mM

TE	
Tris-HCl, pH 8	10 mM
EDTA, pH 8	1 mM

2.2 METHODS

2.2.1 DNA ISOLATION

Plasmid DNA after cloning was extracted without the use of a commercial kit. All steps are carried out at room temperature. Bacteria were pelleted at 11,000 rcf for 1 minute and the pellet resuspended in 200 µl resuspension buffer. After addition of 200 µl lysis buffer samples were incubated for 3 minutes before 200 µl neutralization buffer was added. Samples were centrifuged 10 minutes at 11,000 rcf and the supernatant transferred into a new tube containing 600 µl 2-propanol. After thoroughly mixing samples they were centrifuged for 10 minutes at 11,000 rcf. Supernatant was removed and pellets washed with 300 µl 70% EtOH (v/v), centrifuged at 11,000 rcf for 5 minutes and pellets dried before resuspension in 30 µl H_2O or TE buffer. Other plasmid preparations were done using commercial kits according to the manufacturer's instructions. Macherey-Nagel NucleoSpin® Plasmid (740588.250) for small scale purifications of 1-2 ml, Macherey-Nagel NucleoBond® PC 100 (740573.100) for 20-100 ml and Qiagen Plasmid Maxi prep (12163) for 100-200 ml of bacterial culture.

2.2.2 DNA PURIFICATION

Gel extraction of DNA bands and purification of PCR reactions and restriction digests were done with the Macherey-Nagel NucleoSpin® Gel and PCR Clean-up kit (740609.250) according to manufacturer's instructions. Volume of elution buffer was between 20 and 40 µl (depending on amount of input DNA).

2.2.3 AGAROSE GEL ELECTROPHORESIS

Agarose was dissolved in 0.5% TBE. 0.8% (w/v) agarose was used except for quality control of qRT-PCR primers for which a 2% (w/v) gel was used to verify single bands. Gels were cast with the Bio-Rad Mini-Sub Cell GT Cell or Sub-Cell GT Cell system and samples mixed with 6x DNA loading dye and run at 120V until sufficient separation was reached.

2.2.4 GATEWAY CLONING

Gateway cloning was done according to Gateway Technology user guide and the manuals of the BP Clonase II mix and the LR Clonase II mix with minor changes. To clone the gene of interest (GOI) into pDONR221, the GOI was amplified with Phusion Hot Start II DNA polymerase. The PCR conditions were adjusted for every GOI according to the manufacturer's instructions. Primers included recombination sites for the BP clonase (Table 12). PCR reactions were run on an agarose gel and the band of the correct size extracted. The purified amplicon was

used in a standard 10 µl BP reaction with 50 – 150 ng final amount of amplicon. The reaction was left at room temperature over night. After a 10 minute Proteinase K digest, subcloning efficiency DH5α were transformed according to the manufacturer's instructions using the complete BP reaction. Individual clones were sent for sequencing.

For LR reactions 150 ng of entry clone and the desired destination vector each were used in a 10 µl reaction for one hour at room temperature. After the 10 minute Proteinase K digest the complete reaction was transformed into Subcloning Competent DH5α.

Table 12: attB primer design guidelines for Gateway Cloning.

	5' end	attB site	Kozak sequence	Template specific
Forward	GGGG	ACA-AGT-TTG-TAC-AAA-AAA-GCA-GGC-TTC	ACC-ATG	NNN…
Reverse	GGGG	AC-CAC-TTT-GTA-CAA-GAA-AGC-TGG-GTC-		NNN…

2.2.5 NEBUILDER HIFI ASSEMBLY CLONING

NEBuilder cloning was done using PCR fragments. Primers were designed using the NEBuilder Assembly Tool adjusting the settings to Phusion Hot Start polymerase and 2-3 fragment cloning[141]. PCR reactions were digested with DpnI (30 minutes 37°C, 20 minutes 80°C) to prevent possible carryover of template DNA during the gel purification. 100 ng backbone amplicon were mixed with the insert in a 1:3 molar ratio for a 20 µl reaction. The sample was incubated at 50°C for one hour and the complete reaction transformed into DH5α or ccdB Survival™ 2 in the case of Gateway destination vectors carrying the ccdB kill gene.

2.2.6 RNA ISOLATION AND QRT-PCR ANALYSIS

RNA was extracted using the Macherey-Nagel NucleoSpin® RNA kit (740955.250) according to manufacturer's instructions. Samples were eluted in 40 – 60 µl nuclease free water and concentration measured using a NanoDrop Lite device (Thermo Scientific). cDNA was prepared with Bio-Rad iScript according to the manufacturer's instructions using 250 ng total RNA in a 20 µl reaction. cDNA was diluted 1:1 with water and used for qRT-PCR analysis. qRT-PCR analysis was done using Bio-Rad iTaq enzyme according to the manufacturer's instructions using a 15µl reaction with 250 nM of each primer and 2 µl diluted cDNA. Samples run on a Bio-

Rad CFX96 Touch. Analysis was done with the Bio-Rad CFX Manager 3.0.1224.1015 using HPRT1 and / or β-actin for normalization and a ΔΔCq analysis.

2.2.7 PROTEIN EXTRACTION AND CONCENTRATION DETERMINATION

Cells were washed with PBS to remove FBS prior to lysis. Then cells were lysed by addition of RIPA buffer to the well of the cell culture plate. After 5 minutes at room temperature the lysate was transferred into a 1.5 ml microcentrifuge tube, spun down at 11,000 rcf for 5 minutes to pellet cell debris. The supernatant was transferred into a new tube for storage at -80°C. Protein concentration was determined using the BioRad DC Protein Assay Kit with the microplate protocol. 5 µl diluted lysate or BSA standard per well were diluted with buffer A'. After addition of 200 µl reagent B samples were incubated for 15 minutes and the OD_{750} measured. Protein concentration was calculated using the BSA standard curve.

2.2.8 SDS-PAGE

SDS-PAA gels were cast with the Bio-Rad Mini-PROTEAN system using gels with 1.5 mm strength. The separating gel was overlaid with water-saturated 2-butanol until polymerized. 2-butanol was removed and washed away with H_2O 5 times. The separating gel was overlaid with the stacking gel and a 10 or 15 well comb was added. Gels were stored wrapped in water-soaked paper tissues at 4°C for up to one week. The samples were mixed with 4x Lämmli buffer and heated to 95°C for 5 minutes. 5 µl Precision Plus Dual Color marker were used. Gels were run at 25 mA per gel until the bromophenol blue ran out.

2.2.9 WESTERN BLOT

The Bio-Rad Tank blot system was used. The wet blot was assembled as shown in Figure 4. Gels were blotted at 100V for 1h in pre-cooled transfer buffer with a cool-pack added to the tank. After the transfer the membrane was blocked for 2 hours shaking at room temperature in antibody dilution buffer (see Table 4).

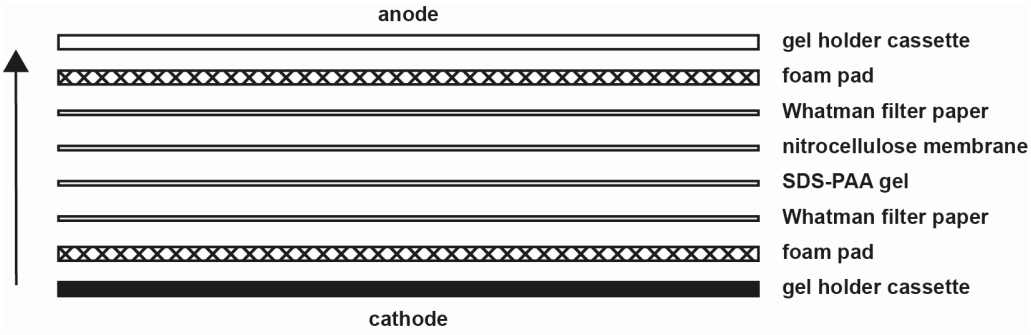

Figure 4: Schematic of Western blot assembly for tank blot. Components are assembled as shown. The arrow indicates the direction in which proteins move.

For ECL based detection, incubation with primary antibody for the protein of interest was done at 4°C over night. Blots were washed 3x 5 minutes with TBS-T shaking at room temperature before incubating with secondary antibody in blocking buffer for 1 hour at room temperature shaking. The membrane was washed 3x 5 minutes with TBS-T again and ECL was added on top of the membrane according to the manufacturer's instructions for 3-5 minutes. Excess ECL reagent was drained carefully and the membrane put into a clear plastic bag that was taped into the X-ray cassette for development. For the loading control the membrane was put in stripping buffer for two hours at room temperature. After 4x washing with excess of TBS-T to remove the stripping buffer the membrane was blocked again and the β-actin loading control was done as described above. Quantification was done using Fiji[142].

When the LI-COR Odyssey CLx imaging system was used, primary antibodies for both the protein of interest and the β-actin loading control were incubated in parallel at 4°C over night. After 3x washes 5 minutes each with TBS-T, the secondary antibodies were added and incubated for 1 hour at room temperature protected from light. The secondary antibody was washed away with 3x TBS-T for 5 minutes each and directly used for detection. Quantification of the Western blot signals was done with LI-COR Image Studio Lite 5.2.

2.2.10 Design and Cloning of shRNAs

shRNA targeting sequences were either obtained from publications or from the Genetic Perturbation Platform (GPP) (http://portals.broadinstitute.org/gpp/public/). For each target mRNA 2-3 shRNAs from GPP were chosen based on the highest adjusted score (shRNA design ruleset version 9, http://portals.broadinstitute.org/gpp/public/resources/rules). The resulting shRNA oligos (see Table 13) were ordered from Eurofins Genomics.

Table 13: Design template for shRNAs. To design forward and reverse oligo the sense and antisense sequence of the shRNA target sequence are inserted as indicated. Annealed oligos can be cloned into pLKO.1 digested with EcoRI and AgeI.

Forward	5' CCGG - 21 bp sense - CTCGAG - 21 bp antisense – TTTTTG 3'
Reverse	5' AATTCAAAAA - 21 bp sense – CTCGAG - 21 bp antisense 3'

5-10 µg pLKO.1 were digested with 2µl AgeI-HF (CutSmart buffer) at 37°C over night. The reaction was purified with the Macherey-Nagel NucleoSpin® Gel and PCR Clean-up kit. The DNA was then digested with 2µl EcoRI (EcoRI buffer) at 37°C over night. The sample was run on an agarose gel and the correct band of 7kb was cut out and purified with the same Gel and PCR Clean-up kit as before.

2.5 µg forward and reverse oligo each were diluted to 50 µl in 1x NEB buffer 2 or 2.1. Oligos were heated to 95°C for 5 minutes and then put at room temperature to cool down slowly. 150ng of linearized pLKO.1 were mixed with 2µl freshly annealed oligonucleotides, 2µl 10x T4 DNA ligase buffer, and 1µl T4 DNA ligase. Ligation was done at 16°C over night. The AgeI restriction site is lost due to the sequence of the annealed oligonucleotides. The whole reaction was transformed into Subcloning Efficiency DH5α according to the manufacturer's protocol. Successful cloning was controlled by AgeI-HF and NcoI restriction digest to verify removal of the AgeI site, and sequencing using a U6 primer.

2.2.11 Production and use of lentiviral vectors

HEK 293T cells with passage numbers below 25 were used for virus production. 5/6th of a fully confluent T75 flask was seeded on six 10 cm dishes in 10 ml IMDM medium. When cells were approximately 90% confluent, medium was changed again and cells transfected. For each 10 cm flask a transfection mix was prepared as follows: 4 µg psPAX2, 4 µg pMD.2G, and 8 µg expression plasmid were diluted in 250 µl OptiMEM. 48 µl of 1 µg/µl PEI were mixed with 202 µl OptiMEM in a separate tube. Both mixtures were combined, thoroughly mixed and incubated at room temperature for 20 minutes. Afterwards the transfection mix was added dropwise onto the cells and medium changed the next day. After three days, virus containing supernatant was taken, centrifuged at 1,000 rcf for 5 minutes and filtered (0.45µM). Purified virus was then concentrated at 134,000 rcf in an SW 32 Ti rotor or an SW 40 Ti (Beckman-Coulter) at 4°C for 2 hours. After removal of the supernatant between 100 and 300µl OptiMEM was added and virus left over night at 4°C before resuspending and aliquoting virus for storage at -80°C.

For transduction of T84 cells 20-100 µl of concentrated lentivirus stock were diluted in 4 ml of DMEM/F12 with 10 µg/ml polybrene and added onto very sparsely seeded cells in a 6 well plate. After 3 days the media was replaced with selection medium containing 5 - 10 µg/ml puromycin, 700 µg/ml neomycin, or 10 µg/ml blasticidin. Selection was continued until non-transduced control cells were dead.

2.2.12 Production of chemically competent DH10Bac

DH10Bac were cultured in 4 ml LB-kanamycin over night at 37°C shaking. This was used to seed 300 ml LB-kanamycin culture which was grown shaking at 37°C until an OD_{595} of 0.5 was reached. Bacteria were pelleted at 1700 rcf and 4°C. From this point on all steps were done on ice. The supernatant was removed and bacteria resuspended in 50 ml ice-cold 50 mM $CaCl_2$. After 30 minutes on ice cells were pelleted at 1700 rcf and 4°C for 15 minutes. The supernatant was removed and bacteria carefully resuspended in 24 ml of cryo solution (50 mM $CaCl_2$ + 15% (v/v) glycerol). After 30 minutes incubation on ice 100 µl aliquots were prepared in pre-cooled 1.5ml microcentrifuge tubes and immediately frozen in liquid nitrogen prior to storage at -80°C.

2.2.13 Production of recombinant bacmids

The protein of interest was cloned into a Baculovirus destination with an LR reaction. A destination vector clone was isolated with the Macherey-Nagel NucleoSpin® Plasmid kit (740588.250) and transformed into chemically competent DH10Bac. 100 µl self-made competent DH10Bac were thawed on ice, 100-300 ng of DNA were added and bacteria incubated on ice for 30 minutes followed by 30 seconds heat shock at 42°C and 3 minutes incubation on ice. Bacteria were recovered in 1 ml SOC medium and kept shaking 5 hours at 37°C. Bacteria were spun down at 11,000 rcf for 1 minute and spread on LB-agar plates containing 50 µg/ml kanamycin, 7 µg/ml gentamicin, 10 µg/ml tetracycline, 100 µg/ml X-Gal, and 40 µg/ml IPTG. After 2-3 days white colonies were picked and grown in 4 ml LB medium containing 50 µg/ml kanamycin, 7 µg/ml gentamicin, and 10 µg/ml tetracycline for another 2-3 days.

All steps of the bacmid isolation were carried out at room temperature if not mentioned otherwise. 2 ml bacteria were pelleted at 3,000 rcf for 15 minutes. The pellet was resuspended in 300 µl solution I (15 mM Tris-HCl, pH 8.0, 10 mM EDTA, 100 µg/mL RNase A) and lysed by addition of 300 µl solution II (0.2 N NaOH, 1% SDS). After 5 minutes the pH was neutralized by addition of 300µl ice cold 3M potassium acetate pH 5.5. Samples were kept on ice for 10 minutes

and centrifuged at 14,000 rcf. The supernatant was transferred into a new microcentrifuge tube containing 800 µl 2-propanol. Samples were mixed and incubated on ice for 5 – 10 minutes. DNA was pelleted by 20 minutes centrifugation at 14,000 rcf. The supernatant was removed and pellets washed in 500 µl 70% (v/v) EtOH. After a last centrifugation step of 20 minutes at 14,000 rcf the pellet was dried and carefully resuspended in 40 µl TE buffer by flicking the tube and stored at 4°C. Resuspension by pipetting was avoided so as to not damage the large bacmid DNA.

2.2.14 PRODUCTION AND USE OF BACMAM VECTORS

$8x10^5$ Sf9 cells per well were seeded in 6 well plates. After one hour cells were sufficiently attached for transfection. The medium was replaced with 2 ml of unsupplemented Grace's Insect Medium while the transfection mixes were prepared. 1 µg of bacmid DNA and 6 µl Cellfectin II Reagent were diluted in 100 µl unsupplemented Grace's Insect Medium each. Samples were combined, thoroughly mixed and incubated for 15 minutes at room temperature. Afterwards 800 µl unsupplemented Grace's Insect Medium were added and the complete transfection mix was used to replace the medium on the insect cells. After 5 hours the transfection mix was replaced with 2ml Sf-900 III SFM medium.

After 72 – 96 hours cells showed signs of late stage infection, i.e. formation of syncytia, cell detachment, and clear expression of recombinant proteins if they are coupled to a fluorescent marker. The supernatant was removed and centrifuged at 1,000 rcf for 5 minutes to remove cells and debris. The supernatant, the viral P1 stock, was transferred to a new tube and stored at 4°C protected from direct light. The complete P1 stock was used to infect 15 ml Sf9 cells in a 25 ml spinner flask with a density of $1.5x10^6$/ml. After incubation of 3-5 days cells will show syncytia formation and recombinant protein expression. Cells were spun down at 1,000 rcf for 15 minutes, supernatant transferred into a new tube, and FBS added for a final concentration of 3% (v/v). Production of a P3 viral stock was done similar to the P2 stock with between 80 and 120 ml cells being infected with between 1 and 3 ml P2 stock, depending on the cell volume and quality of the P2 stock. P2 and P3 stocks were either stored at 4°C protected from light or concentrated by spinning them down at 80,000 rcf in a SW 32 Ti rotor (Beckman Coulter) for 75 minutes at 4°C. Afterwards the supernatant was removed and 2-4 ml Sf-900 III SFM medium with 3 % (v/v) FBS added. The pellet was resuspended and frozen in aliquots at -80°C.

2.2.15 GROWING OF REOVIRUS

L929 cells were grown in suspension culture and kept at $7x10^5$ cells per ml. Once a sufficiently large volume is reached, cells were spun down at 600 rcf for 15 minutes, resuspended to $2x10^7$ cells/ml and infect with Reovirus strain Type 3 clone 9 (T3C9; originally obtained from Bernard N. Fields) with an MOI of 5. The virus was allowed to adsorb to for 1 hour with gentle shaking every 20 minutes. Then cells were diluted to $5x10^5$ cells/ml with a 1:1 mix of fresh medium and conditioned medium. After 48h cell viability was assessed by trypan blue staining regularly until a viability of about 50% was reached. Cells were pelleted at 740 rcf, and resuspended in HO buffer so that $2x10^8$ cells per 8 ml can be frozen at -80°C in a 50 ml tube. This is fraction represents one gradient used for purification as described below.

2.2.16 REOVIRUS PURIFICATION

A gradient is thawed at 37°C and then chilled on ice. Deoxycholate is added to a final concentration of 0.1% (w/v) and tube further incubated on ice for 10-30 minutes. 50% (v/v) -20°C CFC-113 were added and sample emulsified with an ultrasonic homogenizer (Hielscher UP200Ht, power = 50W, amplitude = 100%). The sample was put back on ice to check if the solution remains emulsified after 30 seconds, if this was not the case then the emulsification was repeated. The sample was centrifuged at 9,000 rcf. The aqueous phase is transferred into a new tube and 40% (v/v) -20°C CFC-113 added. Homogenization and centrifugation are repeated as above. The aqueous phase is transferred into a new tube making sure not to transfer any of the CFC-113 layer. Virus was loaded on top of a cesium chloride gradient (2.5 ml each of 1.25 g/ml and 1.45 g/ml). Samples were centrifuged at 111,000 rcf and 4°C over night causing the appearance of two separate bands. The bottom of the tube was pierced to extract the lower band containing infectious virus. The virus is dialyzed against virus buffer over night at 4°C and then stored at 4°C.

2.2.17 REOVIRUS TITRATION

To determine infectivity of reovirus stocks the TCID50 was determined using an In-Cell Western. T84 cells were seeded on a 96 well plate. When confluent, cells are infected with a 1:10 serial dilution beginning with at 1:100. Infection was done in 200 µl volume in triplicates. After 16 hours cells are fixed with 2% (w/v) PFA in PBS for 20 minutes. PFA was removed and cells permeabilized two times for two minutes each with PBS + 0.1% (v/v) Triton X-100., and blocked with 1% (w/v) BSA in PBS for 30 minutes. Infection was detected using an antibody against the

viral non-structural protein μNS for 1 hour. Cells were washed twice with PBS + 0.1% (v/v) Tween-20. The secondary antibody (IRDye 800CW) and Draq5 were both diluted 1:10,000 in blocking buffer. After one hour incubation, samples were washed with three times with PBS and imaged using a LI-COR Odyssey CLx reader. The TCID50/ml was calculated as described by Hierholzer and Killington and FFU/ml approximated as described by Horzinek using a Excel sheet created by Marko Binder (Marco Binder, Dept. Infectious Diseases, Molecular Virology, Heidelberg University)[143,144].

2.2.18 PREPARATION OF ACID ETCHED COVERSLIPS

Coverslips were transferred into a glass beaker and covered with 37% HCl. After 24 to 48 hours the acid was removed and coverslips rinsed with H_2O to neutralize the pH. Coverslips were stored covered in 70% EtOH.

2.2.19 IMMUNOFLUORESCENCE

Cells were grown on coverslips in 24 well plates. T84 cells were grown on acid etched coverslips, all other cells on untreated coverslips. Medium was removed, cells rinsed with PBS once and then fixed in 2% (w/v) paraformaldehyde for 20 min at room temperature or over night at 4°C. Cells were permeabilized with PBS + 0.5% (w/v) Triton X-100 for 15 minutes. 1% (w/v) BSA in PBS was used for blocking and dilution of the primary antibody. After one hour incubation, samples were washed 3x 5 minutes each with PBS + 0.1% (w/v) Tween-20. Secondary antibodies were diluted in PBS + BSA as well and cells incubated for 30 min. After 3x 5 min washes with PBS + 0.1% (w/v) Tween-20, samples were rinsed in H_2O and mounted on a microscopy slide with ProLong Gold Antifade Mountant with or without DAPI.

For T84 cells grown on transwells, the same protocol as above was followed with the following changes: The membrane was cut out before the sample was put into the primary antibody. All washing steps were done by dipping the membrane into PBS + 0.1% Tween-20 several times. All imaging analysis was done using Fiji[142].

2.2.20 PI(3)P STAINING

The protocol was initially published by G. Hammond [145] and adapted by Volker Haucke (Leibniz-Forschungsinstitut für Molekulare Pharmakologie, Berlin). All steps are done at room temperature. Cells were rinsed with 1x PBS and fixed with 2% (w/v) PFA + 2% (w/v) sucrose for 15 min. After three washes with freshly prepared 1xPBS + 50 mM NH_4Cl cells were

permeabilized with 20 µM Digitonin in buffer A. Cells were rinsed three times with buffer A and blocked (buffer A + 50 mM NH4Cl + 5% (v/v) normal goat serum (NGS)) in the presence of 0.026 µg/ml purified GFP-FYVE for 45 minutes. After two washes with buffer A, coverslips were incubated in a 50 µl drop of buffer A + 5% (v/v) NGS with 1:500 dilution of rabbit anti-GFP. Two washes for 5 min. each with buffer A were followed by 45 incubation with buffer A + 5% (v/v) NGS + 1:200 dilution of anti-rabbit secondary antibody. Cells were washed another four times five minutes each with buffer A. 1 µM DAPI were added to the first washing step. After five minutes post-fixation with 2% PFA + 2% sucrose samples were washed another three times for five minutes each with PBS + 50 mM NH_4Cl and mounted with ProLong Antifade Mountant.

2.2.21 Cell culture

All mammalian cells were grown at 37°C with 5% CO_2 in the medium given in Table 2. Sf9 insect cells were grown in 125 ml spinner flasks (CELSTIR flask, Wheaton) at 28°C without CO_2 in a Memmert IPP55 incubator with a bioMIXdrive 4 (2mag AG) at 105 rpm. T84 cells were polarized by seeding them on 6.5 mm transwells with 3 µM pore polycarbonate membranes (Corning, 3415). 10^5 cells were seeded per transwell. Media was changed the next day. When the polarization was followed, media was changed every day and TEER measured afterwards using the EVOM2 epithelial voltohmmeter (World Precision Instruments). If cells only needed to polarize, i.e. TEER of ≥ 1000 Ω, media was changed the day after seeding and every second day afterwards until all transwells were polarized.

2.2.22 Luciferase Assay

Cells were grown in 24 well plates. Medium was removed and cells lysed in 300 µl Luciferase Assay Buffer for 15 minutes at room temperature. 80 µl of lysate were transferred into three wells of a white, 96 well half area plate and 80 µl Luciferase Assay buffer were added to each well. Samples were mixed thoroughly and luciferase activity read with a Tecan Infinite 200 Pro without attenuation with one second integration time and without settle time. Average and standard deviation of each sample triplicate were used.

2.2.23 ELISA

ELISA for IFNλ, IL-6, and IL-8 was done to the manufacturer's instructions with the exception of halving all volumes as half area plates were used. For IL-6 and IL-8 samples were diluted 1:2, for IFNλ 1:5.

2.2.24 Flow Cytometry Analysis of Transgene Expression

Samples were taken during routine passaging and transferred into a test tube with cell strainer cap. Cells were analyzed on a BD FACS Canto II. Side scatter, front scatter, and fluorescence were adjusted using wildtype cells. Between 10,000 and 50,000 cells were used. Analysis was done with FlowJo 10.

3 RESULTS

3.1 VPS34 INHIBITION

3.1.1 VERIFY EFFICIENCY OF VPS34-IN1 AND SAR405 IN T84 CELLS

The aim of this project is to manipulate endosomal PI(3)P levels to elucidate the role of this lipid pool in cellular polarity and in regulating innate immune responses. The fastest way to assess this question is by inhibitor treatment. The two major players in establishing and maintaining the endosomal PI(3)P pool are the PI3-kinase vacuolar sorting protein 34 (VPS34, PIK3C3) and phosphatases of the myotubularin family (MTMs)[146]. The VPS34 inhibitors VPS34-IN1 and SAR405 were chosen due to their specificity[147,148]. To verify that these two inhibitors work in our system, we performed an indirect immunofluorescence assay to control for the depletion of PI(3)P. However, the PIP antibody did not lead to any detectable staining. Due to the low transfection efficiency of our polarized T84 cells (Sup. Figure 1) we chose an alternative staining approach that combines a purified PIP-binding domain with antibody staining (Figure 5 A). A purified PI(3)P binding protein domain coupled to GFP was added during the blocking step. This was subsequently detected with a GFP antibody and a fluorescently tagged secondary antibody. This approach results a punctuate staining in A549 cells largely overlapping with early endosomes stained with the early endosome antigen 1 (EEA1) (Figure 5 B).

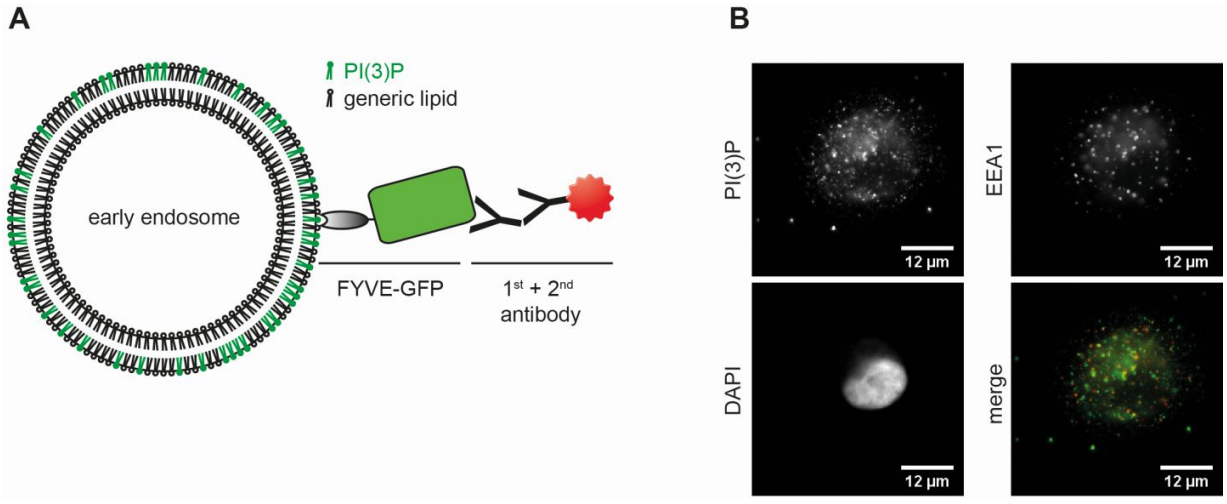

Figure 5: Staining protocol for endosomal PI(3)P. A) Schematic of the protocol. PI(3)P is bound by purified FYVE-GFP which is subsequently detected with an anti-GFP antibody and an Alexa Fluor coupled secondary antibody. B) Example of endosomal PI(3)P staining in A549 cells. The lipid pool (PI(3)P) shows strong similarity to early endosome antigen 1 (EEA) was a marker for early endosomes. Scale bar: 12 µM.

After confirmation of our staining approach, T84 cells were either mock treated (DMSO) or treated with 1 µM or 5 µM VPS34-IN1 for 15 minutes, 16 hours, and 24 hours and stained for PI(3)P (Figure 6). These times were chosen to test if the inhibitor has a fast mode of action or if longer pre-treatment will be necessary for further experiments (15 minutes), as a control for the time needed for a single viral lifecycle (16 hours), and to determine if we will be able to culture cells for a longer period of time with daily media changes to replenish the inhibitor (24 hours). Mock treated samples show punctuated signals corresponding to endosomal markers such as EEA1 (Figure 5 B) or Rab5[149–152]. These pools are severely reduced after only 15 minutes with 1 µM VPS34-IN1 (Figure 6 A). As the staining does not re-appear after 16 or 24 hours, overnight treatments or polarization timecourses with daily media changes will be possible. Specificity and off-target effects of VPS34-IN1 were tested with concentrations of up to 1 µM in the original publication. On the microscope, or by increasing the contrast, one can clearly see that the PI(3)P pools are still there only with a lower intensity (Figure 6 B)[148]. Therefore we tested a higher concentration as well. 5 µM VPS34-IN1 decreases the PI(3)P signal within 15 minutes and up to 24 hours (Figure 6 A). But unlike 1 µM VPS34-IN1 even with increased contrast no remaining PI(3)P staining can be observed (Figure 6 B).

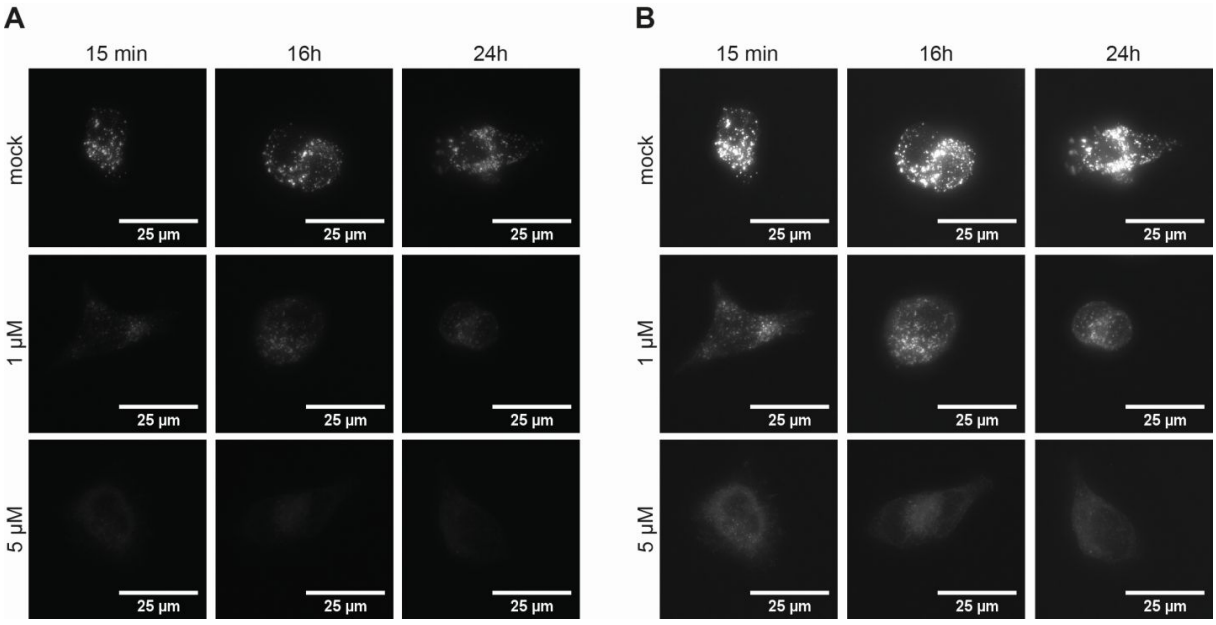

Figure 6: Timecourse experiment using the VPS34 inhibitor VPS34-IN1 in T84 cells. A) PI(3)P indirect immunofluorescence of T84 cells that were either mock treated (DMSO) or treated with VPS34-IN1 for 15 minutes, 16 hours, or 24 hours. B) Same images as in A but with increased brightness and contrast. All images show a z-stack maximum intensity projection of representative cells. Scale bar: 25 µM.

The second inhibitor, SAR405, has been reported to be very specific with an IC_{50} of 1.5 nM for VPS34 while other class I and class II PI3-kinases as well as mTOR are inhibited with IC_{50} values of over 10 µM[147]. This inhibitor was tested in a similar manner as the VPS34-IN1. 1 µM was chosen as it is at the lower range of activity in our system (see Figure 7). 6 µM was chosen because it is the concentration that was used to show the importance of VPS34 in epithelial integrity using spheroid formation in the related colon carcinoma cell line Caco-2[103]. As seen for VPS34-IN1, a 15 minute incubation with 1 µM SAR405 strongly reduces the PI(3)P pools. An effect that can still be observed up to 24 hours, allowing for a rapid removal of PI(3)P as well as overnight treatments (Figure 7 A). As with VPS34-IN1, remaining signal can be observed (Figure 7 B). When 6 µM SAR405 was used only an unspecific background can be seen (Figure 7).

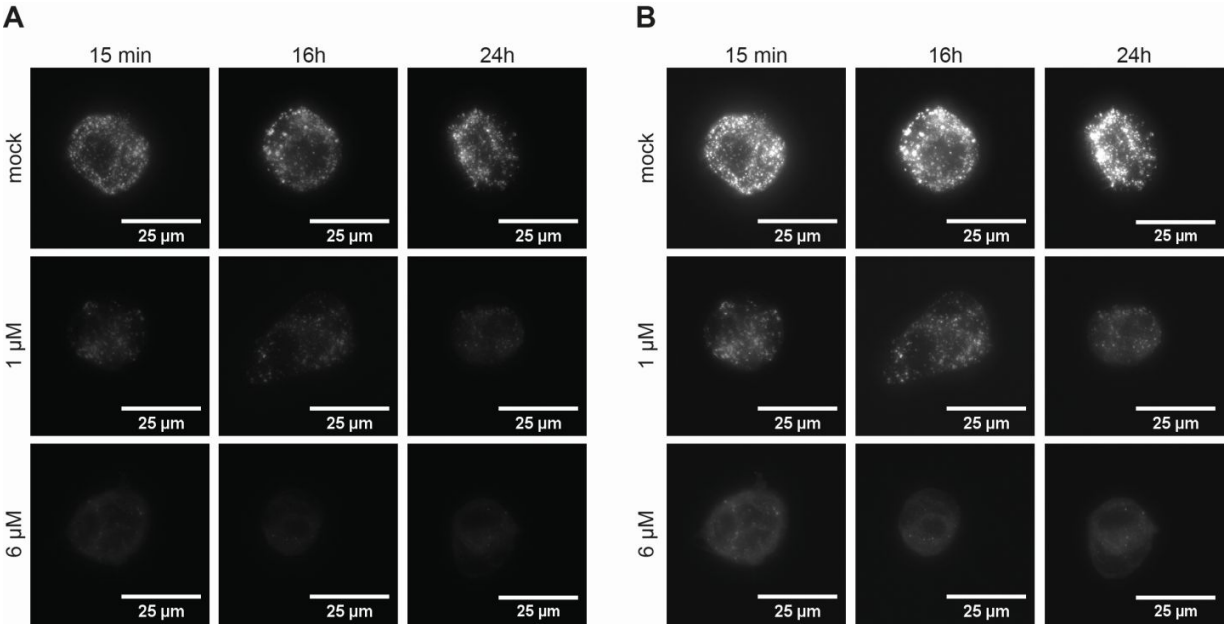

Figure 7: Timecourse experiment using the VPS34 inhibitor SAR405 in T84 cells. A) PI(3)P indirect immunofluorescence in T84 cells that were either mock treated (DMSO) or treated with SAR405 for 15 minutes, 16 hours, or 24 hours. B) Same images as in A but with increased brightness and contrast. All images show a maximum intensity projection of a Z-stack of representative cells. Scale bar: 25 µM.

This data show that both inhibitors work in T84 cells and that inhibition results in a fast reduction in PI(3)P levels after only 15 minutes while still maintaining activity after 24 hours (Figure 6 and Figure 7).

3.1.2 VPS34 INHIBITION AND POLARIZATION

As a first set of experiments the impact of inhibitor mediated PI(3)P depletion on polarization was tested. Polarity in intestinal epithelial cells refers to the asymmetrical distribution of lipids, proteins, RNA, and organelles along the apico-basal axis. Polarity can be monitored by marker proteins of the apical or basolateral membranes. However, due to the need to polarize T84s on non-transparent transwell inserts were are unable to monitor the process of polarization live and fixation of these samples will not allow us to follow the same cell population over time[153–155]. Therefore we decided to use a less invasive way of measuring polarity: the trans-epithelial electrical resistance (TEER). When T84 cells are grown on permeable transwell inserts, over time they will form an epithelial layer with cell-cell connections and polarize (Figure 8 A). The tight junctions in between the cells act as a barrier between the apical and basal compartment creating an electrical resistance between the compartments that can be monitored over the course of an experiment (Figure 8 B). As described in the introduction, there is a strong link between polarity and properly formed tight-junctions. Therefore the buildup of the TEER can be used to follow formation of tight-junctions, which in turn can serve as a marker of polarity (Figure 8 C). In our setting, using T84 cells on 6.5 mm transwells with 3 μM pores, we consider the epithelium tight and cells polarized at 1000 Ohm. Furthermore, it is an important readout as it tells us if there is a tight monolayer that prevents passive diffusion. This is a prerequisite if cells are to be infected from either the apical or basal site which requires an intact monolayer to maintain this separation.

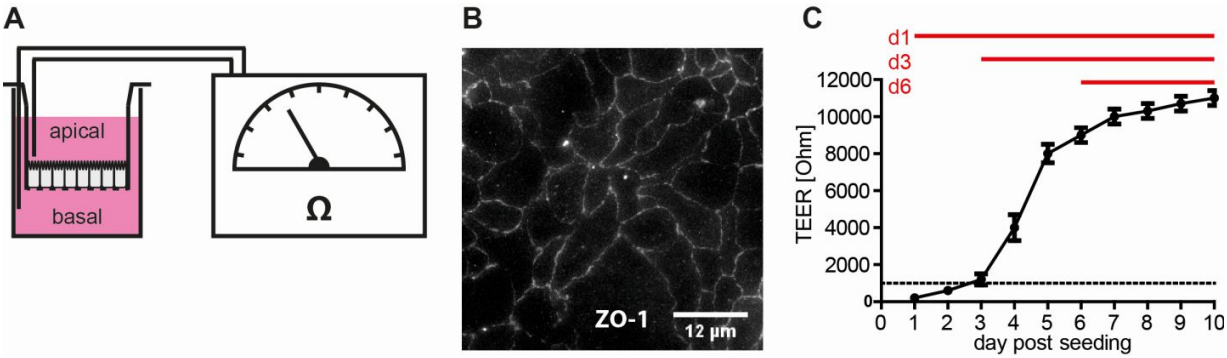

Figure 8: Schematic of how formation of a polarized epithelium is monitored. A) Schematic of experimental setup. Cells are grown on the permeable membrane of a transwell insert. Formation of the tight-junctions will separate the apical from the basal compartment. Using electrodes the trans-epithelial electrical resistance (TEER) can be measured. B) Example of fully formed tight junctions in T84 cells by staining the tight-junction protein ZO-1. Scale bar: 12 µM. C) Schematic of the development of TEER over time and experimental setup for polarization of inhibitor treated cells. The dashed line at 1000 Ohm indicates when tight junctions of the epithelium are considered to be formed. Medium is changed every day and cells are either mock treated or treated with inhibitor at different times post seeding. Cells are then kept in inhibitor until the end of the experiment.

To follow polarization, T84 cells were seeded on transwells. Medium was changed the next day and fresh medium containing either DMSO (black lines) or 1 µM VPS34-IN1 (red lines) was added to the transwells. While control cells polarized normally (Figure 9 A), addition of the inhibitor on day 1 post seeding inhibited the rate of polarization (Figure 9 B). The same trend can be seen when the inhibitor was added at day 3 post seeding (Figure 9 C). Interestingly, when the inhibitor was added to fully polarized cells, 6 days post seeding, a fast response to the drug can be observed and the TEER increase is severely hampered. (Figure 9 D).

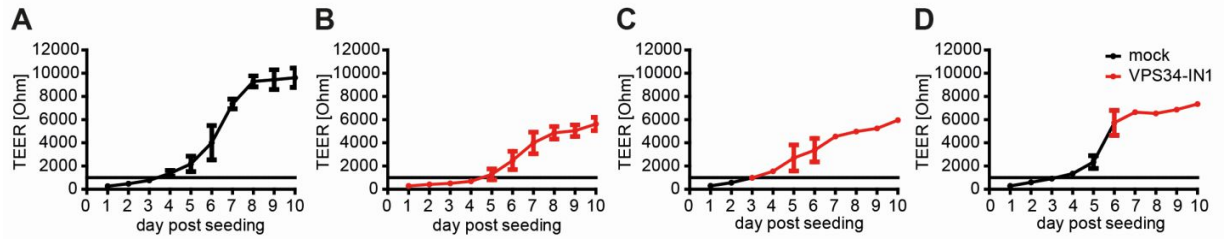

Figure 9: T84 wildtype polarization with 1 µM VPS34-IN1. T84 cells were seeded onto transwell inserts. 24 hours post-seeding medium was change and replaced with either DMSO (A) or treated with 1 µM VPS34-IN1 beginning at day 1 (B), day 3 (C), or day 6 (D) after seeding and kept with inhibitor for the remainder of the experiment. For each condition two transwells were used. The average and standard deviation are shown. One representative experiment is shown, see Sup. Figure 2 for full dataset.

Even though treatment with 1 µM VPS34-IN1 had a clear impact on the TEER (Figure 9), cells still were able to polarize, meaning they reached TEER values of over 1000 Ohm. As treatment with 1 µM VPS34-IN1 only decreases the endosomal PI(3)P pool, the experiment was repeated using 5 µM VPS34-IN1 which was shown to completely remove endosomal PI(3)P (Figure 10).

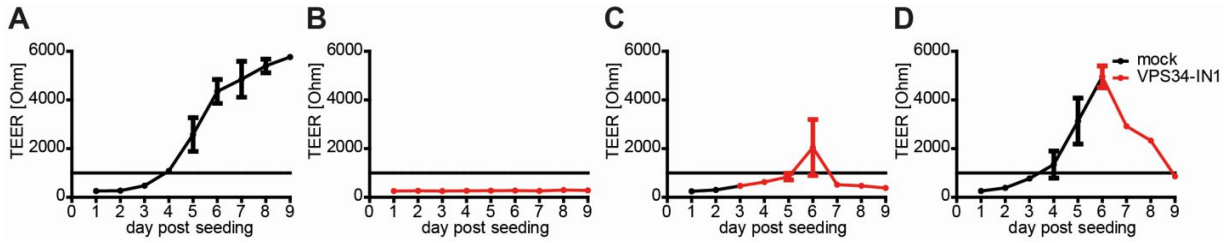

Figure 10: T84 wildtype polarization with 5 µM VPS34-IN1. T84 cells were seeded onto transwell inserts. 24 hours post-seeding medium was change and replaced with either DMSO (A) or treated with 5 µM VPS34-IN1 beginning at day 1 (B), day 3 (C), or day 6 (D) post seeding and kept with inhibitor for the remainder of the experiment. For each condition two transwells were used. The average and standard deviation are shown. One representative experiment is shown. See Sup. Figure 3 for full dataset.

As before, mock cells polarized normally (Figure 10 A). But unlike when cells were treated with 1 µM VPS34-IN1, addition of 5 µM VPS34-IN1 at day 1 post seeding prevented cells from polarizing as seen by the low TEER (Figure 10 B). The effect on TEER development is even more pronounced compared to 1 µM VPS34-IN1 when the inhibitor is added 3 or 6 days post seeding (Figure 10 C and D). TEER development is not only slowed down or stalled, it even decreases. This is especially pronounced when VPS34 is inhibited 6 days post seeding (Figure 10 D).

Previous results have shown that reducing the endosomal PI(3)P pool by VPS34 inhibition slows down polarization (Figure 9 and Figure 10) and even reduces TEER after cells have clearly polarized (Figure 10 D). To verify that the results are due to VPS34 inhibition and not off-target effects, the polarization timecourse was repeated with a second inhibitor, SAR405. Here we have chosen to use 6 µM as it is the concentration where the endosomal PI(3)P pool is completely depleted (Figure 7), and this concentration was used to show the importance of VPS34 on epithelial integrity in a similar cell line[103]. As with the previous experiments, addition of the inhibitor 24 hours post seeding prevents normal polarization with cells barely getting over 1000 Ohm (Figure 11 B) and much slower development compared to mock treated cells (Figure 11 A). Addition of SAR405 3 days after seeding slows down polarization compared to mock

treated cells but the TEER still increases over time (Figure 11 C), and if the inhibitor is added when high TEER values have been reached, between 6000 and 7000 Ohm, the TEER drops slightly over the next few days (Figure 11 D).

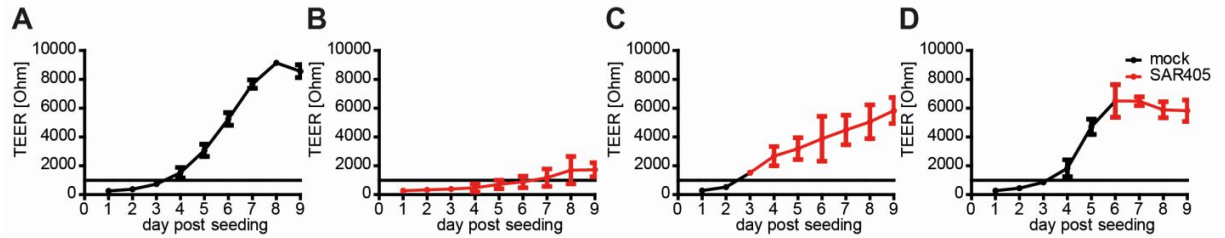

Figure 11: T84 wildtype polarization with 6 µM SAR405. T84 cells were seeded onto transwell inserts. 24 hours post-seeding medium was change and replaced with either DMSO (A) or treated with 6 µM SAR405 beginning at day 1 (B), day 3 (C), or day 6 (D) post seeding and kept with inhibitor for the remainder of the experiment. For each condition two transwells were used. The average and standard deviation are shown. One representative experiment shown, see Sup. Figure 4 for full dataset.

To exclude that low or dropping TEER values, especially after 5 µM VPS34-IN1 and 6 µM SAR405 treatment, were not due to cell death, the membranes were stained with DAPI at the end of the experiment (Figure 12). Only when treated at day one monolayers had holes. Treatment at any other time still allowed cells to form monolayers.

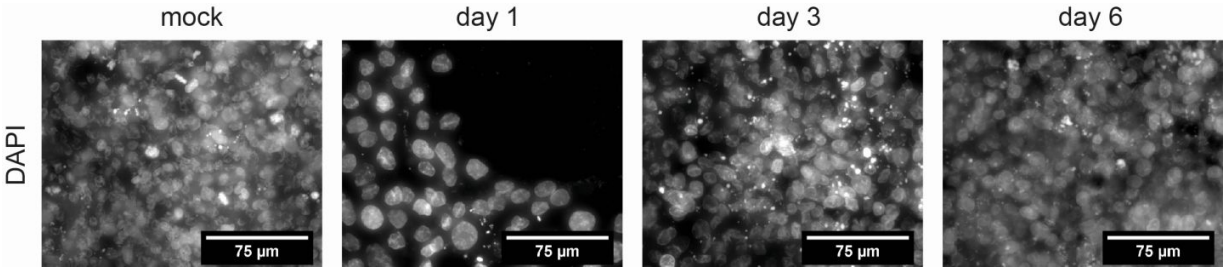

Figure 12: DAPI staining of cells treated with 5 µM VPS34-IN1 for nine days. Cells were stained with DAPI at the end of the experiment. One representative example is shown for the experiment with the strongest impact on polarity (Sup. Figure 3 A). Scale bar: 75 µM.

Together these results show that PI(3)P is critical for polarization in our T84 cell model. Complete removal of PI(3)P greatly impacts the cells ability to form and maintain their polarized nature, while even low levels of PI(3)P are sufficient to maintain polarity.

3.1.3 VPS34 INHIBITION AND IMMUNITY

Due to the role of PI(3)P, in polarity and epithelial integrity, endosomal trafficking, and TLR signaling, we wanted to test the impact of inhibitor mediated PI(3)P depletion on mammalian reovirus (MRV) Type 3 Dearing (T3D) infection[86,92,93,103,108,109,156]. Previous work in the lab has determined that T3D is capable of infecting T84 cells from both their apical and basolateral membranes[157,158]. After virus entry and uptake, the viruses are trafficked into the endosome where they are further processed and released into the cytosol for viral replication to begin. During the course of infection, T3D is detected by the innate immune system through the Toll-like receptors within the endosome[159]. This detection leads to the induction of cytokines, which can be detected through an ELISA readout. Three different ELISA read-outs, IFNλ, IL-6 and IL-8, have been chosen due to their induction following viral infection and their importance in epithelial cells. Interferon lambda (IFNλ), also known as interferon type 3 (IFN3), mainly acts on epithelial cells due to the restricted expression of its receptor[160]. Additionally, work in the lab has shown that IFNλ protects intestinal cells from T3D infection and its protective activity extends to the intestinal epithelium, even to rotavirus infection, a virus closely related to MRV[161]. Interleukin-6 (IL-6) was shown to be produced by numerous cells, including IECs, and is involved in tissue repair[162,163]. Interleukin-8 (IL—8) is produced by IECs as well and acts as a chemoattractant for neutrophils, natural killer cells (NK cells), T cells etc [164].

Initially we wanted to determine whether cells required pre-treatment with the inhibitors prior to infection and which time post-infection lead to the highest induction of cytokines. T84 cells were seeded and allowed to attach over night. The next morning they were pre-treated with either with 5 μM VPS34-IN1 or mock treated (DMSO) for one hour. Afterwards cells were infected with reovirus for 16 or 24 hours in the presence of absence of 5 μM VPS34-IN1. The ELISA results for IFNλ, IL-6, and IL-8 show that 24 hours post-infection leads to the largest induction of all cytokines. Interestingly, addition of 5 μM VPS34-IN1 reduces the cells immune response for all three cytokines (Figure 13). Furthermore it is apparent that pre-stimulation for one hour does not result in a greater reduction compared to cells which received the inhibitor at the same time as infection. This fits well with the rapid effect of VPS34-IN1 as can be seen in Figure 6. As SAR405 acts as rapidly as VPS34-IN1 (Figure 6 and Figure 7), we decided to continue all experiments without inhibitor pre-treatment.

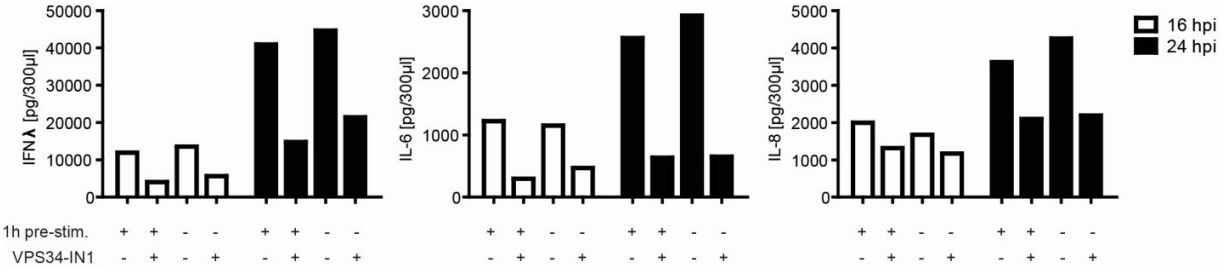

Figure 13: Determination of timing of inhibitor addition. T84 cells were seeded 24 hours prior to infection. Cells were pre-treated with DMSO or 5 µM VPS34-IN1 and then subsequently infected with T3D. Samples were harvested after 16 and 24 hours and used for ELISA analysis. Data of technical triplicates shown.

To determine if the SAR405 also inhibits the production of cytokines after T3D infection we used a similar protocol as described above. T84 cells were seeded 24 hours prior to infection and cells were treated with DMSO or 6 µM SAR405 for 24 hours (Figure 14). However, unlike the VPS34-IN1, the SAR405 inhibitor led to an increase in the production of all three cytokines. A similar increase in cytokine production, e.g. IL-6, upon TLR2 and TLR4 stimulation of bone marrow derived dendritic cells (BMDCs) upon SAR405 treatment has been shown[165]. But in this publication, BDMCs treated with 1 µM VPS34-IN1 also had an increased immune response, unlike what we have seen with 5 µM VPS34-IN1 in T84 cells (Figure 13). This difference between the two inhibitors in T84 cells as well as between T84 cells and BMDCs could be due to off-target effects when using a high concentration of either inhibitor (Figure 13).

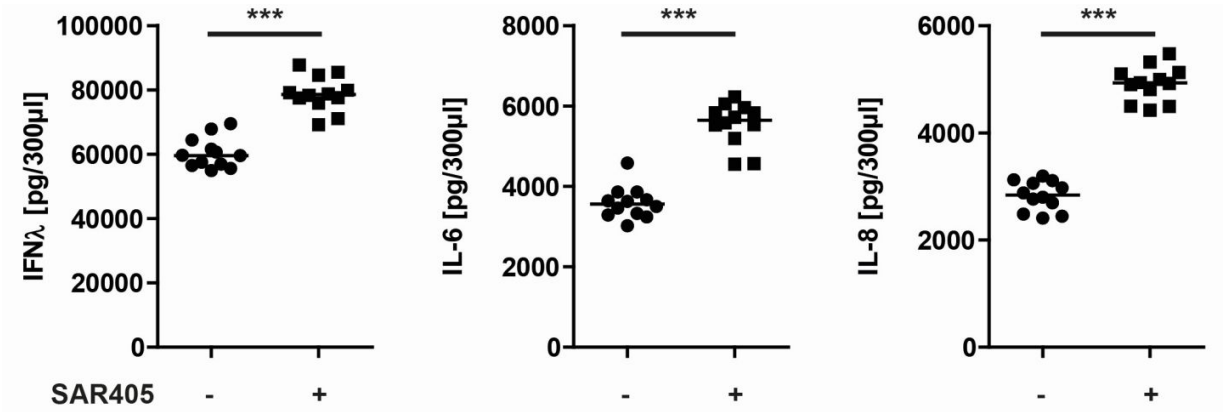

Figure 14: VPS34 inhibition with 6 µM SAR405 and immunity to reovirus infection. T84 cells were seeded 24 hours prior to infection. Cells were infected with T3D in the presence or absence of 6 µM SAR405. Samples were harvested after 24 hours and used for ELISA analysis. Results for IFNλ, IL-6, and IL-8 show a significant increase in the immune response. N=12, significance was tested with an unpaired, two-tailed t-test. $P > 0.05$; * = $P \leq 0.05$; ** = $P \leq 0.01$; *** = $P < 0.001$.

To further investigate the possibility of side effects of the inhibitors used, the experiment was repeated using 1 µM VPS34-IN1 (Figure 15). Once a lower inhibitor concentration was used, the previously observed reduced immune response could not be reproduced, and cells treated with a lower VPS34-IN1 concentration showed no significant change in the immune response for all three cytokines tested.

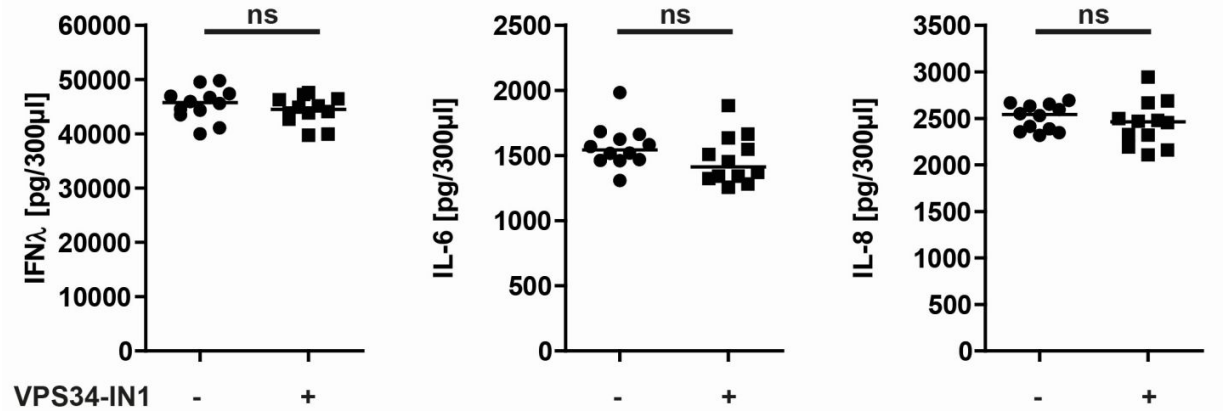

Figure 15: VPS34 inhibition with 1 µM VPS34-IN1 and immunity to reovirus infection. T84 cells were seeded 24 hours prior to infection. Cells were infected with T3D in the presence or absence of 1 µM VPS34-IN1. Samples were harvested after 24 hours and used for ELISA analysis. Results for IFNλ, IL-6, and IL-8 show no significant increase in the immune response. N=12, significance was tested with an unpaired, two-tailed t-test. ns = not significant. $P > 0.05$; * = $P \leq 0.05$; ** = $P \leq 0.01$; *** = $P < 0.001$.

Lastly, we wanted to test the impact of the inhibitors on the viral infectivity. Therefore T84 cells were infected with a serial dilution of reovirus T3D in the presence or absence of both inhibitors. Infectivity was determined by staining the viral non-structural protein µNS. Relative infectivity was determined by comparison of inhibitor treated samples to mock treated infections (Figure 16). While both inhibitors seem to reduce the infectivity of reovirus T3D in T84 cells at the concentrations used for the experiments above, these results are not significant.

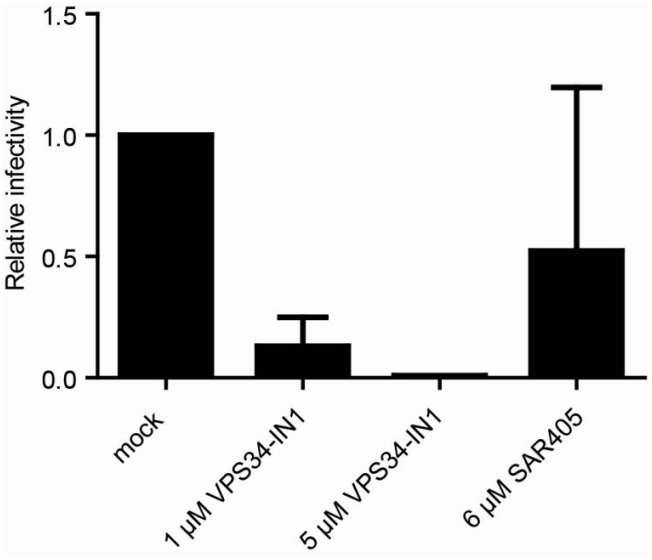

Figure 16: Relative infectivity of reovirus in presence of VPS34 inhibitors. Cells were infected with serial dilutions of reovirus T3D in the presence or absence of both inhibitors. Infection was determined by immunofluorescence analysis of the non-structural protein µNS. Infectivity is shown relative to non inhibitor treated samples (mock). Average and standard deviation of two independent experiments with technical triplicates are shown.

These results show that both inhibitors prevent or slow down polarization, as indicated by the decreased TEER (Figure 9, Figure 10, and Figure 11). Their impact on immunity on the other hand is inconclusive and would argue for off-target effects (Figure 13, Figure 14, and Figure 15). While a reduced immune response at 5 µM VPS34-IN1 would fit well with the lower infectivity (Figure 13), 1 µM VPS34-IN1 also reduces infectivity but does not change the immune response (Figure 15), and the reduced infectivity of SAR405 even results in a higher immune response (Figure 14). This further indicates that these results are not significant (Figure 16).

3.2 KNOCK-DOWN OF VPS34 AND MTM1

3.2.1 VERIFICATION OF KNOCK-DOWN EFFICIENCY IN T84 CELLS

As our previous results indicate that the inhibitors lead to off target effects we chose to evaluate the role of PI(3)P by knock-down its metabolizing enzymes[103,149,166]. The two major players in early endosome PI(3)P metabolism are the PI3-kinase VPS34 and the PI3-phosphatases of the MTM family, especially MTM1[91]. Loss of MTM1 is associated with x-linked myotubular myopathy (XLMTM) and the XLMTM patient derived cell line shows defective transferrin exocytosis and endosomal β1-integrin accumulation. Also increased PI(3)P levels on early endosomes and impaired recycling from endosomes to the plasma membrane have been reported[78,91,146,167]. In total, two shRNAs against MTM1 and three shRNAs against VPS34 were chosen. The targeting sequences were either taken from the database of the Genetic Perturbation Portal (GPP) of the Broad Institute (shMTM1 #1, shVPS34 #1 and shVPS34 #2) or based on previously published siRNA sequences (shMTM1 #2 and shVPS34 #3)[78,168]. T84 cells were transduced by lentiviral vectors expressing one of the shRNAs or a scrambled control shRNA

As epithelial cells, T84 cells tend to grow close to one another and form cell-cell-connections as they would in an epithelium. We have seen before that T84 cells have a reduced metabolism when they have sufficient cell- cell contacts. Once cells grow as a tight epithelium or in islands close to one another they are poorly transduced by viral vectors, or at least show little to no trans-gene expression. We also observed that while sparse cells can be easily selected by 5 µg/ml puromycin, a confluent monolayer of T84 cells can survive several days in 20 µg/ml puromycin. Furthermore, during my master thesis I have shown that knock-down by several rounds AAV-delivered shRNAs does reduce the mRNA levels but does not have an impact on the protein. Only when we used lentiviral vectors and several rounds of passaging cells at low confluency, protein levels decreased (Sup. Figure 5). Therefore, to achieve an efficient knock-down, we need to transduce and select T84 cells at a very low density and split regularly to maintain a relatively low density for at least two weeks before we can detect a clear knock-down. At this time, cells were harvested and the expression level of VPS34 and MTM1 were assessed (Figure 17 A). Compared to the scrambled shRNA control, all shRNAs with the exception shVPS34 #1 had reduced the mRNA levels to less than 30%. Based on these results, cell lines expressing shMTM1 #1 or shVPS34 #3 were used. Additionally, to confirm that the knock-down was maintained through serially passaging of our cells, a second confirmation of both the mRNA

and protein levels was performed. While the mRNA levels were slightly higher than the original screen, around 27% in both lines, Western blots confirmed that the proteins were reduced (Figure 15 B and C). Taken together, these results show that knock-down cell lines were successfully established.

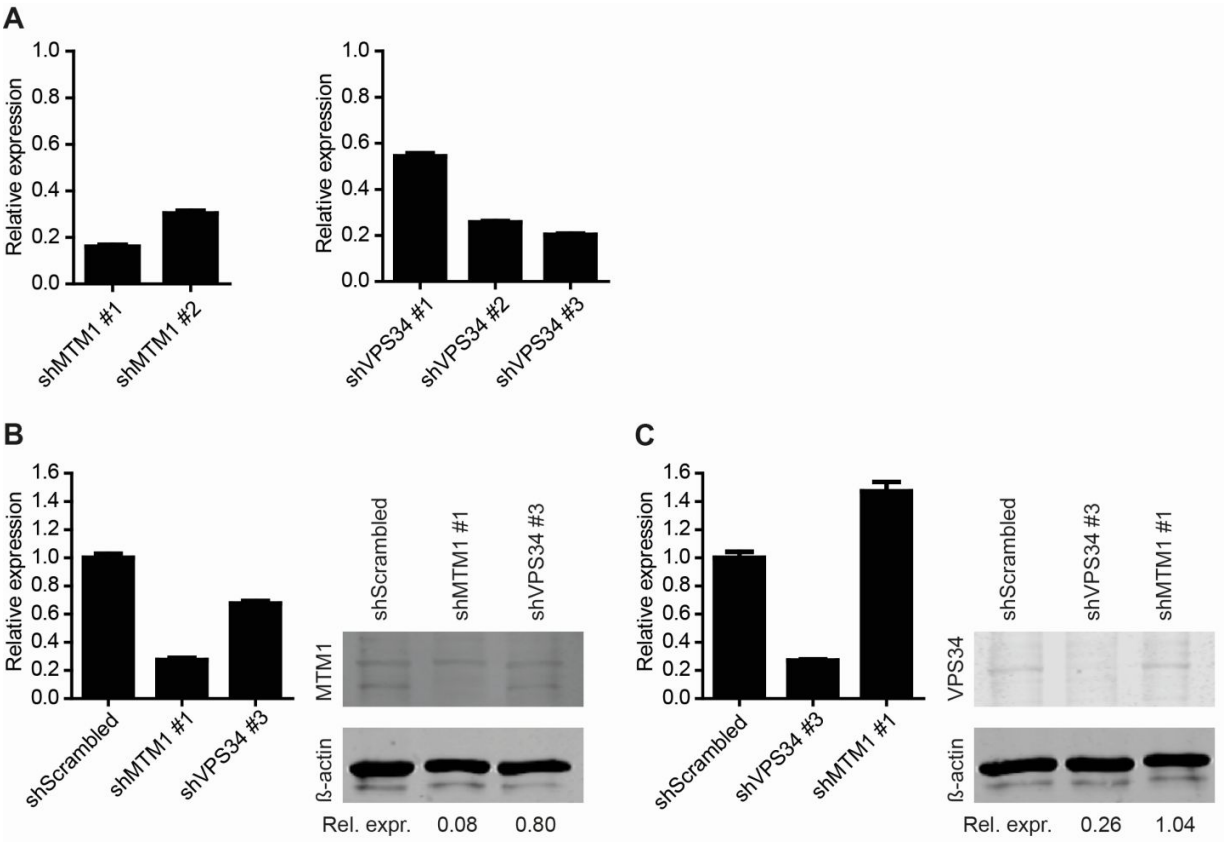

Figure 17: Knock-down of MTM1 and VPS34 in T84 cells. A) T84 cells transduced by lentiviruses expressing shRNAs against VPS34 or MTM1 were validated by qPCR. All five shRNAs were tested in order to determine with which cell line to continue. Expression is shown relative to a scrambled shRNA. B) MTM1 mRNA and protein levels in scrambled control, shMTM1, and shVPS34 knock-down cell lines. C) VPS34 RNA and protein levels in scrambled control, shVPS34, and shMTM1 cell lines. Relative expression of the protein was calculated by band intensities and using the actin signal for normalization.

3.2.2 VPS34 AND MTM1 KNOCK-DOWN IN POLARITY

As with the VPS34 inhibitor experiments, we assessed the role of VPS34 and MTM1 on the ability of T84 cells to polarize. T84 cells knocked-down for VPS34 or MTM1 were seeded on transwells and their TEER was evaluated over polarization. Development of the TEER was followed for nine to ten days in three independent experiments (Figure 18). All three cell lines were still able to polarize as shown by the TEER values of over 1000 Ohm. The scrambled control cells polarize as like wildtype cells. They reach a polarized state within two to three days

and are able to build up high TEER values. The MTM1 knock-down cells behave very similar, possibly polarizing slightly faster. VPS34 knock down cells on the other hand clearly polarize slower and do not reach as high TEER values

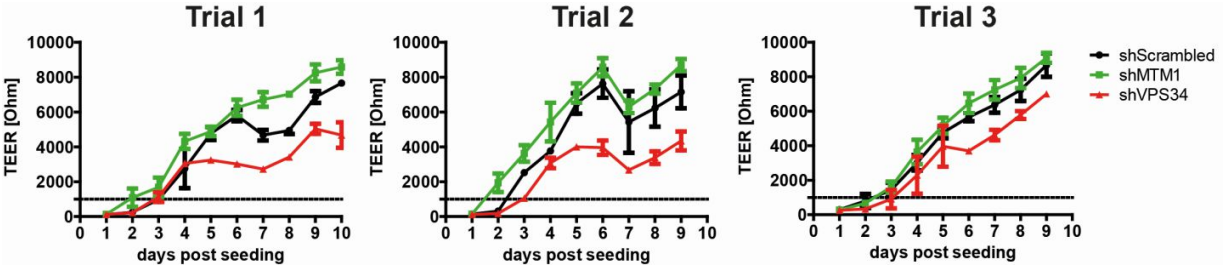

Figure 18: Polarization timecourses of MTM1 and VPS34 knock-down cells. T84 cells expressing shScrabled or knock-down shRNA for either MTM1 or VPS34 were seeded onto transwells. For each experiment, all three cell lines were seeded at identical density seeded on four transwells. Polarization was followed for nine to ten days. Three independent polarization timecourse experiments are shown. Average and standard deviation are shown.

3.2.3 VPS34 AND MTM1 KNOCK-DOWN IN IMMUNITY

Next, the impact of both knock-downs on immunity was tested. For that, T84 cells were infected with reovirus T3D as for the inhibitor experiments before and supernatants harvested after 24 hours. The immune response was tested by ELISA for IFNλ, IL-6, and IL-8 (Figure 19). IFNλ expression increased in MTM1 knock-down cells while the response decreased in VPS34 knock-down cells. The increased response to the MTM1 knock-down was also observed for IL-6 but VPS34 knock-down did not change the IL-6 levels. The results for IL-8 were slightly more difficult to interpret as individual samples show a much higher spread but overall it seems that the IL-8 levels are slightly reduced in both knock-downs. In summary, we have shown a role for VPS34 in polarity as well as for VPS34 and MTM1 in the innate immune response.

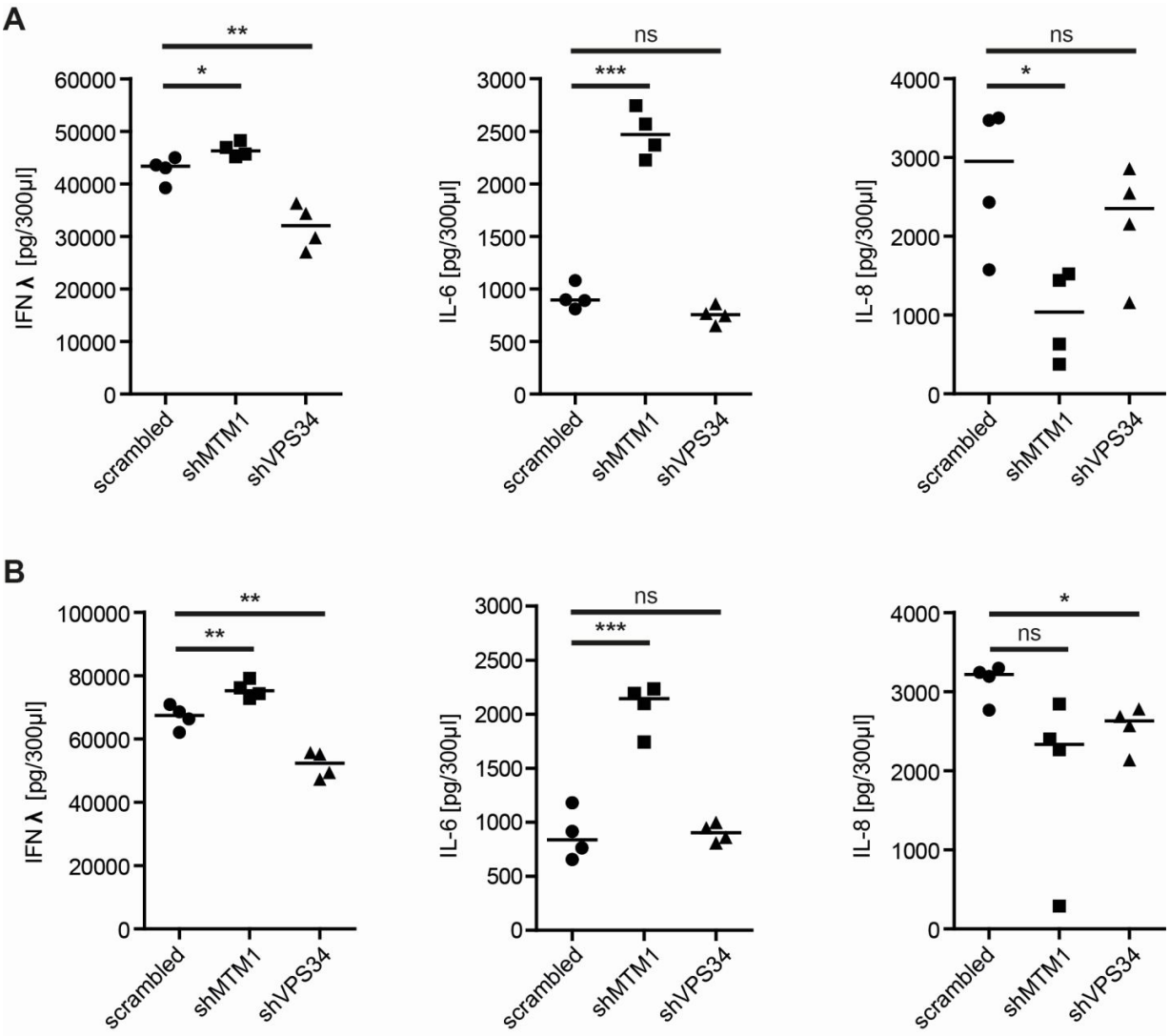

Figure 19: Immune response in MTM1 and VPS34 knock-down cell lines. T84 cells expressing a scrambled shRNA, shMTM1 or shVPS34 were infected with reovirus T3D. Supernatants were harvested 24 hours later and analyzed for IFNλ, IL-6, and IL-8. A and B show results from two different ELISA plates per readout. N=4 per plate, significance was tested with a two-tailed, unpaired t-test: ns = not significant, $P > 0.05$; * = $P \leq 0.05$; ** = $P \leq 0.01$; *** = $P < 0.001$.

3.3 Chemically Induced Dimerization System to Reduce Early Endosome PI(3)P Level

3.3.1 Verification the Chemically Induced Dimerization System Works

So far we have used two different methods of interfering with the cellular PI(3)P levels, either by chemical inhibition or knock-down of metabolizing enzymes. Both methods have yielded different results, e.g. the stronger impact on TEER development upon SAR405 treatment compared to knock-down (Figure 11 and Figure 18) or an increased immune response upon SAR405 treatment while VPS34 knock-down either reduces the IFNλ and IL-8 response and does not change the IL-6 response (Figure 14 and Figure 19). Besides the possibility of off-target effects of the inhibitors, the difference between inhibition and knock-down could result from the fact that the inhibitors only reduce the lipid level while a knock-down reduces protein level. As both of these proteins also interact with other proteins, loss of a protein could have an impact beyond the loss of its catalytic activity[96,169]. Also, VPS34 is part of two different complexes. Complex I is found on phagosomal/autophagosomal membranes while complex II is found on endosomal membranes[96,147,170]. Both methods used for target VPS34 in general, thereby interfering with both complexes. To prevent that, we decided to continue with a method allowing us to change PI(3)P composition in a more precise way.

We chose to remove PI(3)P from early endosomes because it is the predominant phosphoinositide and has been shown to be involved in processes such as maturation from early to late endosomes, endocytosis in hepatocytes, and EGF receptor signaling[86,146,148,150,171–173]. Therefore targeting early endosomes should impact cellular trafficking which is necessary for polarity and polarized sorting. We decided to utilize a chemical dimerization system to specifically remove PI(3)P from early endosomal membranes (Figure 20). Rapamycin is a small, cell permeable molecule used as an immunosuppressant. It acts by binding the FK506 Binding Protein 1A, 12kDa (FKBP12) which then inhibits mTOR by binding to its FKBP and rapamycin binding (FRB) domain[174]. To use this as a tool, we fused the FRB domain to Rab5 and the FKBP domain to the PI(3)P phosphatase MTM1. We utilized a mutated FRB domain, FRB*, so we can use AP21967 (rapalog) which does not interact with mTOR (Figure 20 A)[174]. If rapalog is added, it forms a complex with FRB* and FKBP which recruits MTM1 to the early endosome. We used either full-length wildtype (wt) human MTM1 or full-length human MTM1-C375S, a phosphatase-dead mutant that has been previously characterized[175,176].

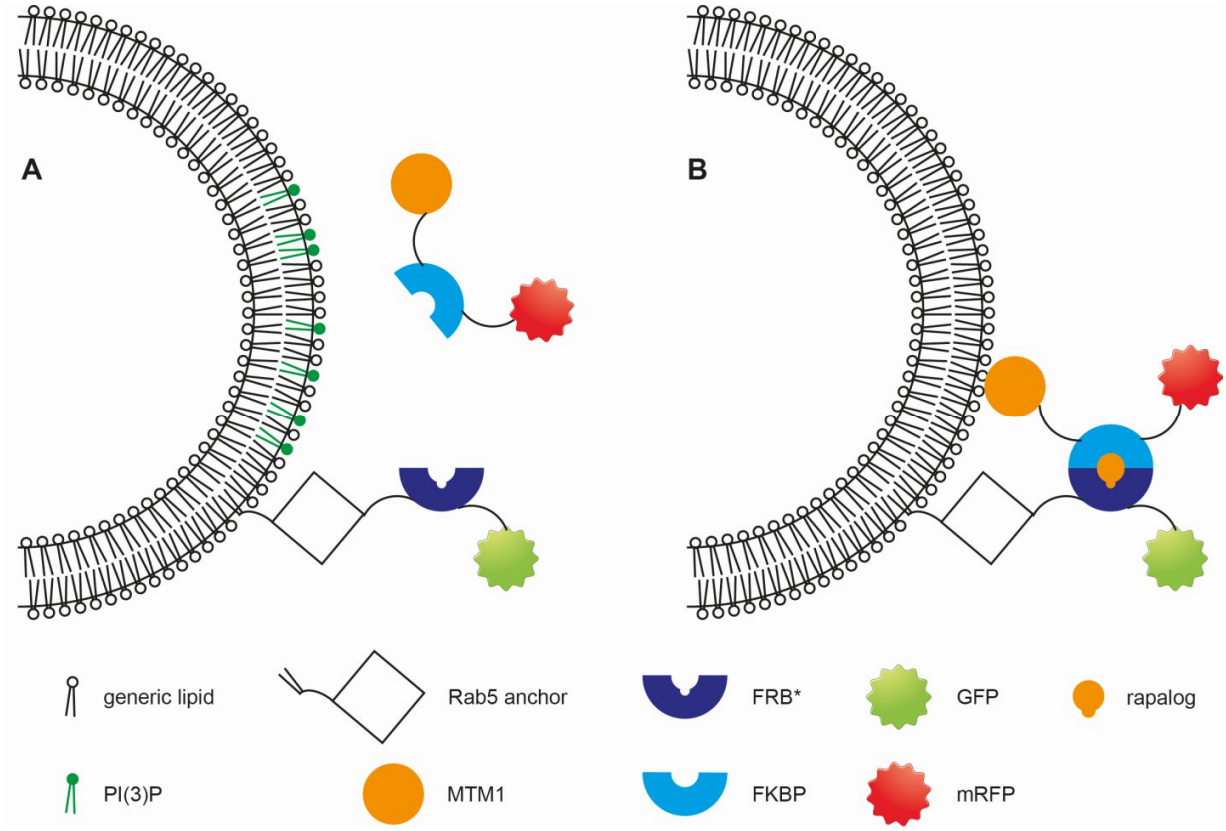

Figure 20: Schematic of the chemically induced dimerization system. A) Cells express the early endosome marker Rab5 as an anchor. Rab5 is fused to GFP and the FRB* domain (Rab5-GFP-FRB*). The enzyme MTM1 is linked to the FKBP domain and mRFP (mRFP-FKBP-MTM1). The enzyme is cytoplasmic and does not remove the endosomal PI(3)P. B) When the chemical dimerizer (rapalog) is added it forms a trimeric complex with the FRB* and FKBP domain recruiting the enzyme to the endosome which depletes the PI(3)P pool.

To prove the functionality of this system, we need to be able to detect the loss of PI(3)P on early endosomes upon recruitment of MTM1 wildtype but not MTM1-C375S. Unfortunately we cannot use the staining procedure described above as it uses an GFP antibody to detect PI(3)P (Figure 5 A) and the Rab5 anchor is GFP-tagged as well (Figure 20). Therefore chose an indirect approach using changes in endosome morphology upon PI(3)P depletion. Enlarged endosomes and tubularization have been described before upon VPS34 knock-down and PI(3)P depletion by MTM1 using a chemical dimerization approach[171,177]. To test this in our hands, we used HEK 293T cells. Unlike T84 cells, they can easily be transfected with a PI(3)P sensor thus obviate the need to stain PI(3)P by immunofluorescence. HEK 293T cells were transfected with Rab5-CFP-FRB*, mRFP-FKBP-MTM1-wt or MTM1-C375S, and FYVE-GFP as a PI(3)P sensor (Figure 21). Without inducing dimerization, the Rab5 anchor shows the expected punctuate structures

fitting well with its endosomal localization. Also Rab5 anchor localization overlaps with the signal from the PI(3)P sensor FYVE-GFP (Figure 21 A, top panel). Upon addition of the dimerizer (rapalog), the cytoplasmic enzyme is recruited to the endosomes thereby changing their morphology and the PI(3)P signal becomes dispersed within the cell (Figure 21 A, lower panel). When the same experiment is performed with the catalytically inactive C375S mutant, PI(3)P levels are not depleted and endosome morphology remains unchanged (Figure 21 B). This proves that our system can remove PI(3)P when MTM1-wt but not MTM1-C375S is recruited and that this results in morphological changes of the early endosomes. Next, the same cell lines were treated with 6 μM SAR405, a concentration sufficient for decreasing PI(3)P levels (Figure 7). In this experiment enlarged endosomes upon PI(3)P depletion can be observed as well, further strengthening the argument that loss of PI(3)P but not recruitment of an enzyme by itself is the reason (Figure 21 C). The same changes in early endosome morphology can be seen in T84 cells expressing Rab5-GFP-FRB* anchor and mRFP-FKBP-MTM1-wt. Upon addition of the dimerizer (rapalog) MTM1 is recruited to early endosomes which become enlarged (Figure 21 D). Therefore confirming that the system can be used to deplete PI(3)P from early endosomes in T84 cells.

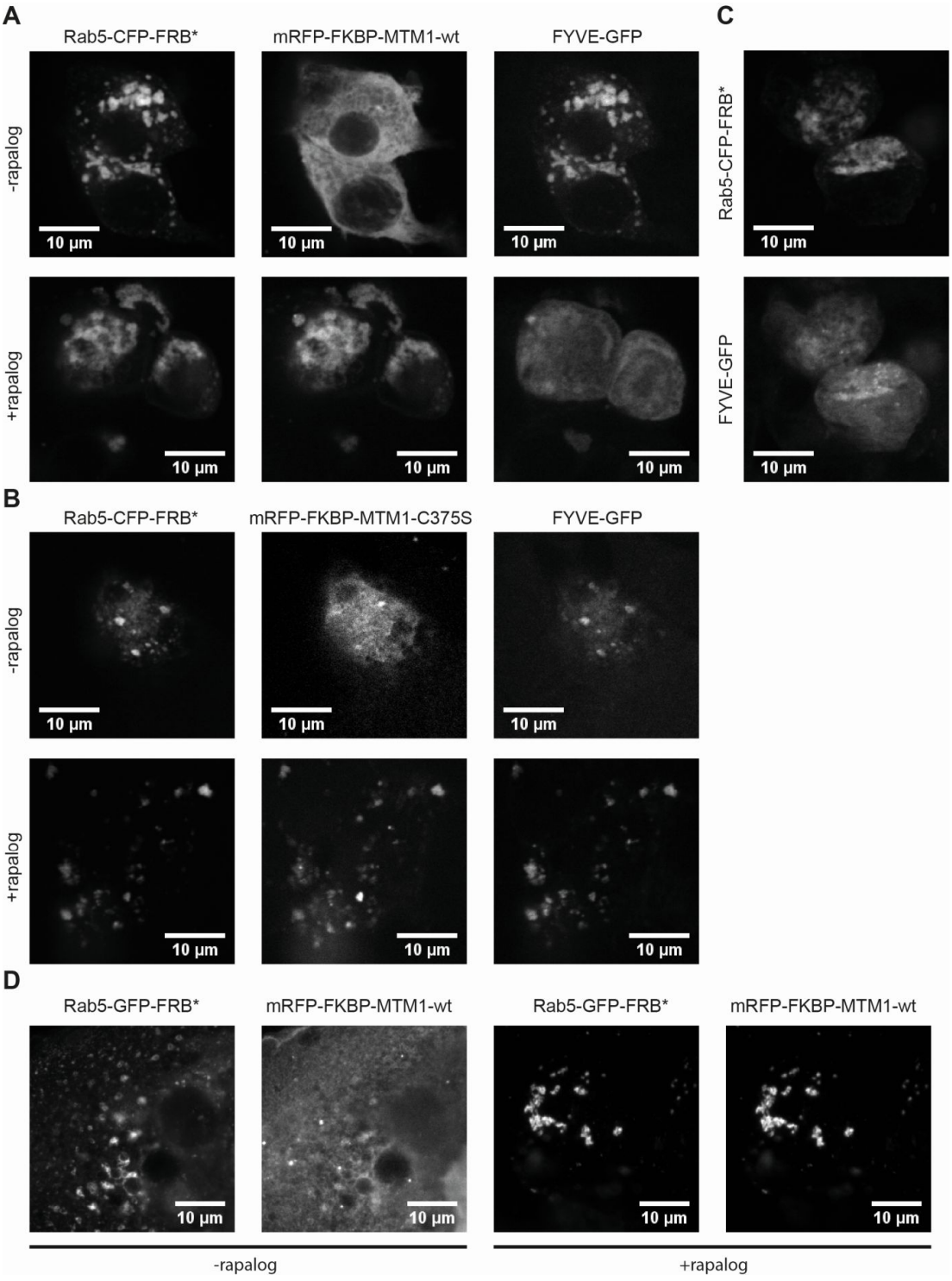

Figure 21: Proof of principle of the chemically induced dimerization system. A) HEK 293T expressing Rab5-CFP-FRB* anchor, mRFP-FKBP-MTM1-wt, and FYVE-GFP were treated with EtOH or rapalog for two hours. Cells were fixed and observed by epifluorescence. B) Experiment as in A but with MTM1-C375S. C) HEK 293T cells expressing Rab5-CFP and FYVE-GFP treated with 6 µM SAR405 for 60 minutes. D) Same as A expect using T84 cells. A-D Representative image is shown. Scale bar: 10 µM.

3.3.2 *Early Endosome PI(3)P Depletion and Polarization*

After establishment of T84 cell lines expressing both the Rab5-GFP-FRB* anchor and either MTM1-wt or MTM1-C375S, we tested the importance of endosomal PI(3)P on polarization (Figure 22). We used a similar experimental set-up as was previously used in the our VPS34 inhibitor treated cells (Figure 8 C), where the dimerizer was added at different times after seeding (1d, 4d, and 7d for Rab5 + MTM1 expressing cells; 1d, 3, and 6d for T84 wildtype cells) and polarization was followed for up to 12 days. Cells expressing the Rab5 anchor and wildtype MTM1 polarize when dimerization is not induced (Figure 22 A) while induction of dimerization and depletion of PI(3)P by addition of rapalog one day after seeding prevents polarization. When PI(3)P is depleted after cells are polarized (TEER > 1000 Ohm) there is only very little increase in TEER compared to the mock control (see Sup. Figure 6 for full dataset). When the experiment is done with cells expressing the Rab5 anchor but the phosphatase dead MTM1-C375S, the results are very similar to cells expressing the wildtype enzyme (Figure 22 B). If the recruitment is induced one day after seeding cells do not polarize anymore and when it is added after cells are polarized the TEER does not increase anymore (see Sup. Figure 7 for full dataset). To test whether this is due to phosphatase-independent functions of MTM1, because MTM1-C375S forms heptameric rings with endogenous wildtype MTM1 stimulating its activity[178], or the dimerizer itself, we tested polarization of T84 wildtype cells in the presence of rapalog (Figure 22 C). As with the MTM1 expressing cell lines, addition of rapalog one day after seeding prevents polarization. Also addition at later timepoints does interfere with the TEER values, which develop slower and do not reach as high values as the control cells (see Sup. Figure 8 for full dataset). This argues that the effect on polarization we see in cells expressing the chemical dimerizer system is at least partly due to the dimerizer itself.

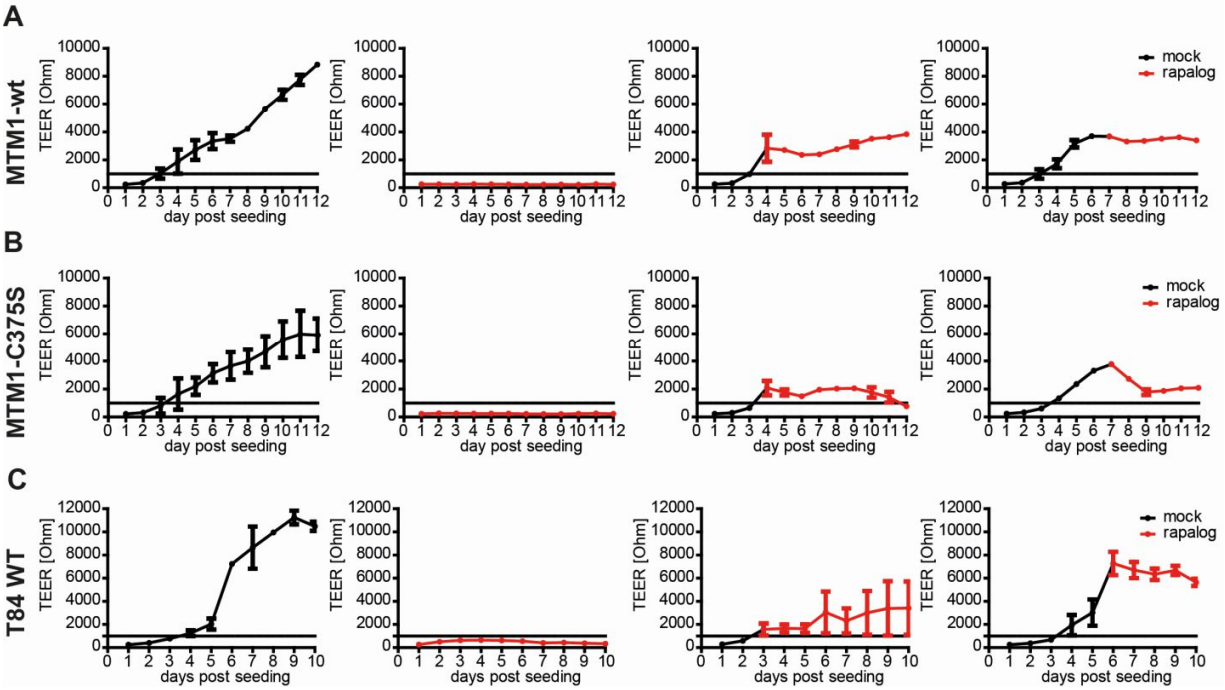

Figure 22: T84 cell polarization upon MTM1-mediated PI(3)P depletion. T84 cells expressing the early endosome anchor (Rab5-GFP-FRB*) were seeded onto transwell inserts and allowed to polarize. Rapalog was added at indicated times post-seeding. (A) T84 also express recruitable MTM1 wildtype or (B) phosphatase dead MTM1-C375S. (C) T84 wildtype cells were used as a control. (A-C) Polarization was followed by measuring the TEER. Every condition was done in duplicates and the average and standard deviation are shown.

3.3.3 Early Endosome PI(3)P Depletion and Immunity

Next we wanted to test the impact of PI(3)P depletion on Rab5-positive early endosomes on the immune response. To that end, T84 cells expressing the Rab5 anchor and either MTM1 wildtype or MTM1-C375S were used. As we knew from the previous experiment that the chemical dimerizer itself is sufficient to interfere with polarization (Figure 22 C), we also included T84 wildtype cells. All cells were seeded at identical numbers and infected with reovirus T3D 24 hours post-seeding. Supernatants were harvested at 24 hours post infection to analyze the immune response by ELISA for IFNλ, IL-6, and IL-8 (Figure 23).

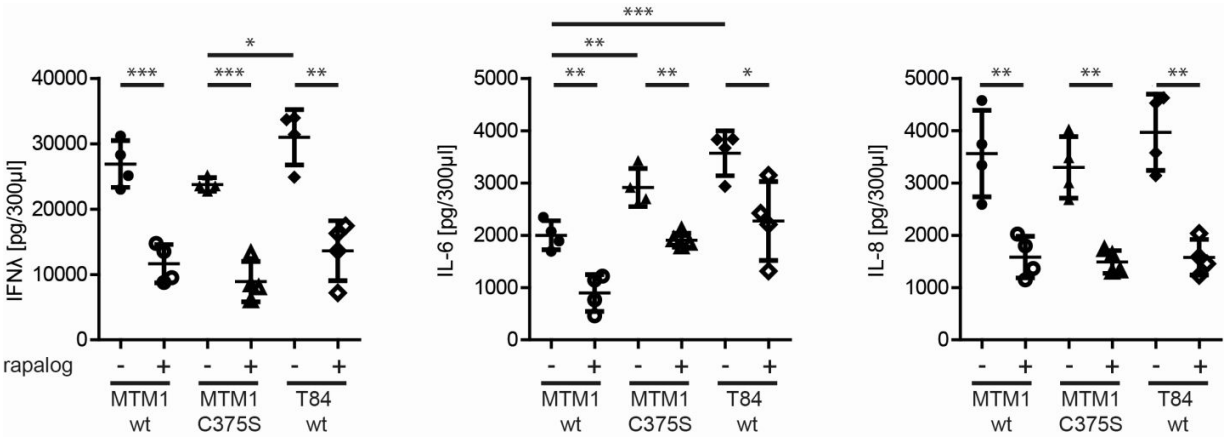

Figure 23: Immune response upon PI(3)P depletion by rapalog. T84 cells expressing Rab5 anchor and MTM1-wildtype, Rab5 anchor and MTM1-C375S, or T84 wildtype were infected in the presence and absence of the chemical dimerizer (rapalog). Supernatants were harvested 24 hours post infection and ELISA for IFNλ, IL-6, and IL-8 were used as readouts. Significance was tested with an unpaired two-tailed t-test. Only significant changes are shown with P > 0.05; * = P ≤ 0.05; ** = P ≤ 0.01; *** = P < 0.001.

We observed a significant reduction in the IFNλ, IL-6, and IL-8 response when dimerization was induced by addition of rapalog (Figure 23). This reduction was independent of whether wildtype MTM1 or the phosphatase dead MTM1-C375S was recruited to endosomes. The same phenotype could also be observed in the T84 wildtype control cells. This argues that the phenotype is not dependent on PI(3)P but the dimerizer itself. Interestingly, when comparing the immune response in the three cell lines without addition of rapalog, cells expressing MTM1-C375S have a lower IFNλ response than T84 wildtype cells and both cells expressing MTM1-wt or MTM1-C375S show a significantly lower IL-6 response compared to T84 wildtype cells (Figure 23).

The experiments presented in this thesis argue for impaired polarization upon PI(3)P depletion by VPS34 inhibition or knock down. This is in concert with previously published results showing the importance of VPS34 for epithelial integrity[103]. Importance of PI(3)P on immunity was not as clear due to inconsistent results when using two different VPS34 inhibitors or knock down of MTM1 and VPS34. Also we observed that in our system chemical dimerization posed a problem as the dimerizer itself interferes with polarization and immunity.

3.4 Creation of New BacMam Viral Vectors

3.4.1 Persistent BacMam Vector

Viral vectors based on Baculoviruses with mammalian expression cassettes (BacMam) are of interest for numerous reasons as described above. This method of gene delivery has been previously established in the lab for transient delivery of transgenes as the efficiency is much higher than transfection and it is much less cytotoxic. Also the commercial vectors allow easy insertions of the gene of interest by Gateway cloning (Figure 24 A). While this works for transient expression, BacMam is unable to establish stable cell lines as the virus neither integrates nor replicates in mammalian cells. If we wanted to use BacMam in our model cell line for the intestinal epithelium, T84 cells, we require a stable cell line as their low transduction efficiency and their slow growth after selection creates a timeframe during which transient expression is lost (Figure 24 C). Also other model systems used in our lab would benefit from a viral vector with such a high cargo capacity, e.g. primary human tissue grown in three dimensional culture (human intestinal organoids). To that end, we decided to modify the commercial BacMam backbone so it can be stably maintained in mammalian cell lines.

To create a persisting BacMam vector, we inserted a self-cleaving peptide sequence from porcine teschovirus-1 (P2A) followed by the puromycin resistance gene and the S/MAR sequence behind the Gateway cloning cassette (Figure 24 B). When the target gene is translated the P2A peptide will cleave it into two functional proteins allowing for puromycin selection of cells expressing the transgene (Figure 24 B). The S/MAR sequence will anchor the vector DNA to the nuclear matrix making sure it will be replicated and remain mitotically stable. The S/MAR sequence was PCR amplified from an existing plasmid (pMAX-SMAR-GFP-P2A-Puro). The existing BacMam pCMV-DEST backbone was amplified as well creating a linearized amplicon opening up the plasmid between the Gateway cassette and the WPRE sequence. The S/MAR containing PCR product was inserted into pCMV-DEST by NEBuilder HiFi Assembly. When a transgene is inserted into this new BacMam S/MAR plasmid, a large mRNA containing the gene of interest, the puromycin resistance gene and the S/MAR sequence will be transcribed.

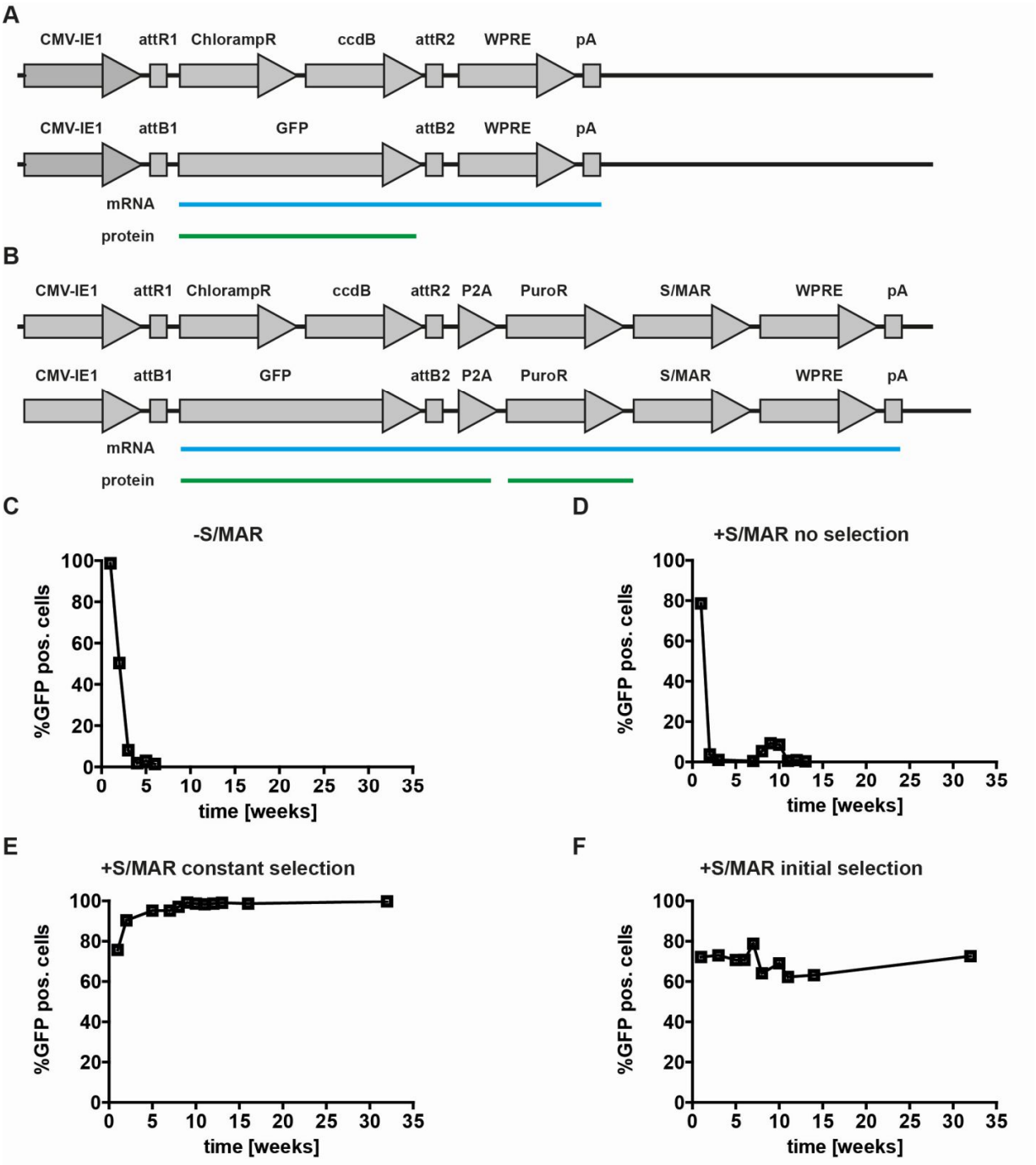

Figure 24: Creation of backbone for recombinant baculoviruses. A) Schematic of the commercial BacMam vector pCMV-DEST with Gateway cloning cassette (top) and as a GFP expression vector (bottom). B) Schematic of the newly created BacMam vector with puromycin resistance gene and S/MAR sequence. The empty vector with the Gateway cloning cassette is depicted on top of an example vector for GFP expression. mRNA and protein produced by either vector are depicted in blue and green respectively. C-F) FACS analysis following GFP expression in HEK 293T cells transduced with the commercial BacMam or the new BacMam S/MAR. C) Cells were transduced with commercial BacMam backbone not carrying the S/MAR sequence or selection marker. **Continued on page 73**

Continued from Figure 24. D) Cells transduced with new BacMam S/MAR that were not selected with puromycin. E) Cells transduced with BacMam S/MAR were kept under selection with 1 µg/ml puromycin for the duration of the experiment. F) Cells with BacMam S/MAR were selected with 1 µg/ml puromycin for one week and cells kept without selection pressure for the rest of the experiment. One week after puromycin removal expression was measured for the first time. CMV-IE1: Cytomegalovirus immediate early promoter; attR1/attR2: recombination sites for Gateway LR reaction; ChlorampR: Chloramphenicol resistance gene; ccdB: kill gene encoding CcdB gyrase poison; WPRE: Woodchuck Hepatitis Virus Posttranscriptional Regulatory Element; pA: polyadenylation signal; GFP: green fluorescent protein; P2A: porcine teschovirus self cleaving peptide; PuroR: puromycin resistance gene; S/MAR: scaffold/matrix attachment region.

The new BacMam S/MAR plasmid was tested by cloning GFP into it, producing viral vectors, and using it to transduce HEK 293T cells. BacMam expressing GFP from the original backbone, without the S/MAR or a selection marker, was used to transduce cells in parallel (Figure 24 C). Two days after transduction virus containing medium was replaced with fresh medium. Cells transduced with BacMam without S/MAR and one sample of BacMam with S/MAR were left without selection to test if S/MAR alone was sufficient to keep GFP expression longer compared to the parental backbone (Figure 24 C and D). Two samples were selected with 1 µg/ml puromycin. One was kept under selection the whole time (Figure 24 E) and the other was selected for only one week and passaged without puromycin for the remaining time (Figure 24 F). Cells transduced with either virus expressed GFP proving that both are functional. Cells transduced with BacMam without the S/MAR sequence lost expression quickly. By week three only 8% of cells still expressed GFP. After six weeks only 1.5% of cells still expressed GFP (Figure 24 C). BacMam expressing the S/MAR sequence mostly lost expression without puromycin selection. Beginning at week three, between 1% and 10% expressed GFP. The low number of expressing cells fits well with reports that only 1-5% of CHO cells transfected with S/MAR plasmids stably anchor and maintain them[138]. When cells transduced with BacMam S/MAR were selected with puromycin, over 95% of cells kept expressing GFP over the course of 32 weeks proving that the puromycin resistance gene as well as the S/MAR sequence are functional and allow the establishment of stable cell lines (Figure 24 E). When after initial selection the puromycin is removed, the percentage of GFP expressing cells remains stable at around 70% indicating that once the extrachromosomal DNA is stably anchored selection pressure can be removed without losing expression (Figure 24 F). Together, these results show that we succeeded in modifying BacMam to express a selection marker and an S/MAR sequence allowing the DNA to be maintained over at least 32 weeks.

3.4.2 BACMAM REPORTER

Now we wanted to utilize the newly created BacMam S/MAR vector. We decided to design a new backbone for reporter constructs. The existing Gateway cassette was replaced with mCherry so that all reporter cells will have constitutive mCherry expression (Figure 25 A and B). The Gateway cassette was moved upstream of the CMV promoter thereby lacking a promoter. In this configuration, Gateway cloning can be used to insert a promoter reporter, e.g. an IFNβ promoter driving expression of luciferase (Figure 25 C).

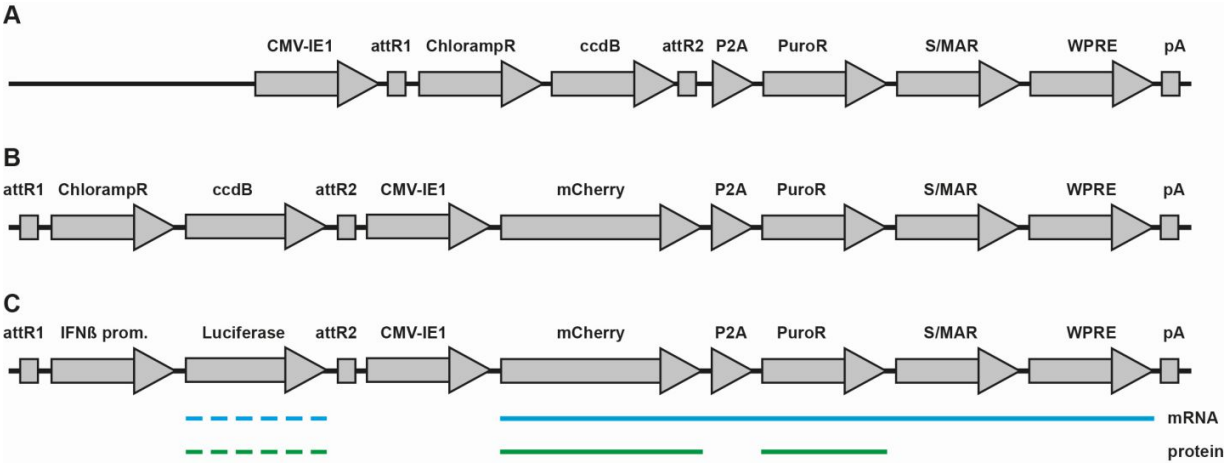

Figure 25: Schematic of the BacMam reporter. A) The new BacMam S/MAR construct. B) BacMam S/MAR was modified to constitutively express mCherry and the puromycin resistance gene. The Gateway cloning cassette was moved upstream without a promoter. C) Same as B except with the IFN beta promoter driving luciferase expression. mRNAs and proteins produced are shown below in blue and green respectively. The dashed lines symbolize expression that depends on reporter activity. CMV-IE1: Cytomegalovirus immediate early promoter; attR1/attR2: recombination sites for Gateway LR reaction; ChlorampR: Chloramphenicol resistance gene; ccdB: kill gene encoding CcdB gyrase poison; WPRE: Woodchuck Hepatitis Virus Posttranscriptional Regulatory Element; pA: polyadenylation signal; GFP: green fluorescent protein; P2A: porcine teschovirus self cleaving peptide; PuroR: puromycin resistance gene; S/MAR: scaffold/matrix attachment region.

A BacMam vector with the IFNβ reporter and a firefly luciferase reporter was used to transduce HEK 293T cells. Cells were kept under selection and expressed mCherry for several months. After about six months, we checked the percentage of reporter positive cells by flow cytometry for mCherry. In line with the results of the BacMam S/MAR vector (Figure 24 E) 100% of the cells expressed mCherry (Sup. Figure 9). Next we wanted to verify that the cells do not only express mCherry but have a functional IFNβ reporter. Therefore we transiently transduced HEK 293T cells and infected them with reovirus two days later or infected the HEK 293T cell line stably expressing the reporter construct for six months. Both cell lines show a

significant induction of luciferase expression when tested 24 hours post reovirus infection (Figure 26). These experiments show that we successfully modified a BacMam expression vector to express a selection marker and an S/MAR sequence allowing for establishment of stable cell lines (Figure 24). Additionally, we further modified this new BacMam vector to allow easy cloning of reporter cassettes using the Gateway system (Figure 25) and verified its functionality (Figure 26).

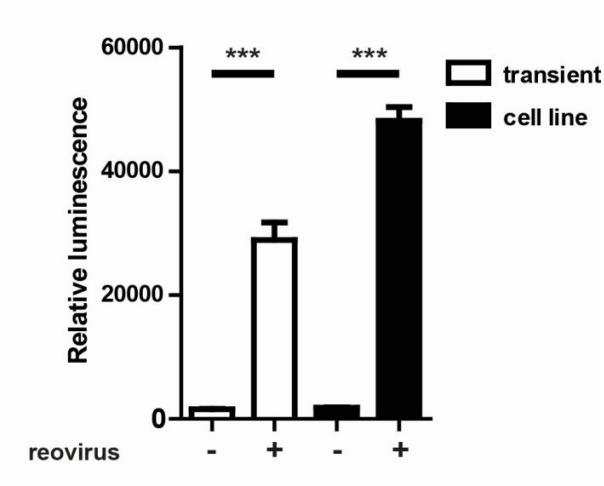

Figure 26: BacMam IFNβ luciferase reporter in HEK 293T cells. Wildtype HEK 293T cells transiently transduced with BacMam IFNβ reporter for 48 hours (white box) or HEK293T cells stably expressing the IFNβ reporter for six months were infected with reovirus. 24 hours post reovirus infection luciferase values were measured. Three independent experiments with standard deviation are shown. The relative luminescence of non infected and infected cells was compared using an unpaired, two-tailed t-test with $P > 0.05$; * = $P \leq 0.05$; ** = $P \leq 0.01$; *** = $P < 0.001$.

4 DISCUSSION

4.1 PHOSPHOINOSITIDE PROJECT

The main objective of this thesis was to elucidate the role of endosomal PI(3)P in establishing and maintaining polarity as well as in immune signaling. PI(3)P is reported to be the predominant phosphoinositide in early endosomes[146]. We could verify this localization in our intestinal epithelial cells where PI(3)P showed a strong overlap with the early endosome marker EEA1 (Figure 5 B). We originally used specific inhibitors of VPS34, the main source of endosomal PI(3)P, to determine the role of PI(3)P on cellular polarization and immune induction[147,148]. First we determined the amount of inhibitors needed to remove PI(3)P from the endosomes. We showed that 1 µM of two selected inhibitors clearly reduced but not completely removed endosomal PI(3)P in T84 cells (Figure 6 and Figure 7). When either 5 µM VPS34-IN1 or 6 µM SAR405 were used, the endosomal PI(3)P staining was completely lost (Figure 6 and Figure 7). Our result that 1 µM VPS34-IN1 significantly reduces but not completely removes PI(3)P fits well with published data[148]. 1 µM SAR405 on the other hand did not seem have any residual PI(3)P in the original publication[147]. This difference between our data and the published data could be due to the different cell lines used. As expected, the higher concentrations worked better for both inhibitors and removed PI(3)P completely (Figure 6 and Figure 7). Both inhibitors shared their quick mode of action and long lasting effect. Even after 24 hours the PI(3)P pools did not reappear at either concentration. The IC_{50} of SAR405 for other PI3-kinasese is over 10 µM so 6 µM SAR405 should still specifically inhibit VPS34[147]. For VPS34-IN1 on the other hand results are not as clear. Depending on which lipid kinase panel was used, several class I and II PI3-kinases had IC_{50} values below 5 µM. We decided to continue with three different conditions. 6 µM SAR405 as it completely removes PI(3)P, does not inhibit other PI3-kinases, and was used in the related cell line Caco-2 to show the importance of VPS34 for epithelial integrity (Figure 7)[103,147] For VPS34-IN1 both 1 µM and 5 µM were used. While 5 µM completely removes endosomal PI(3)P, it could potentially inhibit other kinases as well (Figure 6)[148]. To avoid the possibility of off-target effects we included 1 µM VPS34-IN1 at the risk of insufficient removal of PI(3)P.

Having established the inhibitor is functional, we continued by assessing its impact on polarization. As described in the introduction, there is a strong link between tight junctions and

polarity. Tight junction formation can be followed over time by measuring the trans-epithelial electrical resistance (TEER). Treating T84 wildtype cells with 1 µM VPS34-IN1 had an effect on polarization (Figure 9 and Sup. Figure 2). If added at day one, polarization progressed slower as seen by the longer time needed to reach 1000 Ω (Figure 9 and Sup. Figure 2 A and C). The same delayed polarization could be seen when the inhibitor was added after three days. Addition of the inhibitor at day six, when the cells were fully polarized, again resulted in an abrupt slow down of polarization. Treatment with 5 µM VPS34-IN1 showed the same phenotype seen with 1 µM but the phenotype was even more pronounced (Figure 10 and Sup. Figure 3). Addition of inhibitor at day one prevented polarization as cells even after nine days did not reach 1000 Ω. If added after three days cells did polarize but the values were much lower than in the mock control. Also TEER values decreased over time ending up below 1000 Ω when the timecourse ended at day nine. If cells were already polarized when the inhibitor was added it resulted in an abrupt and drastic decrease in TEER values. Lastly we tested polarization with 6 µM SAR405 (Figure 11 and Sup. Figure 4). Similar to VPS34-IN1, treating cells with SAR405 from day one prevents normal polarization. Only at the end of the timecourse, when the TEER control cells peaked, TEER values reached 1000 Ω. When the inhibitor was added after three or six days, the results were very similar to 1 µM VPS34-IN1 (Figure 9 and Sup. Figure 2). To exclude that the decreased TEER resulted from holes in the monolayer due to cell death, we stained the nuclei with DAPI at the end of the timecourse. Cells still formed monolayers when the inhibitor was added at day three or later (Figure 12). This showed us that neither delayed TEER development nor a significant drop in TEER was due to cell death. Since cells still formed monolayers but the TEER was reduced we assume that the tight-junctions are impaired which is indicating a problem with polarization upon inhibitor induced PI(3)P depletion as was published[103]. PI(3)P recruits the protein WDFY2 which then negatively regulates LKB1. Loss of PI(3)P or VPS34 results in increased LKB1 phosphorylation and activation of AMPK, a pathway that has been known to be involved in tumor development and epithelial polarity[103,179]. Furthermore it is interesting, that Arp2/3 has been shown to mediate the polarized distribution of PAR6 in *C. elegans*[104]. Arp2/3 in turn is regulated by the WASH complex that can bind to PI(3)P and $PI(3,5)P_2$[180]. PAR6 is known to regulate polarity and formation of tight junctions and misregulation results in lower TEER values[181].

Next we wanted to use the VPS34 inhibitors to investigate the role of PI(3)P in immunity. Over the last years, a role for the intestinal virome in health and disease has become clear. Links between the intestinal virome, Crohn's disease and ulcerative colitis have been found[182,183]. It was also shown that murine norovirus (MNV) can replace the microbiome in germ-free mice[184]. MNV re-established normal intestinal morphology, partially protected the mice from chemically induced intestinal damage, and improved symptoms of *Citrobacter rodentium* infection[184]. Therefore we decide to use reovirus, a commonly used model for enteric viruses, to evaluate the role of PI(3)P in detecting and propagating an immune response after viral infection. From experiments in our lab, we know that reovirus efficiently infects T84 cells (Figure 2)[159,161]. Reovirus has a double stranded RNA genome (dsRNA). After entry the virion is trafficked through early and late endosomes before it escapes into the cytoplasm. Reovirus is recognized by TLR3 and RLRs[159,185,186]. Because early to late endosome maturation and TLR3 signaling both utilize endosomal PI(3)P reovirus infection is a relevant model for our purposes. As described in the results section, we chose IFNλ, IL-6, and IL-8 as readouts as they are relevant in intestinal epithelia cells and expressed by T84 cells upon reovirus infection (Figure 14 and Figure 15)[103,160,162–164].

While we knew that both PI(3)P inhibitors worked very fast (Figure 6 and Figure 7), we wanted to test if cells need to be pre-treated prior to infection. Also we wanted to establish whether to harvest samples after 16 or 24 hours (Figure 13). To that end T84 cells were either mock treated or pre-treated with 5 μM VPS34-IN1 for one hour. Afterwards cells were infected with or without 5 μM VPS34-IN1 for 16 and 24 hours. As expected, IFNλ, IL-6 and IL-8 were all produced upon reovirus infection and harvesting at 24 hours post infection yielded higher quantities. Treatment with 5 μM VPS34-IN1 resulted in a reduced immune response for all three readouts (Figure 13). Pre-treatment with VPS34-IN1 did not improve this phenotype which fits very well with the observation that endosomal PI(3)P is already removed after 15 minutes (Figure 6). Contrary to PI(3)P depletion by 5 μM VPS34-IN1, SAR405 treatment resulted in significantly increased IFNλ, IL-6, and IL-8 production. While it contradicts our results for 5 μM VPS34-IN1, an increased IL-6 production upon TLR4 and TLR1/2 stimulation in bone marrow-derived dendritic treated with 1μM VPS34-IN1 or SAR405 cells has been reported[165]. We wanted to exclude that the reduced response with 5 μM VPS34-IN1 was not due to off-target effects due to the relatively high inhibitor concentration. When we repeated the experiment with 1 μM VPS34-

IN1 we did not observe any changes in IFNλ, IL-6, or IL-8 levels upon infection. The fact that 1 µM VPS34-IN1 does not change the immune response but 5 µM shows and effect, could either be due to insufficient removal of PI(3)P with 1 µM VPS34-IN1 or off-target effects with 5 µM VPS34-IN1 (Figure 6)[148]. Taken together, the discrepancy between the two inhibitors makes it impossible to make assumptions about the role of PI(3)P in the immune response to reovirus in T84 cells. Conflicting publications make it even more difficult to determine which phenotype is correct. One publication showed that VPS34 inhibition increased the immune response TLR4 stimulation while another identified the PI(3)P effector WDFY1 as an adaptor in TLR3/4 signaling which would argue for attenuated signaling upon VPS34 inhibition[109,165]. To further clarify which phenotype is correct, we have to use other VPS34 inhibitors, e.g. VPS34 inhibitor 1 (Compound 19, PIK-III analogue) or autophinib[187,188].

Finally we showed that the relative infectivity of reovirus was reduced in T84 cells treated with both VPS34 inhibitors (Figure 16). This would fit nicely with the role of PI(3)P in endosome maturation and the requirement of reovirus to traffic from early to late endosomes before entering the cytoplasm and replication[86,185]. More experiments will be necessary to clarify the role of VPS34 and PI(3)P in reovirus infection.

As the inhibitors could give rise to off target effects and provided conflicting results we moved to a new method to modify endosomal PI(3)P levels by knocking down PI(3)P metabolizing enzymes. The major player in early endosome PI(3)P metabolism are VPS34 (Figure 6 and Figure 7) and MTM1[91]. Of the shRNAs tested against both proteins, all but one (shVPS34 #1) reduced mRNA levels to 30% or less compared to the scrambled control (Figure 17 A). Cell lines expressing shMTM1 #1 and shVPS34 #3 were chosen to continue. They kept their knock-down on the RNA and protein level showing us that the knock-down cell lines were successfully established (Figure 17 B and C). These cell lines were used to test both polarization and immune response. As before, knock-down cell lines were seeded on transwell inserts and the TEER development was followed over nine to ten days (Figure 18). TEER values of scrambled control cells developed as wildtype cells (e.g. Figure 9 A). Interestingly, knock-down of VPS34 changed TEER development. While cells did not polarize much slower, indicated by the time they reached 1000 Ω, their TEER developed slowed down afterwards and stayed lower (Figure 18). This fits well with the observations made in the inhibitor treated cells that did not reach as high TEER values (Figure 9, Figure 10, and Figure 11). The stronger effect of 5 µM VPS34-IN1

or 6 µM SAR405 most likely reflects a more efficient PI(3)P depletion, especially when added at day one where it prevents cells from forming a full monolayer (Figure 12). When the inhibitor was added at later times the results are very similar compared to the VPS34 knock-down. It is still surprising to see that polarization is not impaired given that MTM1 mutations in humans are associated with x-linked myotubular myopathy (XLMTM). Cell lines derived from these patients show increased PI(3)P levels and defective exocytosis which points toward trafficking defects[78]. These cells have an intracellular accumulation of β1-integrin which in polarized epithelial cells is required for establishing apico-basal polarity. The same intracellular aggregation of β1-integrin can be seen in MTM1 knock-down HeLa cells[78]. This either means that trafficking of β1-integrin in these cells differs from T84 cells or the β1-integrin levels at the plasma membrane are still high enough to induce polarization. This could be tested by comparing intracellular and cell surface levels between the knock-down cell lines. Knock-down of MTM1 did not lead to major differences compared to the scrambled control (Figure 18). This indicates that an increase of PI(3)P does not further improve polarization. In order to verify that, an immunostaining of PI(3)P levels in the knock-down cell lines needs to be performed. However, as the knock-down worked efficiently (Figure 17) and VPS34 is the main source of endosomal PI(3)P (Figure 6 and Figure 7) it is very likely that PI(3)P levels are reduced.

As with the inhibitor treated cells we wanted to test the immune response to reovirus infection. Cells were infected with reovirus one day after seeding and samples harvested 24 hours post infection (Figure 19). The IFNλ response is significantly increased in MTM1 knock-down cells while it is significantly decreased upon VPS34 knock-down (Figure 19 A and B). One possible explanation is the PI(3)P binding sorting adaptor WDFY1[109]. Another, and even more intriguing, explanation is based on TLR3 signaling through two different pathways. TLR3 can signal via TRIF, TRAF6, RIP1, TAK1 and NF-κB which leads to the production of proinflammatory cytokines[42]. Signaling via TRIF, TRAF3, TBK1/IKKi drives IRF3 mediated interferon production[42]. Interestingly it was shown that PI(5)P produced by PIKfyve binds TBK1 and IRF3 to mediate IRF3 phosphorylation and activation[189]. This enhances downstream signaling, e.g. IFNβ production[189]. NF-κB mediated cytokine production on the other hand was not influenced by PIKfyve and PI(5)P. This was true for TLR3 and TLR4 signaling and therefore argues for a general method of IRF3 regulation independent of the receptor the signal originally comes from. This is particularly interesting since RLRs signal via IRF3 and NF-κB as well[190].

And while the role of phosphoinositides in innate immunity is normally investigated for TLRs this offers an intriguing mechanism of how phosphoinositides can regulate RLR signaling as well. While it is known that PIKfyve is the kinase producing most of the PI(5)P, the exact pathway is under debate. A direct phosphorylation of phosphatidylinositol is one option. But since it is known that PIKfyve makes $PI(3,5)P_2$ from PI(3)P it is possible that at least some of the cells PI(5)P is produced through an $PI(3,5)P_2$ intermediate and subsequent dephosphorylation by a 3-phosphatase[191]. The latter pathway is interesting since it would link PI(3)P to PI(5)P and thereby to IRF3 mediated interferon production through diverse receptors including RLRs. This could explain the IFNλ response seen (Figure 19). Knock-down of MTM1 increases PI(3)P levels which could shift the equilibrium toward higher $PI(3,5)P_2$ and PI(5)P concentration increasing the IFNλ response. Also MTM1 has been shown to dephosphorylate $PI(3,5)P_2$ *in vitro* to produce PI(5)P[178]. Knock-down of VPS34 on the other hand reduces the PI(3)P level and thereby PI(5)P which would explain the lowered response. To verify the higher or lower IRF3 activation levels in MTM1 and VPS34 knock-down cell lines respectively one could analyze IRF3 phosphorylation levels or relocalization of activated IRF3-GFP into the nucleus[157]. However, this pathway could not explain the IL-6 and IL-8 responses seen as both are produced NF-κB-dependent pathways and should therefore not be affected[192–194].

MTM1 knock-down increases the IL-6 response while VPS34 knock-down does not have any impact. IL-8 on the other hand seems to be reduced in both knock-downs (Figure 19). Since they are both produce in an NF-κB-dependent pathway they should behave similar. As this is not the case, their signaling cascades might differ in certain components making it more or less susceptible to changed PI(3)P levels. It was published that Rac1 and Cdc42 regulate IL-8 secretion in MDCK cells while NF-κB and MAP kinase signaling is not imparied[195]. Both Rac1 and Cdc42 are parts of the epithelial polarity program and PI(3)P is linked to polarity (Figure 9, Figure 10, Figure 11, and Figure 17)[103]. One could imagine that the differences seen in Figure 19 are not due to differences in IL-8 production but secretion. ELISA analysis of cell lysates instead of supernatants could help to answer that question. Also one should keep in mind that knock-down cells have reduced protein levels. Both MTM1 and VPS34 interact with various other proteins and it is perceivable that reduced MTM1 or VPS34 levels interfere with the correct function of one or more of their binding partners[96,169].

Finally we wanted to use a more advanced method of manipulating endosomal PI(3)P by utilizing chemically induced dimerization (CID) (Figure 20). The major advantage of this system is the spatio-temporal control. This is especially important because inhibition and knock-down target both the autophagy and endosome associated VPS34 complexes indiscriminately[96,147]. We chose a Rab5 anchor for early endosomes and the PI(3)P phosphatase MTM1 either as full-length wildtype enzyme or the phosphatase-dead C375S mutant as the players for our system (Figure 20)[175,176]. Furthermore we chose to use a mutated form of the FRB domain, FRB*, as it allows us to use a rapalog instead of rapamycin which would interfere with endogenous mTOR, a central regulator of metabolism[174,196].

To verify loss of PI(3)P upon recruitment of MTM1 wildtype, we would ideally use an anti-GFP antibody (Figure 5 A) but as the Rab5 anchor is fused to GFP, this is not an option (Figure 20). Additionally, due to our cellular system, transfecting a fluorescently tagged PI(3)P sensor was not a viable option (Sup. Figure 1). Therefore, we chose to use an indirect method based on morphology. It was reported that endosomes become enlarged or tubularized upon PI(3)P depletion which we confirmed in the easily transfectable HEK 293T cells[171,177]. When MTM1 wildtype is recruited to early endosomes they lose their PI(3)P and change morphology (Figure 21 A). MTM1-C375S on the other hand is recruited but does not change PI(3)P levels or endosome morphology (Figure 21 B). Since VPS34 inhibition also induces enlarged endosomes (Figure 21 C), we assume that this change is due to loss of PI(3)P and not induced by rapalog or recruitment of MTM1 itself. In fact, when we use our T84 cell line expressing the Rab5-GFP anchor and MTM1 wildtype we can see the same changes in endosome morphology indicating that the system works in T84 cells (Figure 21 D).

To test the impact of PI(3)P on polarization in this inducible system, we followed the same protocol as during the inhibitor treatment but added rapalog instead of VPS34 inhibitors (Figure 8 C). We compared the effect between T84 cell lines expressing a Rab5 anchor and either MTM1 wildtype or MTM1-C375S with normal T84 wildtype cells (Figure 22). Addition of rapalog one day post seeding prevented polarization. As this is the case in MTM1-C375S and wildtype cells, it is not due to loss of PI(3)P but to off target effects of the rapalog. Adding rapalog at later times also interfered with polarization. While cells still polarized, TEER > 1000 Ω, it was clearly slowed down or even decreased. Unfortunately this was true in all three cell lines indicating that the observed phenotype was again due to rapalog treatment itself. We further

checked the immune response in all three cell lines with or without rapalog (Figure 23). Rapalog reduced the immune response independent of the cell line used. Together with the observations of polarization, this further strengthens the argument that rapalog interferes with normal T84 cell function and is not usable for our purpose. Interestingly there are some significant differences in the immune response between the cell lines without rapalog, i.e. lower IFNλ expression in MTM1-C375S cells than in T84 wildtype cells and reduced IL-6 production in MTM1 wildtype and MTM1-C375S compared to T84 wildtype cells (Figure 23). Such differences might be explained by the fact that we are overexpressing full-length MTM1. It is perceivable that the full length enzyme, wildtype and C375S, can interact with their endogenous binding partners mimicking a normal protein overexpression even without inducing dimerization. It was shown that when MTM1-C375S and MTM1 wildtype are overexpressed in HEK 293T cells, MTM1-C375S increases PI(3)P levels relative to MTM1 wildtype[175]. Interestingly, is has been shown that MTM1 can dephosphorylate PI(3,5)P2. The resulting PI(5)P induces MTM1 to form a heptameric ring which acts as an allosteric acitivator[178]. MTM1-C375S can form this ring together with wildtype proteins increasing their activity. This could explain how even a catalytically dead enzyme can change the cellular response, e.g. lower IL-6 response in both MTM1 wildtype and MTM1-C375S. One step to avoid such potential problems in the future would be the use of a truncated protein. However, a larger problem with this system is the dimerizer itself and in order to use a chemical dimerizer system we first need to find a dimerizer lacking cellular targets. One option would be the reversible chemical dimerizer rCD1[197]. While having slightly slower kinetics, it would give us the option to remove MTM1 from the endosomes with addition of FK506 (Tacrolimus). Still one should keep in mind that FK506 itself is an immunosuppressant that binds to FKBP to inhibit calcineurin and has to be tested for its impact on T84 polarity and immunity[198].

During this project we could verify a role of VPS34 and PI(3)P in cellular polarization by using inhibitors or knock-down. This fits with recently published results regarding the role of VPS34 in maintaining epithelial integrity[103]. The impact on immunity is less clear due to conflicting results of the two VPS34 inhibitors used. The results in our knock-down cell lines are interesting, especially the impact on IFNλ which fits well with the link between PI(3)P, PI(5)P and IRF3 mediated interferon expression. The results regarding IL-6 and IL-8 are unfortunately not as clear and will require further investigation. Furthermore we managed to establish a

chemically induced dimerization system in T84 cells and verify its functionality. Unfortunately, while being a very promising approach, the side effects of rapalog keep us from using it for now. If another dimerizer is found that does not interfere with our cells and if truncated enzymes are used this could become a fantastic tool allowing us to dissect the role of individual phosphoinositides in polarity and immunity with an unprecedented spatio-temporal control.

4.2 BacMam Project

The goal of this project was to establish a persisting BacMam vector using an S/MAR sequence. We modified a commercial BacMam that is already used in our lab and allows us efficient cloning with the Gateway system (Figure 24 A). We inserted the puromycin resistance gene downstream of the Gateway cloning cassette (Figure 24 B), and a self-cleaving P2A sequence from porcine teschovirus-1 allowing us to split the protein of interest from the resistance gene upon translation. Further downstream we inserted the S/MAR sequence facilitating the episomal maintenance[128]. We chose this method as it does not require expression of a viral oncogene or integration into the host cell genome and should therefore have a better biosafety profile[120,122–124]. Also the S/MAR sequence has been suggested to prevent epigenetic silencing of the CMV promoter and specifically links the plasmid to nuclear compartments in which active transcription takes place[138,139]. We then transduced HEK 293T cells with viral vectors expressing GFP either from the original backbone without S/MAR (Figure 24 C) or from the new S/MAR backbone (Figure 24 D-F). As expected, cells transduced with the commercial BacMam lost expression within two to three weeks (Figure 24 C)[123]. Only a few percent of cells transduced with BacMam S/MAR without selection kept their expression (Figure 24 D). This was not unexpected as it was reported that only between one and five percent of CHO cells transfected with an S/MAR plasmid will maintain it[129,137,138]. When cells were kept under constant selection, within a short time all cells expressed GFP and kept expression for over 30 weeks (Figure 24 E). To verify the report that no selection pressure is required for maintenance of S/MAR plasmids once they are stably anchored, we removed the selection pressure from one sample after one week (Figure 24 F)[129,137,138]. Indeed we can see that the S/MAR sequence maintains the vector. Between 60 and 80 percent of cells keep expressing GFP for over 30 weeks. The lower percentage of GFP positive cells compared to cells under constant selection indicates that not all cells had stably anchored the vector DNA at the time the selection pressure was removed (Figure 24 E and F).

Next we wanted to modify the BacMam S/MAR vector to allow expression of reporter constructs. Therefore we moved the Gateway cloning cassette upstream of the CMV promoter and inserted mCherry between the CMV promoter and the puromycin resistance gene (Figure 25 B). This construct allows us easy cloning of reporters into the promoterless Gateway cassette, antibiotic selection and tracking of transduced cells through mCherry expression. To test the

construct we cloned a firefly luciferase driven by an IFNβ promoter (Figure 25 C). This construct was used to make stable HEK 293T cell lines which kept expression for about six months (Sup. Figure 9). This cell line and HEK 293T cells transiently transduced with the same BacMam vector were infected with reovirus and the luciferase activity measured (Figure 26). Both, transient and stable expressing cells, showed a clear induction of the IFNβ reporter upon infection proving the BacMam reporter construct is functional.

Taken together these results show that we successfully created a persistent BacMam and further modified it to allow for reporter gene expression (Figure 24 B and Figure 25). Both constructs are functional and were able to drive expression in HEK 293T cells for up to half a year (Figure 24 C-F, Figure 26, and Sup. Figure 9). This is, to our knowledge, the first time a persistent baculovirus vector is described that does not rely on integration or viral genes. Vectors established by others either use integration via the sleeping beauty transposon or AAV ITRs and the AAV rep gene or rely on the EBV origin of replication which requires expression of the viral oncogene EBNA1[120,122–124]. While an S/MAR sequence has been integrated into a baculovirus genome before, it did not result in prolonged expression, possibly due to the lack of antibiotic selection[199]. They also did not try to maintain the whole viral genome. The transgene was recombined into a minicircle, small circular DNA that is devoid of bacterial sequences and maintained via an S/MAR sequence[200]. This required simultaneous transduction with a second baculovirus[199].

Next we will have to verify that the vector really is maintained episomally and does not integrate. Also it has to be tested for stable expression in T84 cells or even human intestinal organoids. It would be interesting to further modify the reporter backbone by adding a second reporter for interferon stimulated genes (ISGs). This would allow us to follow both induction of interferon and the downstream signaling. This would be especially interesting in three dimensional cell culture, i.e. spheroids or human intestinal organoids.

5 REFERENCES

1. Ebnet, K. *Cell polarity. 1, 1,*. (2015).
2. Bentley, M. & Banker, G. The cellular mechanisms that maintain neuronal polarity. *Nat. Rev. Neurosci.* **17,** 611–622 (2016).
3. Peterson, L. W. & Artis, D. Intestinal epithelial cells: regulators of barrier function and immune homeostasis. *Nat. Rev. Immunol.* **14,** 141–153 (2014).
4. Klunder, L. J., Faber, K. N., Dijkstra, G. & van IJzendoorn, S. C. D. Mechanisms of Cell Polarity–Controlled Epithelial Homeostasis and Immunity in the Intestine. *Cold Spring Harb. Perspect. Biol.* **9,** a027888 (2017).
5. Abreu, M. T. Toll-like receptor signalling in the intestinal epithelium: how bacterial recognition shapes intestinal function. *Nat. Rev. Immunol.* **10,** 131–144 (2010).
6. Kiela, P. R. & Ghishan, F. K. Physiology of Intestinal Absorption and Secretion. *Best Pract. Res. Clin. Gastroenterol.* **30,** 145–159 (2016).
7. Muniz, L. R., Knosp, C. & Yeretssian, G. Intestinal antimicrobial peptides during homeostasis, infection, and disease. *Front. Immunol.* **3,** 310 (2012).
8. Schonhoff, S. E., Giel-Moloney, M. & Leiter, A. B. Minireview: Development and differentiation of gut endocrine cells. *Endocrinology* **145,** 2639–2644 (2004).
9. Kaelberer, M. M. & Bohórquez, D. V. The now and then of gut-brain signaling. *Brain Res.* (2018). doi:10.1016/j.brainres.2018.03.027
10. Mabbott, N. A., Donaldson, D. S., Ohno, H., Williams, I. R. & Mahajan, A. Microfold (M) cells: important immunosurveillance posts in the intestinal epithelium. *Mucosal Immunol.* **6,** 666–677 (2013).
11. Lloyd-Price, J., Abu-Ali, G. & Huttenhower, C. The healthy human microbiome. *Genome Med.* **8,** (2016).

12. Rodriguez-Boulan, E. & Macara, I. G. Organization and execution of the epithelial polarity programme. *Nat. Rev. Mol. Cell Biol.* **15,** 225–242 (2014).

13. O'Brien, L. E. *et al.* Rac1 orientates epithelial apical polarity through effects on basolateral laminin assembly. *Nat. Cell Biol.* **3,** 831–838 (2001).

14. Bryant, D. M. *et al.* A molecular network for de novo generation of the apical surface and lumen. *Nat. Cell Biol.* **12,** 1035–1045 (2010).

15. Martin-Belmonte, F. *et al.* PTEN-mediated apical segregation of phosphoinositides controls epithelial morphogenesis through Cdc42. *Cell* **128,** 383–397 (2007).

16. Bryant, D. M. *et al.* A molecular switch for the orientation of epithelial cell polarization. *Dev. Cell* **31,** 171–187 (2014).

17. Mrozowska, P. S. & Fukuda, M. Regulation of podocalyxin trafficking by Rab small GTPases in 2D and 3D epithelial cell cultures. *J. Cell Biol.* **213,** 355–369 (2016).

18. Caplan, M. J. *et al.* Dependence on pH of polarized sorting of secreted proteins. *Nature* **329,** 632–635 (1987).

19. Román-Fernández, A. & Bryant, D. M. Complex Polarity: Building Multicellular Tissues Through Apical Membrane Traffic. *Traffic Cph. Den.* **17,** 1244–1261 (2016).

20. Gassama-Diagne, A. *et al.* Phosphatidylinositol-3,4,5-trisphosphate regulates the formation of the basolateral plasma membrane in epithelial cells. *Nat. Cell Biol.* **8,** 963–970 (2006).

21. Füllekrug, J., Shevchenko, A., Shevchenko, A. & Simons, K. Identification of glycosylated marker proteins of epithelial polarity in MDCK cells by homology driven proteomics. *BMC Biochem.* **7,** 8 (2006).

22. Benton, R. & St Johnston, D. Drosophila PAR-1 and 14-3-3 inhibit Bazooka/PAR-3 to establish complementary cortical domains in polarized cells. *Cell* **115,** 691–704 (2003).

23. Morais-de-Sá, E., Mirouse, V. & St Johnston, D. aPKC Phosphorylation of Bazooka Defines the Apical/Lateral Border in Drosophila Epithelial Cells. *Cell* **141,** 509–523 (2010).

24. Harris, T. J. C. & Peifer, M. The positioning and segregation of apical cues during epithelial polarity establishment in Drosophila. *J. Cell Biol.* **170,** 813–823 (2005).

25. Suzuki, A. *et al.* aPKC acts upstream of PAR-1b in both the establishment and maintenance of mammalian epithelial polarity. *Curr. Biol. CB* **14,** 1425–1435 (2004).

26. Plant, P. J. *et al.* A polarity complex of mPar-6 and atypical PKC binds, phosphorylates and regulates mammalian Lgl. *Nat. Cell Biol.* **5,** 301–308 (2003).

27. Tanos, B. & Rodriguez-Boulan, E. The epithelial polarity program: machineries involved and their hijacking by cancer. *Oncogene* **27,** 6939–6957 (2008).

28. Wang, X., Kumar, R., Navarre, J., Casanova, J. E. & Goldenring, J. R. Regulation of vesicle trafficking in madin-darby canine kidney cells by Rab11a and Rab25. *J. Biol. Chem.* **275,** 29138–29146 (2000).

29. Vogel, G. F. *et al.* Cargo-selective apical exocytosis in epithelial cells is conducted by Myo5B, Slp4a, Vamp7, and Syntaxin 3. *J. Cell Biol.* **211,** 587–604 (2015).

30. Lock, J. G. & Stow, J. L. Rab11 in recycling endosomes regulates the sorting and basolateral transport of E-cadherin. *Mol. Biol. Cell* **16,** 1744–1755 (2005).

31. Klinkert, K., Rocancourt, M., Houdusse, A. & Echard, A. Rab35 GTPase couples cell division with initiation of epithelial apico-basal polarity and lumen opening. *Nat. Commun.* **7,** 11166 (2016).

32. Mrozowska, P. S. & Fukuda, M. Regulation of podocalyxin trafficking by Rab small GTPases in epithelial cells. *Small GTPases* **7,** 231–238 (2016).

33. Kumichel, A., Kapp, K. & Knust, E. A Conserved Di-Basic Motif of Drosophila Crumbs Contributes to Efficient ER Export: ER Export of Crb. *Traffic* **16,** 604–616 (2015).

34. Lin, Y.-H. *et al.* AP-2-complex-mediated endocytosis of Drosophila Crumbs regulates polarity by antagonizing Stardust. *J. Cell Sci.* **128,** 4538–4549 (2015).

35. Müsch, A., Cohen, D., Kreitzer, G. & Rodriguez-Boulan, E. cdc42 regulates the exit of apical and basolateral proteins from the trans-Golgi network. *EMBO J.* **20,** 2171–2179 (2001).

36. Kroschewski, R., Hall, A. & Mellman, I. Cdc42 controls secretory and endocytic transport to the basolateral plasma membrane of MDCK cells. *Nat. Cell Biol.* **1,** 8–13 (1999).

37. Shin, K., Fogg, V. C. & Margolis, B. Tight junctions and cell polarity. *Annu. Rev. Cell Dev. Biol.* **22,** 207–235 (2006).

38. Hirose, T. *et al.* Involvement of ASIP/PAR-3 in the promotion of epithelial tight junction formation. *J. Cell Sci.* **115,** 2485–2495 (2002).

39. Chen, X. & Macara, I. G. Par-3 controls tight junction assembly through the Rac exchange factor Tiam1. *Nat. Cell Biol.* **7,** 262–269 (2005).

40. Fogg, V. C. Multiple regions of Crumbs3 are required for tight junction formation in MCF10A cells. *J. Cell Sci.* **118,** 2859–2869 (2005).

41. Viloria-Petit, A. M. *et al.* A role for the TGF -Par6 polarity pathway in breast cancer progression. *Proc. Natl. Acad. Sci.* **106,** 14028–14033 (2009).

42. Kawasaki, T. & Kawai, T. Toll-like receptor signaling pathways. *Front. Immunol.* **5,** 461 (2014).

43. Brown, J., Wang, H., Hajishengallis, G. N. & Martin, M. TLR-signaling networks: an integration of adaptor molecules, kinases, and cross-talk. *J. Dent. Res.* **90,** 417–427 (2011).

44. Chow, K. T., Gale, M. & Loo, Y.-M. RIG-I and Other RNA Sensors in Antiviral Immunity. *Annu. Rev. Immunol.* **36,** 667–694 (2018).

45. Botos, I., Segal, D. M. & Davies, D. R. The Structural Biology of Toll-like Receptors. *Structure* **19,** 447–459 (2011).

46. Kawai, T. & Akira, S. The role of pattern-recognition receptors in innate immunity: update on Toll-like receptors. *Nat. Immunol.* **11,** 373–384 (2010).

47. Brubaker, S. W., Bonham, K. S., Zanoni, I. & Kagan, J. C. Innate immune pattern recognition: a cell biological perspective. *Annu. Rev. Immunol.* **33,** 257–290 (2015).

48. Jiang, S., Li, X., Hess, N. J., Guan, Y. & Tapping, R. I. TLR10 Is a Negative Regulator of Both MyD88-Dependent and -Independent TLR Signaling. *J. Immunol. Baltim. Md 1950* **196,** 3834–3841 (2016).

49. Le, H. V. & Kim, J. Y. Stable Toll-Like Receptor 10 Knockdown in THP-1 Cells Reduces TLR-Ligand-Induced Proinflammatory Cytokine Expression. *Int. J. Mol. Sci.* **17,** (2016).

50. Odendall, C. *et al.* Diverse intracellular pathogens activate type III interferon expression from peroxisomes. *Nat. Immunol.* **15,** 717–726 (2014).

51. Cario, E. & Podolsky, D. K. Differential alteration in intestinal epithelial cell expression of toll-like receptor 3 (TLR3) and TLR4 in inflammatory bowel disease. *Infect. Immun.* **68,** 7010–7017 (2000).

52. Lee, J. *et al.* Maintenance of colonic homeostasis by distinctive apical TLR9 signalling in intestinal epithelial cells. *Nat. Cell Biol.* **8,** 1327–1336 (2006).

53. Kubinak, J. L. & Round, J. L. Toll-like receptors promote mutually beneficial commensal-host interactions. *PLoS Pathog.* **8,** e1002785 (2012).

54. Sazanov, L. A. A giant molecular proton pump: structure and mechanism of respiratory complex I. *Nat. Rev. Mol. Cell Biol.* **16,** 375–388 (2015).

55. Perera, R. M. & Zoncu, R. The Lysosome as a Regulatory Hub. *Annu. Rev. Cell Dev. Biol.* **32,** 223–253 (2016).

56. Fahy, E. *et al.* A comprehensive classification system for lipids. *J. Lipid Res.* **46,** 839–861 (2005).

57. Fahy, E. *et al.* Update of the LIPID MAPS comprehensive classification system for lipids. *J. Lipid Res.* **50 Suppl,** S9-14 (2009).

58. Sampaio, J. L. *et al.* Membrane lipidome of an epithelial cell line. *Proc. Natl. Acad. Sci.* **108,** 1903–1907 (2011).

59. Yoshizaki, H., Ogiso, H., Okazaki, T. & Kiyokawa, E. Comparative lipid analysis in the normal and cancerous organoids of MDCK cells. *J. Biochem. (Tokyo)* **159,** 573–584 (2016).

60. Ferrell, J. E. Phosphoinositide metabolism and the morphology of human erythrocytes. *J. Cell Biol.* **98,** 1992–1998 (1984).

61. Milne, S. B., Ivanova, P. T., DeCamp, D., Hsueh, R. C. & Brown, H. A. A targeted mass spectrometric analysis of phosphatidylinositol phosphate species. *J. Lipid Res.* **46,** 1796–1802 (2005).

62. Gil-de-Gomez, L. *et al.* A Phosphatidylinositol Species Acutely Generated by Activated Macrophages Regulates Innate Immune Responses. *J. Immunol.* **190,** 5169–5177 (2013).

63. Arifin, S. A. & Falasca, M. Lysophosphatidylinositol Signalling and Metabolic Diseases. *Metabolites* **6,** (2016).

64. Oka, S., Nakajima, K., Yamashita, A., Kishimoto, S. & Sugiura, T. Identification of GPR55 as a lysophosphatidylinositol receptor. *Biochem. Biophys. Res. Commun.* **362,** 928–934 (2007).

65. Kotsikorou, E. *et al.* Identification of the GPR55 agonist binding site using a novel set of high-potency GPR55 selective ligands. *Biochemistry (Mosc.)* **50,** 5633–5647 (2011).

66. Sud, M. *et al.* LMSD: LIPID MAPS structure database. *Nucleic Acids Res.* **35,** D527-532 (2007).

67. Viaud, J. *et al.* Phosphoinositides: Important lipids in the coordination of cell dynamics. *Biochimie* (2015). doi:10.1016/j.biochi.2015.09.005

68. Mitchell, K. T., Ferrell, J. E. & Huestis, W. H. Separation of phosphoinositides and other phospholipids by two-dimensional thin-layer chromatography. *Anal. Biochem.* **158,** 447–453 (1986).

69. Duex, J. E., Nau, J. J., Kauffman, E. J. & Weisman, L. S. Phosphoinositide 5-phosphatase Fig 4p is required for both acute rise and subsequent fall in stress-induced phosphatidylinositol 3,5-bisphosphate levels. *Eukaryot. Cell* **5,** 723–731 (2006).

70. Bonangelino, C. J. *et al.* Osmotic stress-induced increase of phosphatidylinositol 3,5-bisphosphate requires Vac14p, an activator of the lipid kinase Fab1p. *J. Cell Biol.* **156,** 1015–1028 (2002).

71. Wenk, M. R. *et al.* Phosphoinositide profiling in complex lipid mixtures using electrospray ionization mass spectrometry. *Nat. Biotechnol.* **21,** 813–817 (2003).

72. Shewan, A., Eastburn, D. J. & Mostov, K. Phosphoinositides in cell architecture. *Cold Spring Harb. Perspect. Biol.* **3,** a004796 (2011).

73. Laketa, V. *et al.* PIP_3 induces the recycling of receptor tyrosine kinases. *Sci. Signal.* **7,** ra5 (2014).

74. Laketa, V. *et al.* Membrane-permeant phosphoinositide derivatives as modulators of growth factor signaling and neurite outgrowth. *Chem. Biol.* **16,** 1190–1196 (2009).

75. Farhan, H. & Rabouille, C. Signalling to and from the secretory pathway. *J. Cell Sci.* **124,** 171–180 (2011).

76. Schink, K. O., Tan, K.-W. & Stenmark, H. Phosphoinositides in Control of Membrane Dynamics. *Annu. Rev. Cell Dev. Biol.* **32,** 143–171 (2016).

77. Lorente-Rodríguez, A. & Barlowe, C. Requirement for Golgi-localized PI(4)P in fusion of COPII vesicles with Golgi compartments. *Mol. Biol. Cell* **22,** 216–229 (2011).

78. Ketel, K. *et al.* A phosphoinositide conversion mechanism for exit from endosomes. *Nature* (2016). doi:10.1038/nature16516

79. Krauss, M., Kukhtina, V., Pechstein, A. & Haucke, V. Stimulation of phosphatidylinositol kinase type I-mediated phosphatidylinositol (4,5)-bisphosphate synthesis by AP-2mu-cargo complexes. *Proc. Natl. Acad. Sci. U. S. A.* **103,** 11934–11939 (2006).

80. Posor, Y. *et al.* Spatiotemporal control of endocytosis by phosphatidylinositol-3,4-bisphosphate. *Nature* **499,** 233–237 (2013).

81. Posor, Y., Eichhorn-Grünig, M. & Haucke, V. Phosphoinositides in endocytosis. *Biochim. Biophys. Acta* (2014). doi:10.1016/j.bbalip.2014.09.014

82. Raiborg, C., Schink, K. O. & Stenmark, H. Class III phosphatidylinositol 3-kinase and its catalytic product PtdIns3P in regulation of endocytic membrane traffic. *FEBS J.* **280,** 2730–2742 (2013).

83. Aguet, F., Antonescu, C. N., Mettlen, M., Schmid, S. L. & Danuser, G. Advances in analysis of low signal-to-noise images link dynamin and AP2 to the functions of an endocytic checkpoint. *Dev. Cell* **26,** 279–291 (2013).

84. Stoops, E. H. & Caplan, M. J. Trafficking to the apical and basolateral membranes in polarized epithelial cells. *J. Am. Soc. Nephrol. JASN* **25,** 1375–1386 (2014).

85. Wallroth, A. & Haucke, V. Phosphoinositide conversion in endocytosis and the endolysosomal system. *J. Biol. Chem.* **293,** 1526–1535 (2018).

86. Poteryaev, D., Datta, S., Ackema, K., Zerial, M. & Spang, A. Identification of the switch in early-to-late endosome transition. *Cell* **141,** 497–508 (2010).

87. Vonderheit, A. & Helenius, A. Rab7 Associates with Early Endosomes to Mediate Sorting and Transport of Semliki Forest Virus to Late Endosomes. *PLoS Biol.* **3,** e233 (2005).

88. Wurmser, A. E., Sato, T. K. & Emr, S. D. New component of the vacuolar class C-Vps complex couples nucleotide exchange on the Ypt7 GTPase to SNARE-dependent docking and fusion. *J. Cell Biol.* **151,** 551–562 (2000).

89. Liu, K. *et al.* WDR91 is a Rab7 effector required for neuronal development. *J. Cell Biol.* **216,** 3307–3321 (2017).

90. Rink, J., Ghigo, E., Kalaidzidis, Y. & Zerial, M. Rab conversion as a mechanism of progression from early to late endosomes. *Cell* **122,** 735–749 (2005).

91. Cao, C., Backer, J. M., Laporte, J., Bedrick, E. J. & Wandinger-Ness, A. Sequential actions of myotubularin lipid phosphatases regulate endosomal PI(3)P and growth factor receptor trafficking. *Mol. Biol. Cell* **19,** 3334–3346 (2008).

92. Hazeki, K., Uehara, M., Nigorikawa, K. & Hazeki, O. PIKfyve regulates the endosomal localization of CpG oligodeoxynucleotides to elicit TLR9-dependent cellular responses. *PloS One* **8,** e73894 (2013).

93. Hayashi, K., Sasai, M. & Iwasaki, A. Toll-like receptor 9 trafficking and signaling for type I interferons requires PIKfyve activity. *Int. Immunol.* (2015). doi:10.1093/intimm/dxv021

94. Martens, S., Nakamura, S. & Yoshimori, T. Phospholipids in Autophagosome Formation and Fusion. *J. Mol. Biol.* **428,** 4819–4827 (2016).

95. McEwan, D. G. Host-pathogen interactions and subversion of autophagy. *Essays Biochem.* **61,** 687–697 (2017).

96. Jean, S. & Kiger, A. A. Classes of phosphoinositide 3-kinases at a glance. *J. Cell Sci.* **127,** 923–928 (2014).

97. Jang, D.-J. & Lee, J.-A. The roles of phosphoinositides in mammalian autophagy. *Arch. Pharm. Res.* **39,** 1129–1136 (2016).

98. Peng, J. *et al.* Phosphoinositide 3-kinase p110δ promotes lumen formation through the enhancement of apico-basal polarity and basal membrane organization. *Nat. Commun.* **6,** 5937 (2015).

99. Wu, C., You, J., Fu, J., Wang, X. & Zhang, Y. Phosphatidylinositol 3-Kinase/Akt Mediates Integrin Signaling To Control RNA Polymerase I Transcriptional Activity. *Mol. Cell. Biol.* **36,** 1555–1568 (2016).

100. Xia, H., Nho, R. S., Kahm, J., Kleidon, J. & Henke, C. A. Focal Adhesion Kinase Is Upstream of Phosphatidylinositol 3-Kinase/Akt in Regulating Fibroblast Survival in Response to Contraction of Type I Collagen Matrices via a β_1 Integrin Viability Signaling Pathway. *J. Biol. Chem.* **279,** 33024–33034 (2004).

101. Langlois, M.-J. *et al.* The PTEN Phosphatase Controls Intestinal Epithelial Cell Polarity and Barrier Function: Role in Colorectal Cancer Progression. *PLoS ONE* **5,** e15742 (2010).

102. von Stein, W., Ramrath, A., Grimm, A., Müller-Borg, M. & Wodarz, A. Direct association of Bazooka/PAR-3 with the lipid phosphatase PTEN reveals a link between the PAR/aPKC complex and phosphoinositide signaling. *Dev. Camb. Engl.* **132,** 1675–1686 (2005).

103. O'Farrell, F. *et al.* Class III phosphatidylinositol-3-OH kinase controls epithelial integrity through endosomal LKB1 regulation. *Nat. Cell Biol.* (2017). doi:10.1038/ncb3631

104. Shivas, J. M. & Skop, A. R. Arp2/3 mediates early endosome dynamics necessary for the maintenance of PAR asymmetry in Caenorhabditis elegans. *Mol. Biol. Cell* **23,** 1917–1927 (2012).

105. Kagan, J. C. & Medzhitov, R. Phosphoinositide-mediated adaptor recruitment controls Toll-like receptor signaling. *Cell* **125,** 943–955 (2006).

106. Kagan, J. C. *et al.* TRAM couples endocytosis of Toll-like receptor 4 to the induction of interferon-beta. *Nat. Immunol.* **9,** 361–368 (2008).

107. Chiang, C.-Y., Veckman, V., Limmer, K. & David, M. Phospholipase Cγ-2 and intracellular calcium are required for lipopolysaccharide-induced Toll-like receptor 4 (TLR4) endocytosis and interferon regulatory factor 3 (IRF3) activation. *J. Biol. Chem.* **287,** 3704–3709 (2012).

108. Aksoy, E. *et al.* The p110δ isoform of the kinase PI(3)K controls the subcellular compartmentalization of TLR4 signaling and protects from endotoxic shock. *Nat. Immunol.* **13,** 1045–1054 (2012).

109. Hu, Y.-H. *et al.* WDFY1 mediates TLR3/4 signaling by recruiting TRIF. *EMBO Rep.* **16,** 447–455 (2015).

110. Ridley, S. H. *et al.* FENS-1 and DFCP1 are FYVE domain-containing proteins with distinct functions in the endosomal and Golgi compartments. *J. Cell Sci.* **114,** 3991–4000 (2001).

111. Bonham, K. S. *et al.* A Promiscuous Lipid-Binding Protein Diversifies the Subcellular Sites of Toll-like Receptor Signal Transduction. *Cell* **156,** 705–716 (2014).

112. Sasai, M., Linehan, M. M. & Iwasaki, A. Bifurcation of Toll-like receptor 9 signaling by adaptor protein 3. *Science* **329,** 1530–1534 (2010).

113. Catimel, B. *et al.* The PI(3,5)P2 and PI(4,5)P2 interactomes. *J. Proteome Res.* **7,** 5295–5313 (2008).

114. van Oers, M. M. Opportunities and challenges for the baculovirus expression system. *J. Invertebr. Pathol.* **107 Suppl,** S3-15 (2011).

115. Robert R. Granados, Li, G. & G. W. Blissard. Insect cell culture and biotechnology. *Virol. Sin.* **22,** 83–93 (2008).

116. Monie, A., Hung, C.-F., Roden, R. & Wu, T.-C. Cervarix: a vaccine for the prevention of HPV 16, 18-associated cervical cancer. *Biol. Targets Ther.* **2,** 97–105 (2008).

117. Heimpel, A. M. & Buchanan, L. K. Human feeding tests using a nuclear-polyhedrosis virus of Heliothis zea. *J. Invertebr. Pathol.* **9,** 55–57 (1967).

118. Kost, T. A., Condreay, J. P., Ames, R. S., Rees, S. & Romanos, M. A. Implementation of BacMam virus gene delivery technology in a drug discovery setting. *Drug Discov. Today* **12,** 396–403 (2007).

119. Boyce, F. M. & Bucher, N. L. Baculovirus-mediated gene transfer into mammalian cells. *Proc. Natl. Acad. Sci. U. S. A.* **93,** 2348–2352 (1996).

120. Chen, C.-L. *et al.* Development of hybrid baculovirus vectors for artificial MicroRNA delivery and prolonged gene suppression. *Biotechnol. Bioeng.* **108,** 2958–2967 (2011).

121. Mansouri, M. *et al.* Highly efficient baculovirus-mediated multigene delivery in primary cells. *Nat. Commun.* **7,** 11529 (2016).

122. Turunen, T. A. K., Laakkonen, J. P., Alasaarela, L., Airenne, K. J. & Ylä-Herttuala, S. Sleeping Beauty-baculovirus hybrid vectors for long-term gene expression in the eye. *J. Gene Med.* **16,** 40–53 (2014).

123. Luo, W.-Y. *et al.* Development of the hybrid Sleeping Beauty-baculovirus vector for sustained gene expression and cancer therapy. *Gene Ther.* **19,** 844–851 (2012).

124. Zeng, J., Du, J., Zhao, Y., Palanisamy, N. & Wang, S. Baculoviral vector-mediated transient and stable transgene expression in human embryonic stem cells. *Stem Cells Dayt. Ohio* **25,** 1055–1061 (2007).

125. Wang, L. *et al.* Epstein-Barr virus nuclear antigen 1 (EBNA1) protein induction of epithelial-mesenchymal transition in nasopharyngeal carcinoma cells. *Cancer* **120,** 363–372 (2014).

126. Wilson, J. B., Bell, J. L. & Levine, A. J. Expression of Epstein-Barr virus nuclear antigen-1 induces B cell neoplasia in transgenic mice. *EMBO J.* **15,** 3117–3126 (1996).

127. Mirkovitch, J., Mirault, M. E. & Laemmli, U. K. Organization of the higher-order chromatin loop: specific DNA attachment sites on nuclear scaffold. *Cell* **39,** 223–232 (1984).

128. Wong, S. P., Argyros, O. & Harbottle, R. P. Sustained Expression from DNA Vectors. in *Advances in Genetics* **89,** 113–152 (Elsevier, 2015).

129. Piechaczek, C., Fetzer, C., Baiker, A., Bode, J. & Lipps, H. J. A vector based on the SV40 origin of replication and chromosomal S/MARs replicates episomally in CHO cells. *Nucleic Acids Res.* **27,** 426–428 (1999).

130. Chen, F. *et al.* Episomal lentiviral vectors confer erythropoietin expression in dividing cells. *Plasmid* **90,** 15–19 (2017).

131. Verghese, S. C., Goloviznina, N. A., Skinner, A. M., Lipps, H. J. & Kurre, P. S/MAR sequence confers long-term mitotic stability on non-integrating lentiviral vector episomes without selection. *Nucleic Acids Res.* **42,** e53 (2014).

132. Lin, Y. *et al.* MAR characteristic motifs mediate episomal vector in CHO cells. *Gene* **559,** 137–143 (2015).

133. Hughes, T. S. *et al.* Intrathecal injection of naked plasmid DNA provides long-term expression of secreted proteins. *Mol. Ther. J. Am. Soc. Gene Ther.* **17,** 88–94 (2009).

134. Argyros, O. *et al.* Persistent episomal transgene expression in liver following delivery of a scaffold/matrix attachment region containing non-viral vector. *Gene Ther.* **15,** 1593–1605 (2008).

135. Stehle, I. M., Scinteie, M. F., Baiker, A., Jenke, A. C. W. & Lipps, H. J. Exploiting a minimal system to study the epigenetic control of DNA replication: the interplay between

transcription and replication. *Chromosome Res. Int. J. Mol. Supramol. Evol. Asp. Chromosome Biol.* **11,** 413–421 (2003).

136. Jenke, B. H. C. *et al.* An episomally replicating vector binds to the nuclear matrix protein SAF-A in vivo. *EMBO Rep.* **3,** 349–354 (2002).

137. Schaarschmidt, D., Baltin, J., Stehle, I. M., Lipps, H. J. & Knippers, R. An episomal mammalian replicon: sequence-independent binding of the origin recognition complex. *EMBO J.* **23,** 191–201 (2004).

138. Stehle, I. M. *et al.* Establishment and mitotic stability of an extra-chromosomal mammalian replicon. *BMC Cell Biol.* **8,** 33 (2007).

139. Jenke, A. C. W., Scinteie, M. F., Stehle, I. M. & Lipps, H. J. Expression of a transgene encoded on a non-viral episomal vector is not subject to epigenetic silencing by cytosine methylation. *Mol. Biol. Rep.* **31,** 85–90 (2004).

140. Moffat, J. *et al.* A lentiviral RNAi library for human and mouse genes applied to an arrayed viral high-content screen. *Cell* **124,** 1283–1298 (2006).

141. New England Biolabs Inc. *NEBuilder Assembly Tool*. (2017).

142. Schindelin, J. *et al.* Fiji: an open-source platform for biological-image analysis. *Nat. Methods* **9,** 676–682 (2012).

143. *Virology methods manual*. (Acad. Press, 1996).

144. Horzinek, M. C. & Zeijst, B. A. M. van der. *Kompendium der allgemeinen Virologie: mit 86 Abbildungen und 16 Tabellen*. (Verlag Paul Parey, 1985).

145. Hammond, G. R. V., Schiavo, G. & Irvine, R. F. Immunocytochemical techniques reveal multiple, distinct cellular pools of PtdIns4P and PtdIns(4,5)P(2). *Biochem. J.* **422,** 23–35 (2009).

146. Marat, A. L. & Haucke, V. Phosphatidylinositol 3-phosphates-at the interface between cell signalling and membrane traffic. *EMBO J.* (2016). doi:10.15252/embj.201593564

147. Ronan, B. *et al.* A highly potent and selective Vps34 inhibitor alters vesicle trafficking and autophagy. *Nat. Chem. Biol.* **10,** 1013–1019 (2014).

148. Bago, R. *et al.* Characterization of VPS34-IN1, a selective inhibitor of Vps34, reveals that the phosphatidylinositol 3-phosphate-binding SGK3 protein kinase is a downstream target of class III phosphoinositide 3-kinase. *Biochem. J.* **463,** 413–427 (2014).

149. Franco, I. *et al.* PI3K Class II α Controls Spatially Restricted Endosomal PtdIns3P and Rab11 Activation to Promote Primary Cilium Function. *Dev. Cell* **28,** 647–658 (2014).

150. Tuma, P. L., Nyasae, L. K., Backer, J. M. & Hubbard, A. L. Vps34p differentially regulates endocytosis from the apical and basolateral domains in polarized hepatic cells. *J. Cell Biol.* **154,** 1197–1208 (2001).

151. Schink, K. O., Raiborg, C. & Stenmark, H. Phosphatidylinositol 3-phosphate, a lipid that regulates membrane dynamics, protein sorting and cell signalling. *BioEssays News Rev. Mol. Cell. Dev. Biol.* **35,** 900–912 (2013).

152. Zoncu, R. *et al.* A phosphoinositide switch controls the maturation and signaling properties of APPL endosomes. *Cell* **136,** 1110–1121 (2009).

153. Dugay, F. *et al.* Overexpression of the polarity protein PAR-3 in clear cell renal cell carcinoma is associated with poor prognosis. *Int. J. Cancer* **134,** 2051–2060 (2014).

154. Vaira, V. *et al.* Aberrant overexpression of the cell polarity module scribble in human cancer. *Am. J. Pathol.* **178,** 2478–2483 (2011).

155. Eder, A. M. *et al.* Atypical PKCiota contributes to poor prognosis through loss of apical-basal polarity and cyclin E overexpression in ovarian cancer. *Proc. Natl. Acad. Sci. U. S. A.* **102,** 12519–12524 (2005).

156. Carpentier, S. *et al.* Class III phosphoinositide 3-kinase/VPS34 and dynamin are critical for apical endocytic recycling. *Traffic Cph. Den.* **14,** 933–948 (2013).

157. Stanifer, M. L., Kischnick, C., Rippert, A., Albrecht, D. & Boulant, S. Reovirus inhibits interferon production by sequestering IRF3 into viral factories. *Sci. Rep.* **7,** 10873 (2017).

158. Shah, P. N. M. *et al.* Genome packaging of reovirus is mediated by the scaffolding property of the microtubule network. *Cell. Microbiol.* **19,** (2017).

159. Stanifer, M. L. *et al.* Reovirus intermediate subviral particles constitute a strategy to infect intestinal epithelial cells by exploiting TGF-β dependent pro-survival signaling. *Cell. Microbiol.* (2016). doi:10.1111/cmi.12626

160. Sommereyns, C., Paul, S., Staeheli, P. & Michiels, T. IFN-lambda (IFN-lambda) is expressed in a tissue-dependent fashion and primarily acts on epithelial cells in vivo. *PLoS Pathog.* **4,** e1000017 (2008).

161. Pervolaraki, K. *et al.* Type I and Type III Interferons Display Different Dependency on Mitogen-Activated Protein Kinases to Mount an Antiviral State in the Human Gut. *Front. Immunol.* **8,** 459 (2017).

162. Kuhn, K. A., Manieri, N. A., Liu, T.-C. & Stappenbeck, T. S. IL-6 Stimulates Intestinal Epithelial Proliferation and Repair after Injury. *PLoS ONE* **9,** e114195 (2014).

163. Jones, S. C. *et al.* Expression of interleukin-6 by intestinal enterocytes. *J. Clin. Pathol.* **46,** 1097–1100 (1993).

164. Akdis, M. *et al.* Interleukins (from IL-1 to IL-38), interferons, transforming growth factor β, and TNF-α: Receptors, functions, and roles in diseases. *J. Allergy Clin. Immunol.* **138,** 984–1010 (2016).

165. Pittini, Á., Casaravilla, C., Allen, J. E. & Díaz, Á. Pharmacological inhibition of PI3K class III enhances the production of pro- and anti-inflammatory cytokines in dendritic cells stimulated by TLR agonists. *Int. Immunopharmacol.* **36,** 213–217 (2016).

166. Marat, A. L. *et al.* mTORC1 activity repression by late endosomal phosphatidylinositol 3,4-bisphosphate. *Science* **356,** 968–972 (2017).

167. Laporte, J. *et al.* A gene mutated in X-linked myotubular myopathy defines a new putative tyrosine phosphatase family conserved in yeast. *Nat. Genet.* **13,** 175–182 (1996).

168. Broad Institute. Genetic Perturbation Platform. *Genetic Perturbation Platform* Available at: https://www.broadinstitute.org/genetic-perturbation-platform.

169. Hnia, K., Vaccari, I., Bolino, A. & Laporte, J. Myotubularin phosphoinositide phosphatases: cellular functions and disease pathophysiology. *Trends Mol. Med.* **18,** 317–327 (2012).

170. Backer, J. M. The intricate regulation and complex functions of the Class III phosphoinositide 3-kinase Vps34. *Biochem. J.* **473,** 2251–2271 (2016).

171. Fili, N., Calleja, V., Woscholski, R., Parker, P. J. & Larijani, B. Compartmental signal modulation: Endosomal phosphatidylinositol 3-phosphate controls endosome morphology and selective cargo sorting. *Proc. Natl. Acad. Sci. U. S. A.* **103,** 15473–15478 (2006).

172. Juhász, G. *et al.* The class III PI(3)K Vps34 promotes autophagy and endocytosis but not TOR signaling in Drosophila. *J. Cell Biol.* **181,** 655–666 (2008).

173. Bechtel, W. *et al.* Vps34 deficiency reveals the importance of endocytosis for podocyte homeostasis. *J. Am. Soc. Nephrol. JASN* **24,** 727–743 (2013).

174. Putyrski, M. & Schultz, C. Protein translocation as a tool: The current rapamycin story. *FEBS Lett.* **586,** 2097–2105 (2012).

175. Taylor, G. S., Maehama, T. & Dixon, J. E. Myotubularin, a protein tyrosine phosphatase mutated in myotubular myopathy, dephosphorylates the lipid second messenger, phosphatidylinositol 3-phosphate. *Proc. Natl. Acad. Sci. U. S. A.* **97,** 8910–8915 (2000).

176. Hnia, K. *et al.* Myotubularin controls desmin intermediate filament architecture and mitochondrial dynamics in human and mouse skeletal muscle. *J. Clin. Invest.* **121,** 70–85 (2011).

177. Morel, E. *et al.* Phosphatidylinositol-3-phosphate regulates sorting and processing of amyloid precursor protein through the endosomal system. *Nat. Commun.* **4,** (2013).

178. Schaletzky, J. *et al.* Phosphatidylinositol-5-phosphate activation and conserved substrate specificity of the myotubularin phosphatidylinositol 3-phosphatases. *Curr. Biol. CB* **13,** 504–509 (2003).

179. Shackelford, D. B. & Shaw, R. J. The LKB1–AMPK pathway: metabolism and growth control in tumour suppression. *Nat. Rev. Cancer* **9,** 563–575 (2009).

180. Jia, D. *et al.* WASH and WAVE actin regulators of the Wiskott-Aldrich syndrome protein (WASP) family are controlled by analogous structurally related complexes. *Proc. Natl. Acad. Sci.* **107,** 10442–10447 (2010).

181. Yamanaka, T. *et al.* Mammalian Lgl Forms a Protein Complex with PAR-6 and aPKC Independently of PAR-3 to Regulate Epithelial Cell Polarity. *Curr. Biol.* **13,** 734–743 (2003).

182. Carding, S. R., Davis, N. & Hoyles, L. Review article: the human intestinal virome in health and disease. *Aliment. Pharmacol. Ther.* **46,** 800–815 (2017).

183. Norman, J. M. *et al.* Disease-specific alterations in the enteric virome in inflammatory bowel disease. *Cell* **160,** 447–460 (2015).

184. Kernbauer, E., Ding, Y. & Cadwell, K. An enteric virus can replace the beneficial function of commensal bacteria. *Nature* **516,** 94–98 (2014).

185. Boulant, S. *et al.* Similar uptake but different trafficking and escape routes of reovirus virions and infectious subvirion particles imaged in polarized Madin-Darby canine kidney cells. *Mol. Biol. Cell* **24,** 1196–1207 (2013).

186. Danthi, P., Holm, G. H., Stehle, T. & Dermody, T. S. Reovirus receptors, cell entry, and proapoptotic signaling. *Adv. Exp. Med. Biol.* **790,** 42–71 (2013).

187. Robke, L. *et al.* Phenotypic Identification of a Novel Autophagy Inhibitor Chemotype Targeting Lipid Kinase VPS34. *Angew. Chem. Int. Ed Engl.* **56,** 8153–8157 (2017).

188. Honda, A. *et al.* Potent, Selective, and Orally Bioavailable Inhibitors of VPS34 Provide Chemical Tools to Modulate Autophagy in Vivo. *ACS Med. Chem. Lett.* **7,** 72–76 (2016).

189. Kawasaki, T., Takemura, N., Standley, D. M., Akira, S. & Kawai, T. The second messenger phosphatidylinositol-5-phosphate facilitates antiviral innate immune signaling. *Cell Host Microbe* **14,** 148–158 (2013).

190. Bruns, A. M. & Horvath, C. M. Activation of RIG-I-like receptor signal transduction. *Crit. Rev. Biochem. Mol. Biol.* **47,** 194–206 (2012).

191. Hasegawa, J., Strunk, B. S. & Weisman, L. S. PI5P and PI(3,5)P2: Minor, but Essential Phosphoinositides. *Cell Struct. Funct.* **42,** 49–60 (2017).

192. Libermann, T. A. & Baltimore, D. Activation of interleukin-6 gene expression through the NF-kappa B transcription factor. *Mol. Cell. Biol.* **10,** 2327–2334 (1990).

193. de Haij, S. NF- B Mediated IL-6 Production by Renal Epithelial Cells Is Regulated by C-Jun NH2-Terminal Kinase. *J. Am. Soc. Nephrol.* **16,** 1603–1611 (2005).

194. Elliott, C. L., Allport, V. C., Loudon, J. A., Wu, G. D. & Bennett, P. R. Nuclear factor-kappa B is essential for up-regulation of interleukin-8 expression in human amnion and cervical epithelial cells. *Mol. Hum. Reprod.* **7,** 787–790 (2001).

195. Hobert, M. E., Sands, K. A., Mrsny, R. J. & Madara, J. L. Cdc42 and Rac1 regulate late events in Salmonella typhimurium-induced interleukin-8 secretion from polarized epithelial cells. *J. Biol. Chem.* **277,** 51025–51032 (2002).

196. Li, J., Kim, S. G. & Blenis, J. Rapamycin: One Drug, Many Effects. *Cell Metab.* **19,** 373–379 (2014).

197. Feng, S. *et al.* A Rapidly Reversible Chemical Dimerizer System to Study Lipid Signaling in Living Cells. *Angew. Chem. Int. Ed Engl.* (2014). doi:10.1002/anie.201402294

198. Thomson, A. W., Bonham, C. A. & Zeevi, A. Mode of action of tacrolimus (FK506): molecular and cellular mechanisms. *Ther. Drug Monit.* **17,** 584–591 (1995).

199. Sung, L.-Y. *et al.* Enhanced and prolonged baculovirus-mediated expression by incorporating recombinase system and in cis elements: a comparative study. *Nucleic Acids Res.* **41,** e139–e139 (2013).

200. Nehlsen, K., Broll, S. & Bode, J. Replicating minicircles: Generation of nonviral episomes for the efficient modification of dividing cells. *Gene Ther. Mol. Biol.* **10,** 233–244 (2006).

6 SUPPLEMENTARY

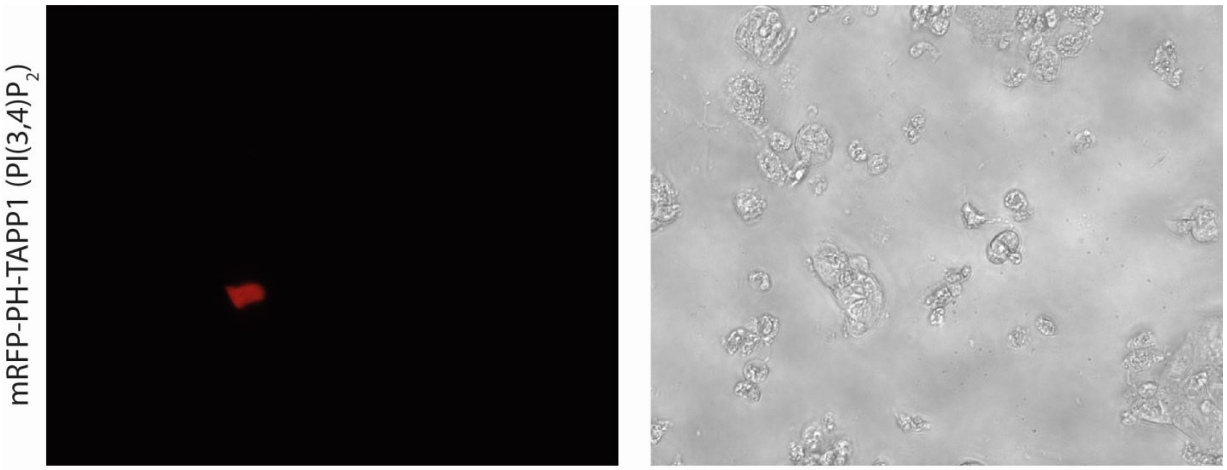

Sup. Figure 1: Transfection of T84 cells is not efficient. T84 cells were transfected with the PI(3,4)P2 sensor mRFP-TAPP1 and were visualized 48 hours post-transfection by epifluorescence (left) or brightfield (right). Representative image is shown.

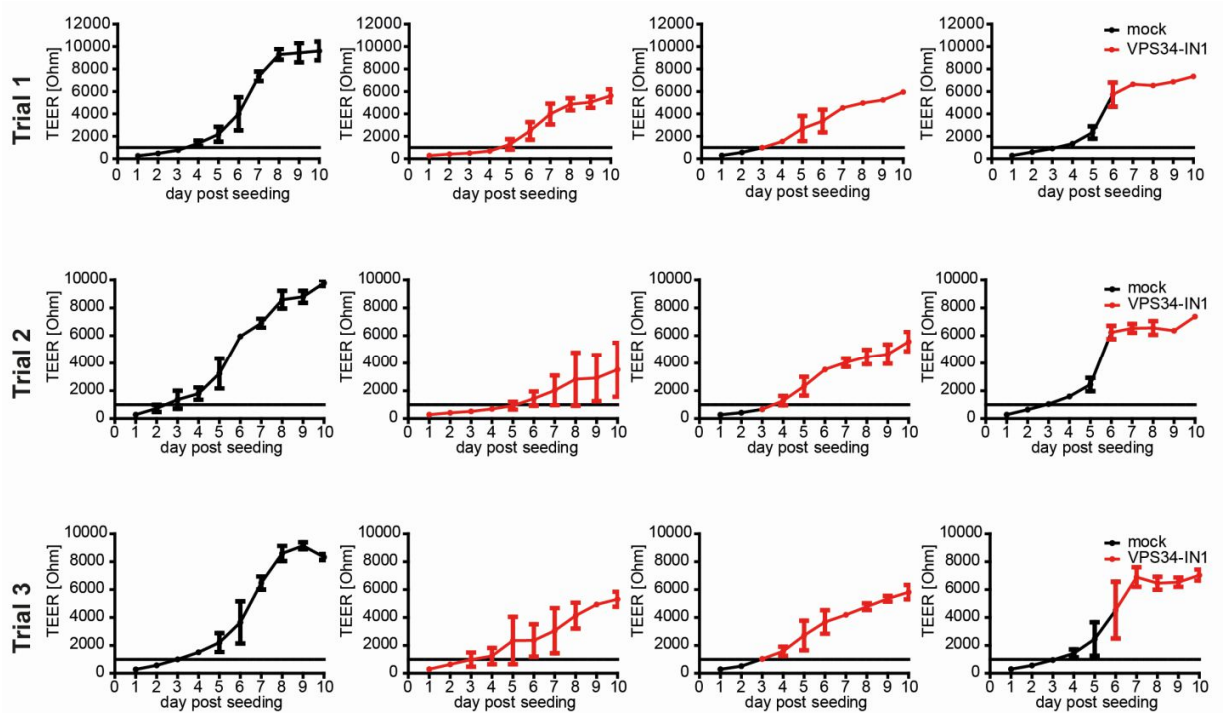

Sup. Figure 2: T84 wildtype polarization with 1 µM VPS34-IN1. T84 cells were seeded onto transwell inserts and their polarization was monitored by TEER measurements. Cells were either mock treated (DMSO) or treated (black) with 1 µM VPS34-IN1 beginning at day 1, day 3, or day 6 post seeding (red) and kept with inhibitor for the remainder of the experiment. Three independent experiments are shown. For each condition two transwells were used and average and standard deviation are shown.

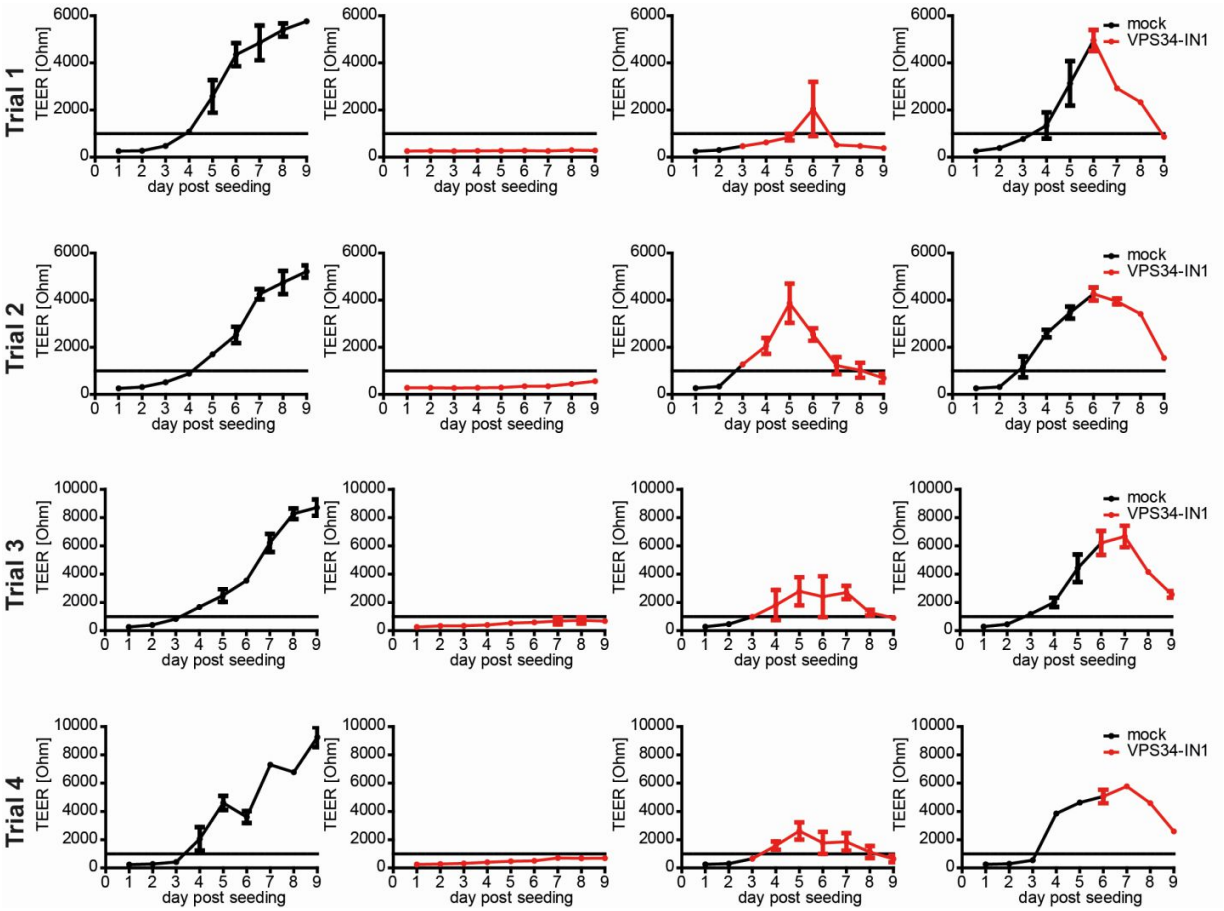

Sup. Figure 3: T84 wildtype polarization with 5 µM VPS34-IN1. T84 cells were seeded onto transwell inserts and their polarization was monitored by TEER measurements. Cells were either mock treated (DMSO) or treated (black) with 5 µM VPS34-IN1 beginning at day 1, day 3, or day 6 post seeding (red) and kept with inhibitor for the remainder of the experiment. Four independent experiments are shown. For each condition two transwells were used and average and standard deviation are shown.

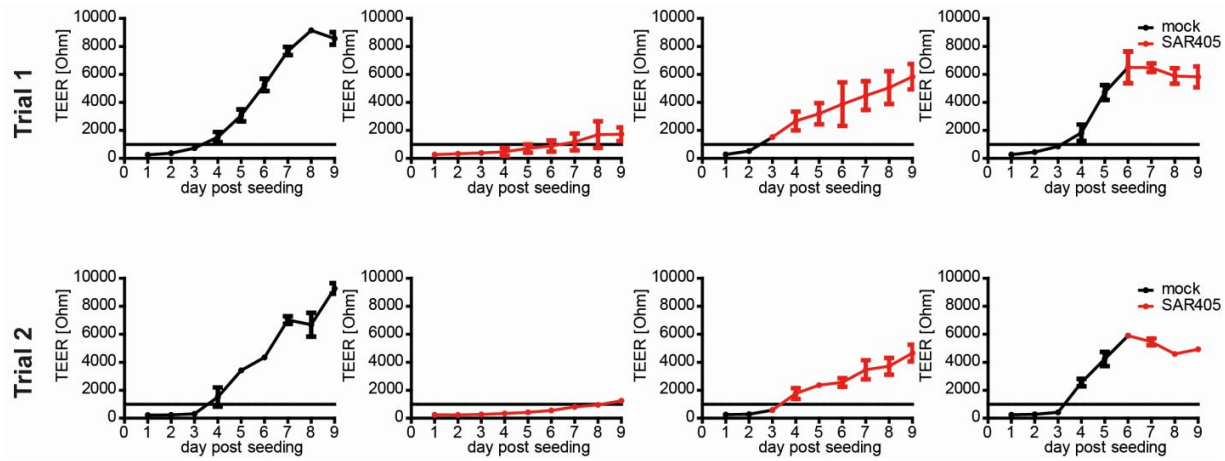

Sup. Figure 4: T84 wildtype polarization with 6 µM SAR405. T84 cells were seeded onto transwell inserts and their polarization was monitored by TEER measurements. Cells were either mock treated (DMSO) or treated (black) with 6 µM SAR405 beginning at day 1, day 3, or day 6 post seeding (red) and kept with inhibitor for the remainder of the experiment. Two independent experiments are shown. For each condition two transwells were used and average and standard deviation are shown.

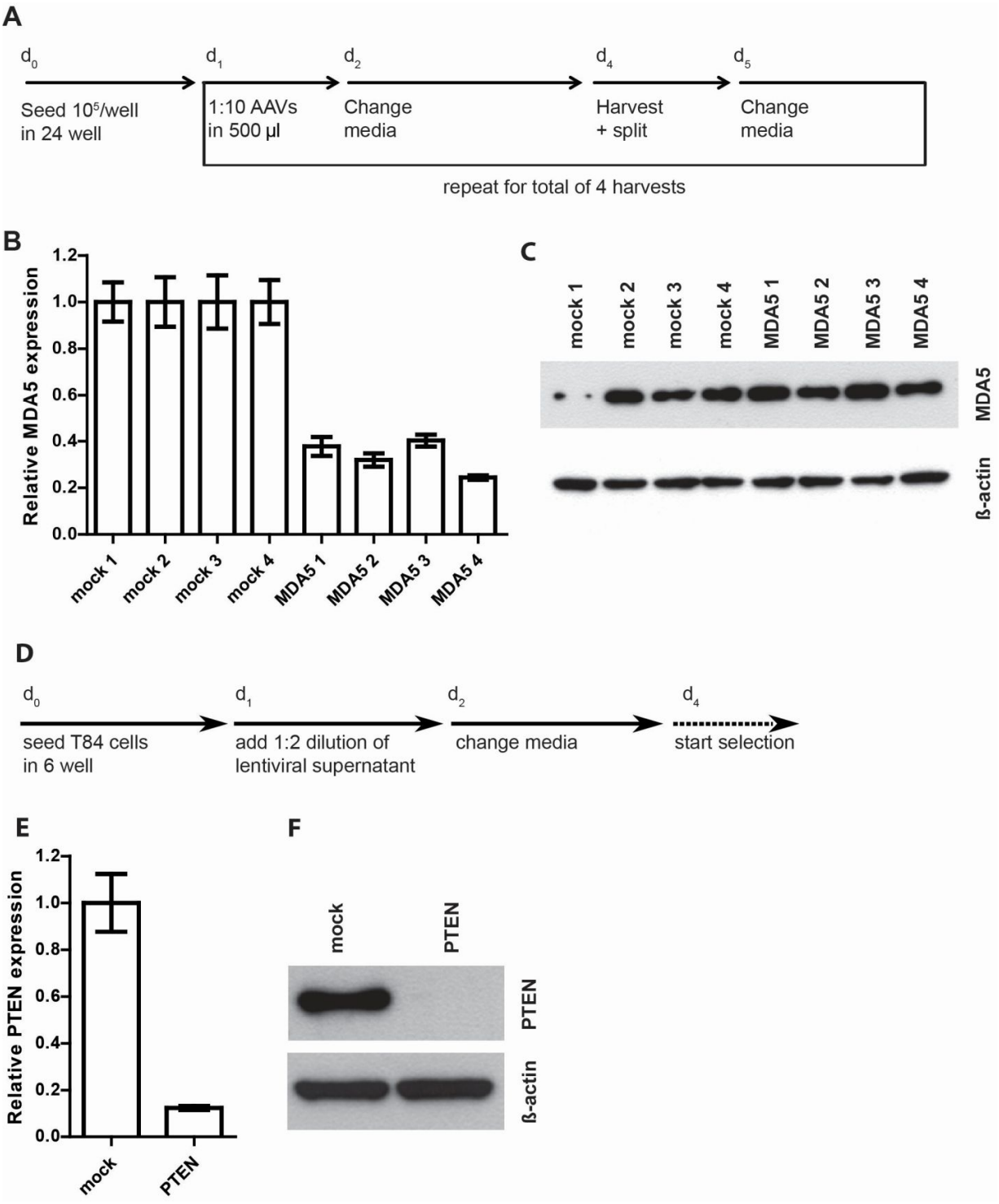

Sup. Figure 5: Knock-down in T84 cells requires low density cells and passaging. A) Experimental procedure for transient knock-down using AAVs. B) Knock-down of MDA5 on RNA level at each time when cells were passaged and re-transduced. C) Western blot analysis of the samples in B. D) Experimental procedure for lentiviral knock-down. E) RNA level of PTEN after several passages of cells at low density for over two weeks. F) Western blot analysis of PTEN protein levels in scrambled control (mock) or knock-down cells (PTEN). This data was taken from my own Master Thesis and has originally been created by myself.

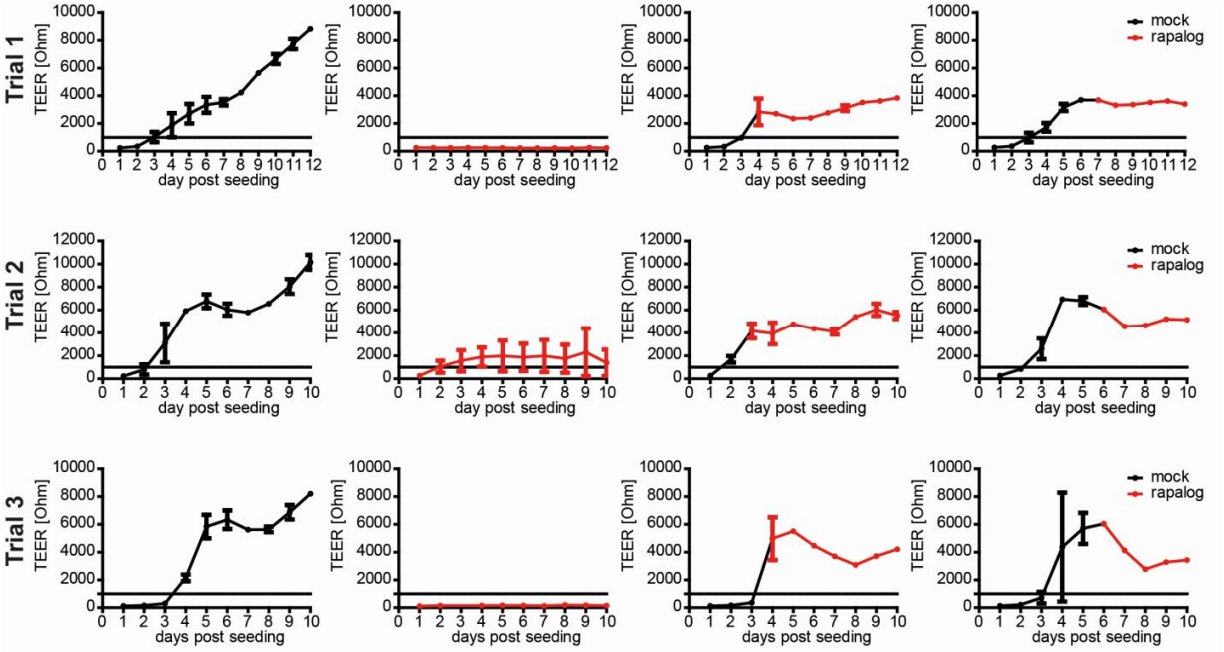

Sup. Figure 6: T84 Rab5-GFP-FRB* + mRFP-FKBP-MTM1-wildtype polarization timecourses with rapalog. T84 cells expressing recruitable MTM1-wt were seeded onto transwell inserts and their polarization was monitored by TEER measurements. Rapalog was added at indicated time points and was maintained throughout the whole experiment. Three independent experiments with two transwells per timepoint are shown. Average and standard deviation are shown.

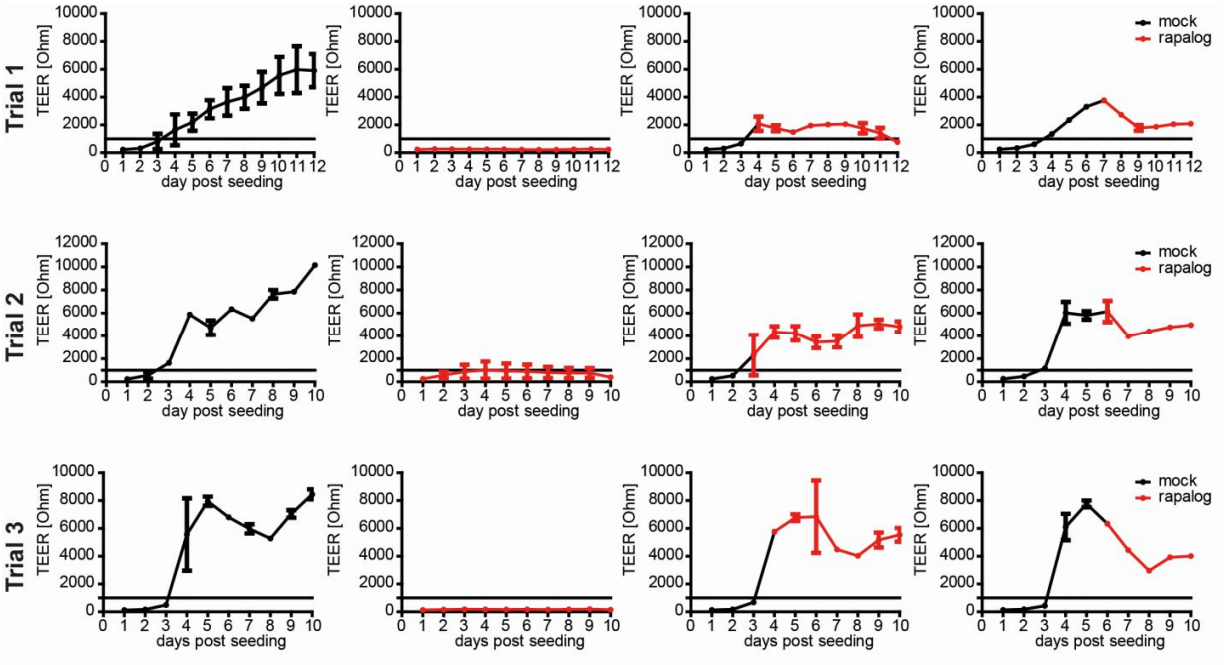

Sup. Figure 7: T84 Rab5-GFP-FRB* + mRFP-FKBP-MTM1-C375S polarization timecourses with rapalog. T84 cells expressing recruitable MTM1-C375S were seeded onto transwell inserts and their polarization was monitored by TEER measurements. Rapalog was added at indicated time points and was maintained throughout the whole experiment. Three independent experiments with two transwells per timepoint are shown. Average and standard deviation are shown.

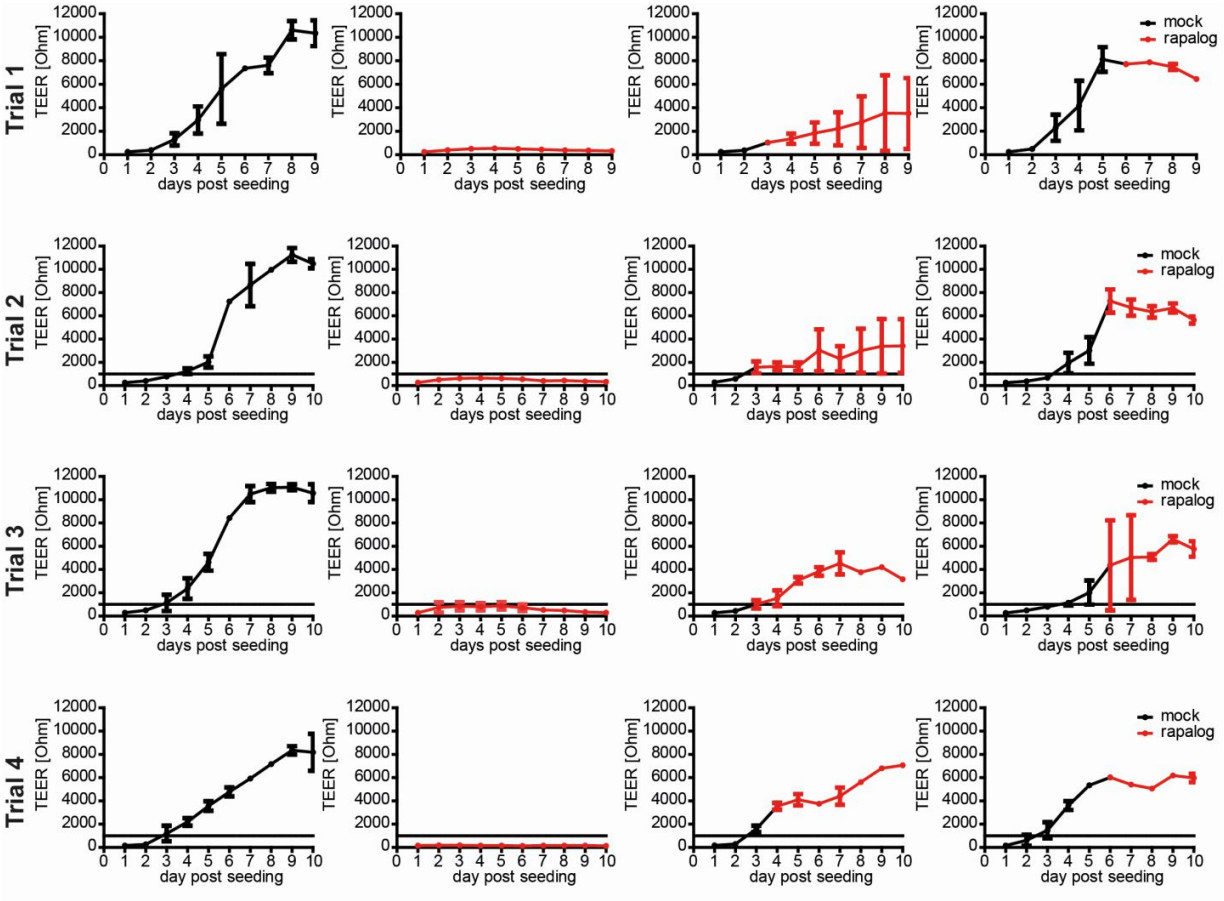

Sup. Figure 8: T84 wildtype polarization timecourses with rapalog. T84 WT cells were seeded onto transwell inserts and their polarization was monitored by TEER measurements. Rapalog was added at indicated time points and was maintained throughout the whole experiment. Four independent experiments with two transwells per timepoint are shown. Average and standard deviation are shown.

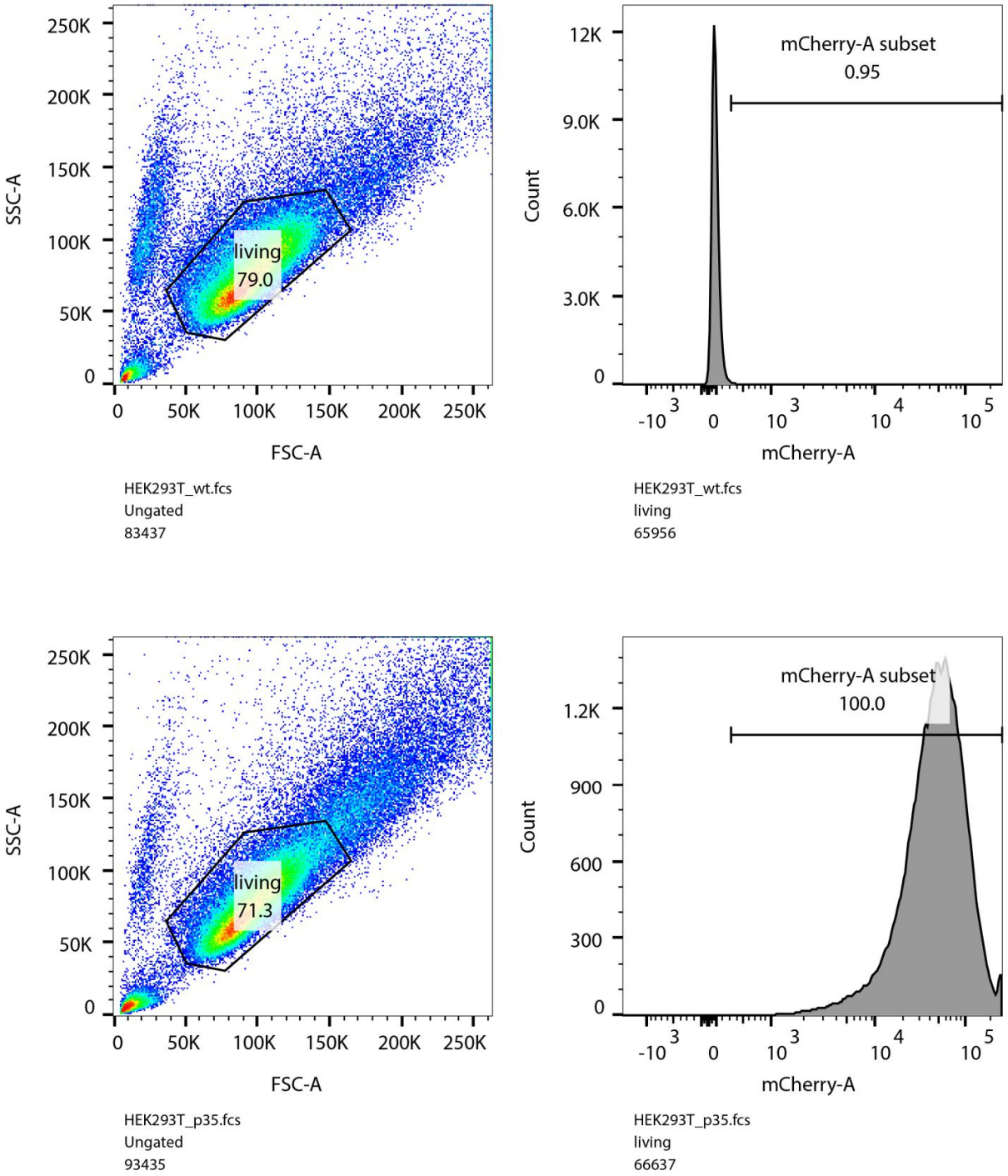

Sup. Figure 9: Gating for HEK 293T wildtype and BacMam p35-luc reporter cells. HEK293T cells were analyzed 6 months after transduction with the BacMam reporter. Gating for living cell population and mCherry expression for wildtype. (top panel) or HEK 293T cells transduced with BacMam p35-luc reporter (bottom panel).